VYSOKÉ UČENÍ TECHNICKÉ V BRNĚ

BRNO UNIVERSITY OF TECHNOLOGY

FAKULTA CHEMICKÁ
ÚSTAV FYZIKÁLNÍ A SPOTŘEBNÍ CHEMIE

FACULTY OF CHEMISTRY
INSTITUTE OF PHYSICAL AND APPLIED CHEMISTRY

THE HYDRATION OF HYALURONIC ACID

HYDRATACE HYALURONOVÉ KYSELINY

DIPLOMOVÁ PRÁCE
DIPLOMA THESIS

AUTOR PRÁCE ALENA PRŮŠOVÁ
AUTHOR

BRNO 2008

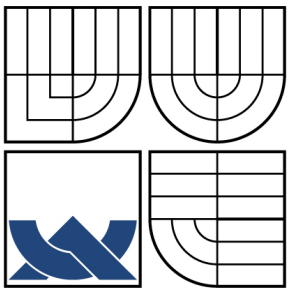

VYSOKÉ UČENÍ TECHNICKÉ V BRNĚ

BRNO UNIVERSITY OF TECHNOLOGY

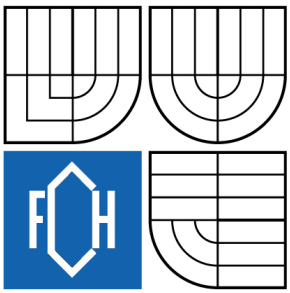

FAKULTA CHEMICKÁ
ÚSTAV FYZIKÁLNÍ A SPOTŘEBNÍ CHEMIE

FACULTY OF CHEMISTRY
INSTITUTE OF PHYSICAL AND APPLIED CHEMISTRY

THE HYDRATION OF HYALURONIC ACID

HYDRATACE HYALURONOVÉ KYSELINY

DIPLOMOVÁ PRÁCE
DIPLOMA THESIS

AUTOR PRÁCE — ALENA PRŮŠOVÁ
AUTHOR

VEDOUCÍ PRÁCE — Ing. JIŘÍ KUČERÍK, Ph.D.
SUPERVISOR

BRNO 2008

Vysoké učení technické v Brně
Fakulta chemická
Purkyňova 464/118, 61200 Brno 12

Zadání diplomové práce

Číslo diplomové práce	**FCH-DIP0141/2007**	Akademický rok: **2007/2008**
Ústav	Ústav fyzikální a spotřební chemie	
Student(ka)	**Průšová Alena**	
Studijní program	Spotřební chemie (M2806)	
Studijní obor	Spotřební chemie (2806T002)	
Vedoucí diplomové práce	**Ing. Jiří Kučerík, Ph.D.**	
Konzultanti diplomové práce		

Název diplomové práce:

Hydratace hyaluronové kyseliny

Zadání diplomové práce:

1. Zpracování literární rešerše na téma hydratace a biopolymery.
2. Seznámení se s technikami ultrazvukové spektroskopie a termické analýzy
3. Provedení vlastních experimentů.
4. Vyhodnocení dosažených výsledků.

Termín odevzdání diplomové práce: 16.5.2008

Diplomová práce se odevzdává ve třech exemplářích na sekretariát ústavu a v elektronické formě vedoucímu diplomové práce. Toto zadání je přílohou diplomové práce.

Alena Průšová	Ing. Jiří Kučerík, Ph.D.	
student(ka)	Vedoucí práce	Ředitel ústavu

V Brně, dne 1.9.2007

doc. Ing. Jaromír Havlica, CSc.
Děkan fakulty

ABSTRACT

Hydration is a crucial factor influencing the secondary structure and consequently the function of molecules present in living systems. Due to mutual affinity of water molecules, they form specific structures which composition and physical properties are affected by the presence of an extraneous molecule. Hyaluronan belongs to the group of biomolecules having large binding and retention capability for water. The aim of this work was to investigate the hydration of different molecular fractions hyaluronan and enumerate the amount of water in individual hydration layers. In the first part, the differential scanning calorimetry was used. On the base of difference in melting temperatures and enthalpies, such approach allowed to recognize three main types of water structures in the hyaluronan solution, so-called 'bulk water'; 'freezing-bound' and the 'non-freezing water'. It has been found that increasing molecular dimension of hyaluronan cause a slight increase in ability to bind both non-freezing and freezing-bound water. In the second part of the work, based on the change in compressibility, the bound water was studied using high resolution ultrasonic spectroscopy. It allowed the extension of experimental conditions from 2 to 60°C and partially supported the results from the first part. Experimental data also showed that hyaluronan is an incompressible molecule and water enumeration is possible using additional densitometry measurement.

ABSTRAKT

Hydratace patří mezi nejdůležitější faktory ovlivňující sekundární strukturu a tím i funkci molekul v živých systémech. Díky vysoké afinitě tvoří molekuly vody specifické struktury jejichž složení a fyzikální vlastnosti jsou ovlivněny přítomností studované látky. Hyaluronan patří mezi biomolekuly s obrovskou schopností vázat a zadržovat vodu. Cílem této práce bylo prozkoumat hydratační vlastnosti hyaluronanu o různé molekulové hmotnosti a vyčíslit množství molekul vody v jednotlivých hydratačních vrstvách. V první části práce byla využita metoda diferenční kompenzační kalorimetrie. Ta umožnila klasifikovat tři základní strukturní typy vody v roztoku hyaluronanu na základě rozdílných teplot a entalpií tání, tzv. „volná-mrznoucí voda“, „mrznoucí-vázaná voda“ a dále „nemrznoucí voda“. Bylo zjištěno, že se vzrůstající molekulovou hmotností hyaluronanu se mírně zvyšuje jak množství vázané tak i nemrznoucí vody. V druhé části diplomové práce, na základě rozdílné kompresibility, byla vázaná voda studována metodou vysoko rozlišovací ultrazvukové spektroskopie. Ta umožnila rozšířit oblast studovaných teplot od 2 do 60°C a částečně podpořila výsledky dosažené v první části práce. Výsledky také ukázaly, že v případě hyaluronanu se jedná o nekompresibilní molekulu a za pomoci dodatečných měření hustoty lze množství hydratační vody stanovit s vysokou přesností.

KEYWORDS

Hyaluronic acids, high resolution ultrasonic spectroscopy, thermal analysis

KLÍČOVÁ SLOVA

Hyaluronová kyselina, vysoce rozlišovací ultrazvuková spektroskopie, termická analýza

PRŮŠOVÁ, A. *Hydratace hyaluronové kyseliny*. Brno: Vysoké učení technické v Brně, Fakulta chemická, 2008. 81 s. Vedoucí diplomové práce Ing. Jiří Kučerík, Ph.D.

DECLARATION

I declare that this thesis has been compiled by myself and on my own and I cited all my information sources completely and correctly. The diploma thesis is in terms of its contents a property of the BUT Faculty of Chemistry and its usage for commercial purposes is subject to a prior consent of the supervisor and the dean.

PROHLÁŠENÍ

Prohlašuji, že jsem diplomovou práci vypracovala samostatně a že všechny použité literární zdroje jsem správně a úplně citovala. Diplomová práce je z hlediska obsahu majetkem Fakulty chemické VUT v Brně a může být využita ke komerčním účelům jen se souhlasem vedoucího diplomové práce a děkana FCH VUT.

.....
podpis diplomanta

Acknowledgements:
I would like to say a word of thanks to my supervisor Ing. Jiří Kučerík, Ph. D., who was guiding my diploma thesis for his enormous patience and helpfulness. Last but not least, I would like to thank to my parents for enabling my studies at the university.

CONTENT

1 INTRODUCTION

During the last decades, significant advances have been made in the development of biocompatible and biodegradable materials for biomedical applications. In the biomedical field, the goal is to develop and investigate materials for use in the human body to restore as well to improve physiologic functions, and enhance survival and quality of life. The development of such materials includes requirements that those should be nontoxic and, in time, being integrated or absorbed into biological environment.

One of an appropriate material seems to be hyaluronan which is already being investigated and in some branches of biomedical applications is already used. For example as vehicle for controlled drug delivery transport system, as a material for scaffold in tissue engineering, as a component of a bandage by wound healing processes, as an alternate fluid in human joints, as a space filling matter in plastic surgery and last but not least as a hydration matter in cosmetics.

These and other reasons were the impulse to do this thesis, which is devoted to the description of the behavior and property of water on the surface of the hyaluronan molecule.

Motto:
...if liquid water is strange, solid water (ice) is even stranger...
Hobbs P.V., 1974

2 STATE OF THE ART

2.1 Hyaluronic acid

The term of hyaluronic acid origins from hyalos (Greek for vitreous humour) and uronic acid because it was first isolated from the vitreous of bovine eyes (by Karl Meyer in 1934) and possesses a high uronic acid content.

Hyaluronic acid also known as sodium hyaluronate or hyaluronan (HYA) is a naturally occurring biopolymer, which serves important biological functions in bacteria and higher animals including humans. Today, this macromolecule is most frequently referred to as hyaluronan, reflecting the fact that it exists in vivo as a polyanion and not in the protonated acid form [1].

Only one kind of hyaluronan exists. It is the archetypal glycosaminoglycan. Similar anionic glycosaminoglycans include the chondroitin, keratan and heparan sulfates which, by contrast, can exist in astronomical numbers of possible isomers, because their sulfate groups can be distributed along the polymer in many different ways [1].

Hyaluronan is water soluble giving viscoelastic fluids [2] and it has a considerably greater ability to trap water than other polyelectrolyte polysaccharides. A 2 % solution of pure hyaluronic acid holds the water so tightly that it looks like a gel showing elastic or pseudoelastic properties [3]. The water-binding capacity correlates with the molecular weight (M_w) [4]. The molecular weight of hyaluronan polymers covers the range from around a hundred thousand up to several million Daltons (up to 10 MDa) [5] and depend on their source and methods of isolation. Each disaccharide unit has a molecular weight of approximately 401 Da [6].

Generally hyaluronan polymers have extraordinarily wide range and often opposing biological functions depending on the size of the molecule. Larger matrix polymers of hyaluronan are space-filling, anti-angiogenic and immunosuppressive while the intermediate-sized polymers comprising 25–50 disaccharides are inflammatory, immunostimulatory and highly angiogenic. Smaller oligosaccharides are antiapoptotic. These low molecular weight oligosaccharides appear to function as endogenous danger signals and induce heat shock proteins [5].

There are 15 g of hyaluronan in the 70 kg individual and daily turnover is 5 g. This high turnover is caused by quite small lifetime of hyaluronan in different types of tissues. In the epidermis the lifetime of hyaluronan is about 20 minutes and in the cartilages the lifetime is about 9 days [7].

2.1.1 Structure of hyaluronan

Hyaluronan is a linear unbranched, high molecular weight, polar polysaccharide of the glycosaminoglycans class. Hyaluronan is composed of repeating polyanionic disaccharide units which consists of N-acetyl-D-glucoseamine and D-glucuronic acid linked by a β 1-4 glycosidis bond. The disaccharides are linked by β 1-3 bonds to form hyaluronan chains (Fig. 1) [8].

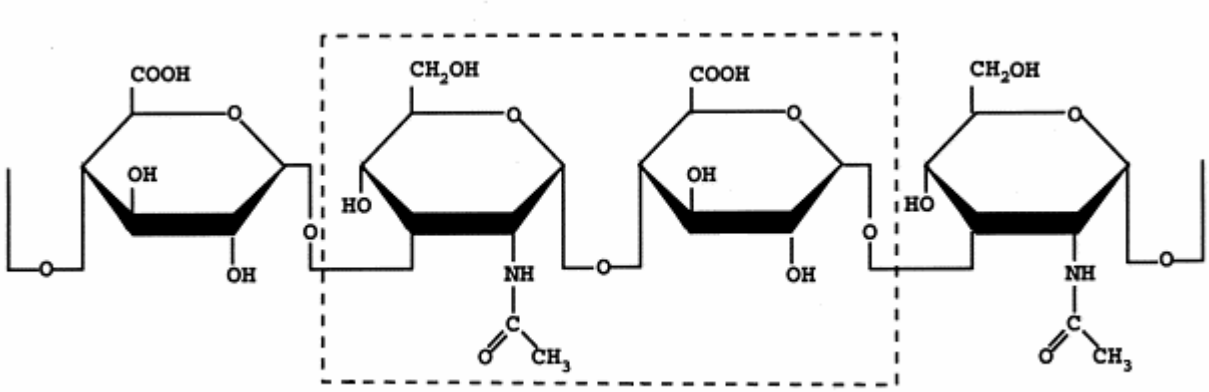

Fig.1 *The formula of disaccharide unit of hyaluronan*. [9]

Both sugar segments are spatially related to glucose (Fig.2) which in the *β* configuration allows all of its bulky groups (the hydroxyls, the carboxylate moiety and the anomeric carbon on the adjacent sugar) to be in sterically favorable equatorial positions while all of the small hydrogen atoms occupy the less sterically favorable axial positions. Thus, the structure of the disaccharide shown in the Fig. 2 is energetically very stable. [1]

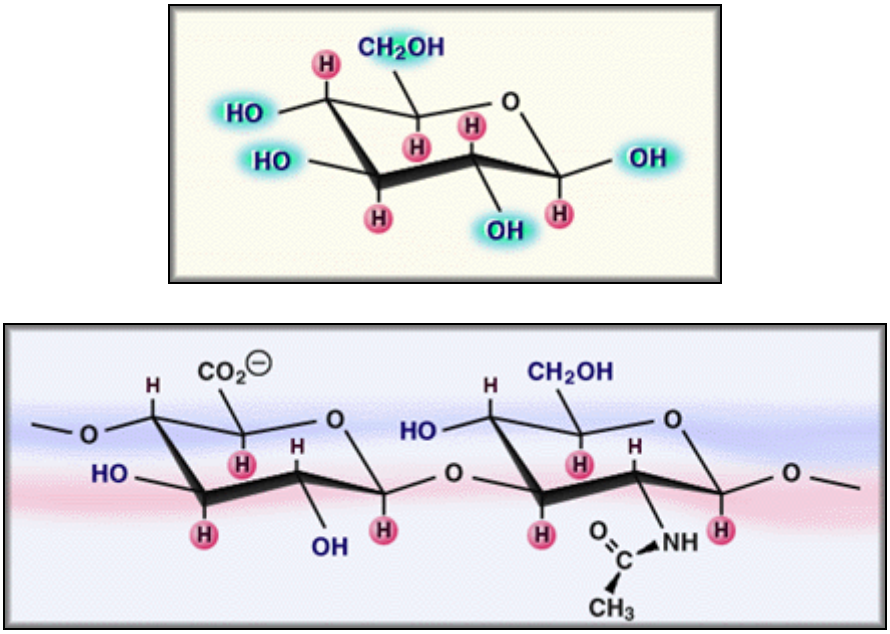

Fig. 2 *Relationship between beta-D-glucose and the repeat disaccharide of hyaluronan; pink H are axial hydrogens that contribute to the hydrophobic face.* [1]

Molecular models based on a combination of data with low resolution X-ray fiber results suggested that an extensive hydrogen-bonded structure was present in hyaluronan [10].

Nuclear magnetic resonance confirmed the presence of this ordered structure in solution, in which each disaccharide unit is twisted through 180 degrees compared with those ahead and behind it in the chain. Two twists (totaling 360 degrees) bring back the original orientation; hence this structure is a two-fold helix. Refined computer simulations suggested that water played an important part in stabilizing the structure [11].

This ribbon like structure shows gentle curves both in plan and elevation projections (Fig. 3), and these are important in determining how hyaluronan molecules can form duplexes with each other.

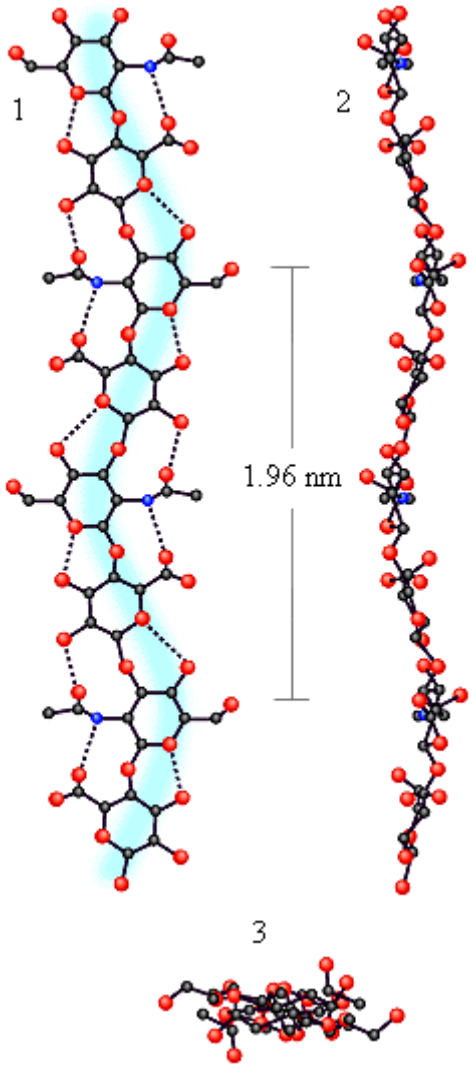

Fig. 3 *Plan (1) and elevation (2) of computer drawn projections of the ribbon like hyaluronan molecule. (3) is the view seen along the two fold helix axis. The N atoms are shown as blue circles.* [10]

The significance of this secondary structure (as distinct from the simple sequence of sugars which is the primary structure) became clearer when it was noticed that hyaluronan in the two-fold helix had an extensive hydrophobic patch, 1 of about 8 CH units, roughly the same size as octanoic acid (Fig. 4). Thus, hyaluronan has the properties of a highly hydrophilic material simultaneously with hydrophobic patches characteristic of lipids, i.e. it is amphiphilic.

Hydrophobic patches can have far-reaching implications for molecules in a water environment. Hydrophobic molecules clump together in water, thus reducing their interface with the solvent. This mechanism drives the formation of membranes, and contributes to the stability of e.g. the double helix in DNA. It is called hydrophobic bonding, although no chemical bond is formed.

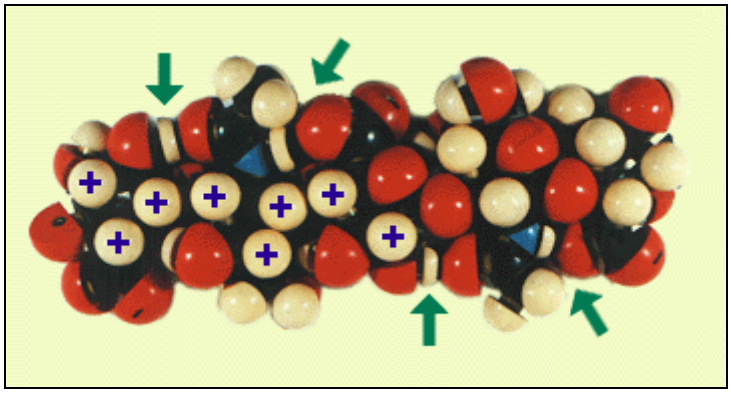

Fig. 4 *Model of a hyaluronan oligosaccharide. The H-bonds arrowed are between the acetamido and neighboring glucuronate units. The H atoms marked with a cross are part of a hydrophobic patch consisting of 8 CH groups.*

Hyaluronan also aggregates with itself, partly helped by bonding between the hydrophobic patches. The flat and tape-like secondary structure (Fig. 3) has fascinating properties; both sides are identical, but one side of the tape runs in the opposite sense to the obverse side; i.e. they are antiparallel. As a consequence of this, what is possible on one side of the tape is also possible on the other. Aggregates can grow from both sides [12].

Electrostatic repulsion between the many negative charges, which would promote dissociation of the aggregates, is countered not only by hydrophobic interactions but also by H-bonding between acetamido and carboxylate groups (Fig. 5). These very short range interactions demand close complementarity between the two participants, and this is best obtained when the hyaluronan interactants are antiparallel to each other (Fig. 5). Only then do the gentle curves in their shapes (Fig. 3) mutually complement each other, and hydrophobic and hydrogen bonding are then optimal.

Rotary shadowing-electron microscopy showed that honeycomb-like meshworks were formed at very low hyaluronan concentrations (1 μg/mL). High molecular mass hyaluronan meshworks at this concentration showed no molecular ends or tails. The meshworks were essentially infinite. Every hyaluronan molecule was connected with all the rest, via the

meshwork. On the contrary, although lower molecular weight hyaluronan formed meshworks at low concentrations, these meshworks were islands, separated from each other [11].

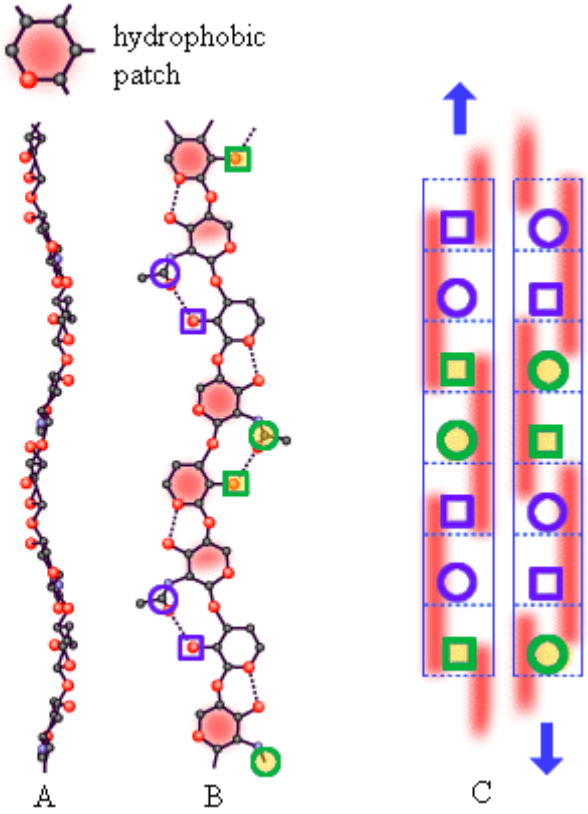

Fig. 5 *A and B are elevation and plan projections respectively of a hyaluronan molecule. The red patches in B are the hydrophobic patches stretching along three sugar units on alternate sides of the polymer chain. Circles represent acetamido and squares represent carboxylate groups. Only the most relevant atoms are shown in A and B. The N atoms are shown as blue circles (see Fig. 3 for complete structures). C is a scheme, seen in side view, of a possible duplex between two molecules of hyaluronan. The two participating molecules are antiparallel to each other. The dotted lines delineate each sugar unit. The red bars are the hydrophobic patches stretching along three sugar units, alternating between front and back of the polymer chain. The blue circles and squares are on the same edge of the molecule and of the duplex (see also B). The curves in each molecule, seen in A and B, closely follow the same course in the antiparallel arrangement so that the two molecules fit well together in the duplex. The hydrophobic patches then engage closely with each other and the acetamido and carboxylate groups are within H-bonding distances* [10], [11].

The interactions which hold meshworks together are fairly weak, so that aggregates form and dissociate, depending on conditions and temperatures. As the hyaluronan concentration increases, the meshwork contains thicker branches, until at concentrations seen, for example, in synovial fluids (less than 1 mg/mL) sheets and tubes of striking morphology are observed by rotary shadowing electron microscopy. The important point is that these meshworks are ordered. The shapes of the hyaluronan secondary structures determine the shapes of the aggregates, and each branch in the meshwork of ambidexterans carries with it two clear

intrinsic directions up or down, established by the hyaluronan chains. This may have organizational consequences, for instance, in guiding morphogenesis.

Chang, Boackle and Armand [13] discovered that hyaluronan was a potent inhibitor of complement activated lysis of red blood cells, but only in a 'denatured' form. Hyaluronan solutions prepared and maintained at ambient temperatures were almost devoid of this activity, but by heating to 100°C and then snap freezing to capture the 'denatured' form, the solution acquired inhibitory power. If it was cooled slowly the hyaluronan had time to 'renature' and the product was a poor inhibitor. Thus, hidden or locked-up biological properties of hyaluronan in solutions at moderate concentrations may be liberated by processes which break up hyaluronan aggregates.

Hydrophobic patches are used during interactions with receptor CD44, bonding proteins of proteoglycans and bonding phospholipids of cell membrane.

2.1.2 Function and occurrence of hyaluronan

Hyaluronan is almost omnipresent however it occurs primarily in the extracellular matrix (ECM) and pericellular matrix, although recently it has been shown to be present intracellularly [14], in the vitreous humour, in the umbilical cords and in the synovial fluid. The hyaluronan together with heparin sulphate comprise the major fraction of the vertebrate ECM [15]. In some case hyaluronan can make a simple ECM in the virtual absence of other macromolecules, e.g., around the ovum and developing embryo [16]. The ECM is comprised of structural proteins, specialized proteins and proteoglycans.

Proteoglycans are found predominantly in the connective tissue and cartilage, a specialized form of connective tissue. The tissue supports and bins other tissues and organs. The proteoglycans within the hyaline cartilage are shaped like a bottle brush, with hyaluronic acid making up the backbone of the brush. Without the strength of the backbone, the proteoglycan falls apart, leaving the cartilage to deteriorate. The cartilage is avascular, as it contains no blood vessels. It is unable to be fed its needed supply of nutrients by the blood. It must be fed by the synovial fluid. The synovial fluid is produced within the synovial membrane and secreted to the extracellular space. Its main function is to act as a lubricant for the joints as it sits within the joint cavities. It also provides nutrients to the joints and the surrounding cartilage, as well as removes the metabolic waste produced by the cartilage [17].

In ECM there is huge amount of water trapped by proteoglycans which are in conjunction with hyaluronan. It is caused by the hydrogen bond formation which results in the unique water-binding and retention capacity of the hyaluronan. It also follows that the water-binding capacity is directly related to the molecular weight of the hyaluronan. Due to this unique property is hyaluronan used in pharmacy, cosmetics and plastics surgery.

Hyaluronan plays important role in wound healing where normalizes cell migration and proliferation. For example after the wounding of skin, the level of hyaluronan within the skin accumulates dramatically. Hyaluronan regulates the rate of epidermal proliferation and differentiation, both during normal homeostasis in the skin as well as after cutaneous injury [18].

Furthermore hyaluronan is involved in tumor progression. In some cancers hyaluronan levels correlate well with malignancy. Hyaluronan is thus often used as a tumor marker. It may also be used to monitor the progression of the disease. Moreover in clinical medicine is hyaluronan used as a marker for other diseases as rheumatoid arthritis and liver pathologies [5].

Due to its high biocompatibility, biodegradability and its common presence in the extracellular matrix of tissues, hyaluronan is gaining popularity as a biomaterial scaffold in tissue engineering research. There are other several types of medical applications of hyaluronan: ophthalmology, orthopedic surgery and rheumatology, otolaryngology, dermatology, endoscopic mucosal resection, cataract surgery, osteoarthritis, pharmacology and drug delivery, postoperative adhesions and so on [19].

2.1.3 Production of hyaluronan

Hyaluronan has been traditionally extracted from rooster combs and bovine vitreous humor etc, generally from the tissues abundant in the hyaluronan. For awareness of it some of them are mentioned in Tab. I. It is difficult to isolate high molecular weight hyaluronan economically from these sources because it forms a complex with proteoglycans [20].

Table I.: Occurrence of hyaluronan in different animal tissues and its content [5]

Tissue or body fluid	Concentration (μg/ml)	Remarks
Rooster comb	7500	The animal tissue with by far the highest hyaluronan content.
Human umbilical cord	4100	Contains primarily hyaluronan with a relatively high M_w.
Human joint (synovial) fluid	1400–3600	The volume of the synovial fluid increases under inflammatory conditions. This leads to decreased hyaluronan concentration.
Bovine nasal cartilage	1200	Often used as a cartilage model in experimental studies.
Human vitreous body	140–340	Hyaluronan concentration increases upon the maturation of this tissue.
Human dermis	200–500	Suggested as a 'rejuvenating' agent in cosmetic dermatology.
Human epidermis	100	Hyaluronan concentration is much higher around the cells that synthesize hyaluronan.
Rabbit brain	65	Hyaluronan is supposed to reduce the probability of occurrence of brain tumors.
Rabbit heart	27	Hyaluronan is a major constituent in the pathological matrix that occludes the artery in coronary restenosis.
Human thoracal lymph	0.2–50	The low M_w of this hyaluronan is explained by the preferential uptake of the larger molecules by the liver endothelial cells.

Human urine	0.1–0.3	Urine is also an important source of hyaluronidase.
Human serum	0.01–0.1	Hyaluronan concentrations increase in serum from elderly people as well as in patients with rheumatoid arthritis and liver cirrhosis.

It is presently impractical to control the molecular weight of the biopolymer while it is synthesized in animal tissue and it is limited by maximum molecular weight 2.5 MDa [5]. Subsequent extraction and purification processes result in an inherent molecular weight reduction. From a social viewpoint, the use of animal-derived biochemicals for human therapeutics is being met with growing resistance, besides ethical arguments, because of the risk of viral infection.

However, because the value of the product was high and the demand increasing there was an interest in developing further production way. The use of bacteria known to produce hyaluronan was an obvious option. Another reason of this way is clear away the problems with contamination with proteins because bacteria have not enzymes for synthesis of proteoglycans.

Thus industry has instead turned to bacterial fermentation processes. It was concluded that the presence of hyaluronan is a common trait in Streptococci. [21]. Group C streptococci (Streptococcus aqui and Streptococcus zooepidemicus) produce extracellular hyaluronan apparently identical in chemical structure to that obtained from eukaryotic material.

This production has a good yield during the growth phase but during the stationary phase it was often degraded by a hyaluronidase [21]. Hence mutants lacking hyaluronidase have been developed to ensure that degradation of the high molecular weight polymer does not occur [4]. Nowadays it is used continues culture production in chemostat.

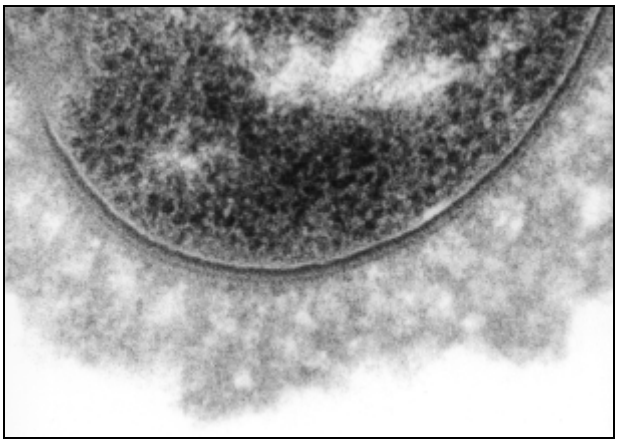

Fig.6 *Extracellular production of hyaluronan, Streptococcus zooepidemicus with hyaluronan capsules* [22].

2.2 Structure of water

Liquid water is an absolute requirement for all active life. It is the most important nutrient throughout the living world. In particular, we cannot live without it for more than about 100 hours, whereas other nutrients may be neglected for weeks or months. Although commonly it is treated rather trivially, no other nutrient is more essential or needed in as great amounts. Liquid water is required for life to start and for life to continue. No enzymes work in the absence of water molecules.

Water plays many roles within the body; as a media for, and contributor to, molecular interactions; as a solvent and separating medium, to carry and distribute nutrients, metabolites, hormones and other materials around the body and within cells; to remove waste products, mainly via the urine and feces; as a reactant in many metabolic reactions; as a thermoregulator due to its high specific heat and heat of evaporation; as a lubricant between bodily structures and in forming mucous as well as facilitating necessary structural shifts in macromolecules such as proteins and nucleic acids; as a structure-former, maintaining cellular shape; and as a protective shock absorber, for example, for the brain [23].

The hydration of molecules follows from the structure of water and its behavior in solution. In the water molecule the oxygen nucleus with +8 charges attracts electrons better than the hydrogen nucleus with its +1 charge. Hence, the oxygen atom is partially negatively charged and the hydrogen atom is partially positively charged. The hydrogen atoms are not only covalently attached to their oxygen atoms but also attracted towards other nearby oxygen atoms. This attraction is the basis of the 'hydrogen' bonds (Fig. 7).

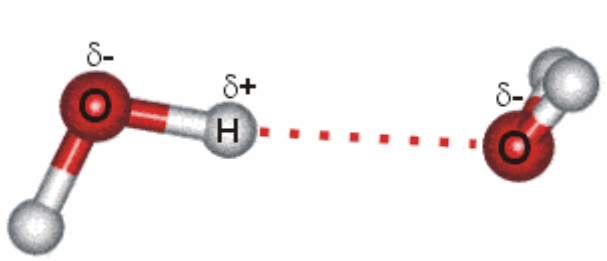

Fig. 7 *The hydrogen bond.*

The water hydrogen bond is a weak bond, never stronger than about a twentieth of the strength of the O-H covalent bond. The attraction of the O-H bonding electrons towards the oxygen atom leaves a deficiency on the far side of the hydrogen atom relative to the oxygen atom. The result is that the attractive force between the O-H hydrogen and the O-atom of a nearby water molecule is strongest when the three atoms are in a straight line (that is, O-H···O) and when the O-atoms are separated by about 0.28 nm. Each water molecule can form two hydrogen bonds involving their hydrogen atoms plus two further hydrogen bonds utilizing the hydrogen atoms attached to neighboring water molecules. These four hydrogen bonds optimally arrange themselves tetrahedrally around each water molecule as found in ordinary ice. In liquid water, thermal energy bends and stretches and sometimes breaks these hydrogen bonds. However, the average structure of a water molecule is similar to

this tetrahedral arrangement. The Fig.8 shows such a typical average cluster of five water molecules.

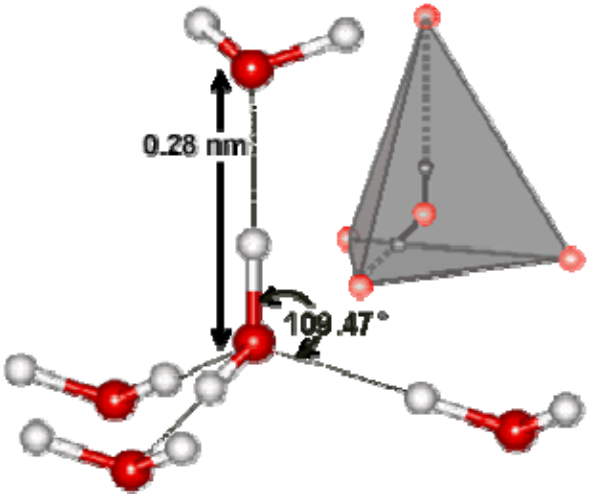

Fig.8 *The cluster of five water molecules in tetrahedrally arrangement.*

In liquid water, the tetrahedral clustering is only locally found and reduces with increasing temperature. In ice this tetrahedral clustering is extensive, producing its crystalline form. The stronger the bonds, the more ordered and static is the resultant structure. The energetic cost of the disorder is proportional to the temperature, being smaller at lower temperatures. This is why the structure of liquid water is more ordered at low temperatures. This increase in orderliness in water as the temperature is lowered is far greater than in other liquids, due to the strength and preferred direction of the hydrogen bonds.

In ice there is the clustering during producing of crystalline form more extensive. There are several types of ice which differ in arrangement of water molecules. We distinguish twenty types of ice which differ in various ambient conditions during their formation (pressure and temperature). Many of the crystalline forms may remain metastable in much of the low-temperature phase space at lower pressures [24].

2.3 Hydration of biopolymers

2.3.1 Polysaccharides hydration

Hydration is a general term concerning the amount of bound water. It has been defined as 'non-bulk' water. Using a simplistic approach to polysaccharide hydration, water can be divided into 'bound water', [25] subcategorized as being capable of freezing or not, and 'unbound water', subcategorized as being trapped or not. 'Unbound' water freezes at the same temperature as normal water (less than 0°C dependent on cooling rate). However some water may take up to 24 hr to freeze. 'Bound freezable' water freezes at a lower temperature than normal water, being easily supercooled. It also exhibits a reduced enthalpy of fusion (melting). Although the inability to freeze is often used to determine bound water, freezing may not a good measure of hydration as it concerns the water content of the glassy state; not aqueous hydration.

In the glassy state the viscosity is extremely high (more than 1012–1013 Pa s), conformational changes are severely inhibited and the material is metastably trapped in a solid but microscopically disordered state. The segmental motion of macromolecules occurs when the temperature increases through the glass transition temperature. The value of T_g (temperature of the glass transition) depends somewhat on the method of its determination; the glass transition, unlike phase changes, occurring over a range of a few Kelvin.

For recognition of the type of water is determined by freezing and melting calorimetry using the enthalpy of the phase change and thermogravimetry, measuring the weight changes due to absorption from set humidity atmospheres. However, non-freezing water may be trapped in a glassy state, lowering diffusion by several orders of magnitude and hindering crystal formation.

In practical experience, the effects of water on polysaccharide and polysaccharide on water are complex and become even more complex in the presence of other materials, such as salts. Water competes for hydrogen bonding sites with intramolecular and intermolecular hydrogen bonding, certainly will determine the carbohydrate's flexibility and may determine the carbohydrate's preferred conformation(s) [26].

2.3.2 Hyaluronan hydration

Hyaluronan is naturally occurring in a living organism, thus the behavior in the ambience condition approximately similar to the living organism (e.g. physiological solution) is significant. In a physiological solution, the backbone of a hyaluronan molecule is stiffened by a combination of the chemical structure of the disaccharide, internal hydrogen bonds and interactions with solvent. The axial hydrogen atoms (Fig. 2) form a nonpolar, relatively hydrophobic face while the equatorial side chains form a more polar, hydrophilic face, thereby creating a twisting ribbon structure. Consequently, a hyaluronan molecule assumes an expanded random coil structure in physiological solutions which occupies a very large domain (Fig. 9). The actual mass of hyaluronan within this domain is very low, about 0.1 % (w/w) or less when the macromolecule is present at a very dilute concentration in saline solution. This means that the domains of individual molecules would overlap each other at concentrations of 1 mg hyaluronan per mL or higher.

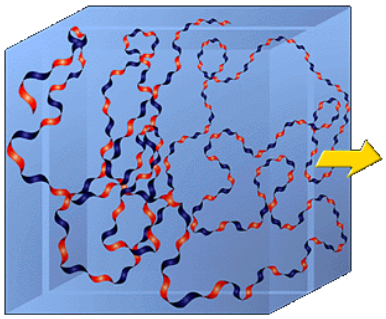

Fig.9 *Model of hyaluronan ribbon in a 3-dimensional domain. The light blue box represents the domain of the molecule in solution. The alternating blue and red strand represents the ribbon structure with blue (hydrophilic) and red (hydrophobic) faces* [1].

The domain structure of hyaluronan has interesting and important consequences. Small molecules such as water, electrolytes and nutrients can freely diffuse through the solvent within the domain. However, large molecules such as proteins will be partially excluded from the domain because of their hydrodynamic sizes in solution. As shown in Fig. 10, the hyaluronan network in the domain allows less and less space for other molecules the larger they are.

This leads both to slower diffusion of macromolecules through the network and to their lower concentration in the network compared to the surrounding hyaluronan free compartments. Interestingly, the hyaluronan chains are constantly moving in the solution, and the effective 'pores' in the network continuously change in size. Statistically, all sizes of pores can exist, but with different probabilities.

This means that in principle, all molecules can pass through a hyaluronan network, but with different degrees of retardation depending on their hydrodynamic volumes.

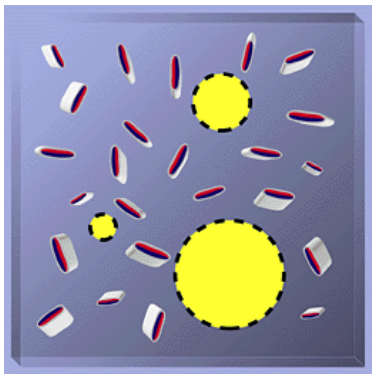

Fig. 10 *Vertical slice from Fig. 9 illustrating average pore size and partial exclusion of large molecules. The red and blue are tracings of regions in Fig. 3 representing portions of the hyaluronan backbone in the representative slice. The fuzzy halo (shading) around the hyaluronan fragments would be the volume of the slice inaccessible to a diffusing molecule. The 3 circles of different size represent areas available to diffusing molecules. The smallest would have access to most of the volume not occupied by hyaluronan while the largest would have access only to the place where it is located and would clearly have a harder time moving through the hyaluronan domain (Fig. 9) than the smaller ones* [1].

3 METHODS AND MEASUREMENTS

3.1 Differential Scanning Calorimetry (DSC)

Differential scanning calorimetry (DSC) belongs to the group of thermoanalytical methods, which are defined as a group of techniques in which a property of the sample is monitored against time or temperature while the temperature of the sample, in a specific atmosphere, is programmed. The programme may involve heating or cooling at a fixed (or variable) rate of temperature change, or holding the temperature constant, or any sequence of these. The basic theories to be used in thermal analysis are equilibrium and non-equilibrium thermodynamics and kinetics [27]. These measurements provide quantitative and qualitative information about physical and chemical changes that involve endothermic processes, heat flow into the sample, or exothermic processes, heat flows out of the sample, or changes in heat capacity which is a glass transition.

The first commercial DSC instrument was introduced by Watson and his co-workers at Perkin Elmer (Model DSC-1) in 1964 [28]. Watson, et al., also appears to be the first to have used the nomenclature differential scanning calorimetry. Their instrument, a power-compensating DSC (Fig. 12), maintained a zero temperature difference between the sample and the reference by supplying electrical energy (hence, the term power-compensation) either to the sample or to the reference, as the case may be, depending on whether the sample was heated or cooled at a linear rate. The amount of heat required to maintain the sample temperature and that of the reference material isothermal to each other is then recorded as a function of temperature. Moreover, in power-compensation DSC, an endothermic transition, which corresponds to an increase in enthalpy, is indicated as a peak in the upward direction (since power is supplied to the sample), while an exothermic transformation, a decrease in enthalpy, is shown as a negative peak [29].

Essentially the heat-flux type (Fig. 11) of DSC measures the difference in temperature between the sample and reference as a function of time, and since the temperature varies linearly with time, as a function of temperature as well. The heat-flux is actually derived from a combination of the ΔT (t) curve and the $d\Delta T(t)/dt$, both of these are transparent to the user since the electronics used yield a direct heat flux value from these terms. An endothermic signal is in the negative direction, while an exothermic signal is the upward direction [29].

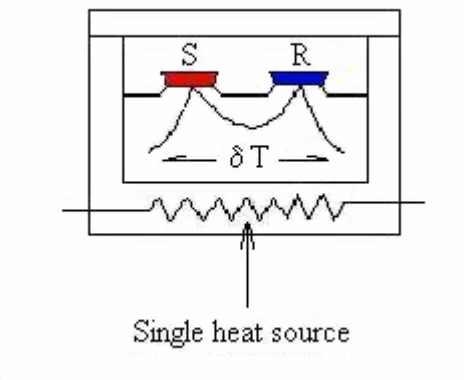

Fig. 11 *The heat flux arrangement.*

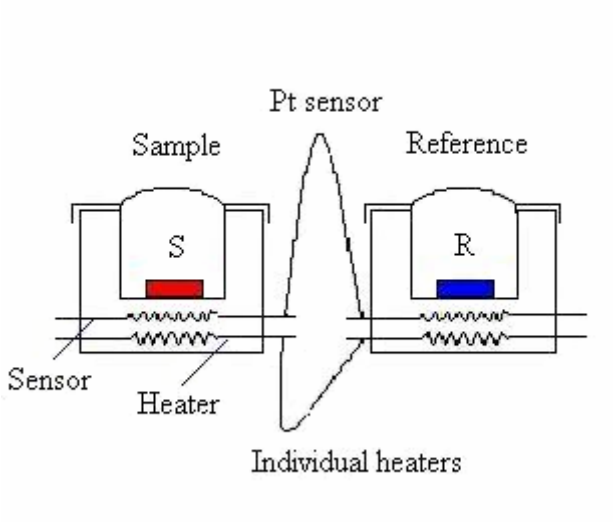

***Fig 12**. The power compensation arrangement.*

Both the heat-flux DSC and power-compensation DSC have their advantages and disadvantages, but, the end result is the same, the two will yield the same information. The advantage of the heat-flux type is that it can accommodate larger sample volumes, has a very high sensitivity, and can go above 1100 K. The disadvantage is that it cannot be scanner at rates faster than 10 K min^{-1} at high temperatures and not faster than 3 K min^{-1} at sub ambient temperatures. The main advantage of the power-compensation calorimeter is that it does not require a calibration in that the heat is obtained directly from the electrical energy supplied to the sample or reference compartment (a calibration is still necessary, however, to convert this energy into meaningful units) and that very fast scanning rates can be obtained. The disadvantage of this system is that the electronic system must be of extremely high sensitivity and large fluctuations in the environment must be absent so as to avoid compensating effects which are not due to the sample. Also, the complexity of the electronics prevents the system from being used above 1100 K [29].

3.1.1 DSC in biomolecules hydration study

DSC method has been already used by Hatakeyama H. where phase transition behavior of water of hyaluronan was investigated in a wide range of water contents. The samples were heated at 10 K min^{-1} after cooling from 330 to 150 K at a cooling rate of 10 K min^{-1}. The sample with concentration 0.5 (g/g) did not show any phase transition except for a shift in the baseline due to glass transition (T_g) [30], [31], [32].

The heat capacity difference at T_g of water-hyaluronan system is particularly large among various water/polyelectrolyte polysaccharide systems. A characteristic feature of the glassy state of hyaluronic acid is explained by a large amount of amorphous ice which is formed during the quenching process in the network structure. From a plot of water-hyaluronan systems T_g decreases markedly until concentration 1.0 (g/g), and reaches a minimum at around concentration 1.1 (g/g) [33], [34].

The melting curves of hyaluronan-water systems show the multiple peaks having a shoulder at the low temperature side of the main peak. It was plotted a dependence which shows the relationship between starting temperature, peak temperature of sub-melting, the melting peak

and temperature of crystallization. Peak temperature of sub-melting and starting temperature of melting linearly increase with increasing temperature of crystallization. In contrast, peaks temperatures of melting are maintained at a constant value. This indicates that melting of irregular ice formed in the hyaluronan network is observed at the lower temperature side peak [35].

Isothermal crystallization of hyaluronan having various concentrations was carried out at different temperatures [36]. It was found that the rate of nucleation of water in hyaluronan gel was almost the same as bulk water. In contrast, the rate of crystal growth of freezing bound water was about 10 times slower than that of bulk water.

This method has been also used for investigation of water interaction with hylan, the formaldehyde cross-linked derivative of hyaluronan. It was likewise observed three types of water, non-freezing, freezing-bound and free water. When the water content of the system is increased, even by up to 10 %, almost all the water remains in the freezing-bound state, with a enthalpy value less than free water. Several metastable states of water can be detected within the structured hylan-water matrix, indicative of defects in the frozen-bound ice structure. The maximum amount of non-freezing water, intimately associated with the hydrophilic groups of hylan, corresponds to 13 mol water per disaccharide unit of the hyaluronan chain. The large capacity shown by hyaluronan entangled networks to build water into their structure could also be responsible for their unusually high viscosity and elasticity after the onset of entanglement. Such viscoelastic properties are the basic for their use in viscosupplementation of arthritic diseased joints [36].

That methods was also successfully used to study hydration of other biopolymers and polymers such as cellulose [37], lignin [38], gellan gum [39], xanthan gum [40], agarose [41], arabic gum [42], [43] carboxymethylcellulose [44], alginic acid [45] poly(vinyl alkohol) [46], sodium cellulose sulphate [3], sodium polystyrene sulphate [3].

3.2 High Resolution Ultrasonic Spectrometry (HRUS)

Ultrasonic spectroscopy is simply spectroscopy employing sound waves. The general principle of this method is measurement of parameters from ultrasonic waves propagating through samples. In particular, it uses high frequency acoustical waves which are synthesized electronically (Fig. 13).

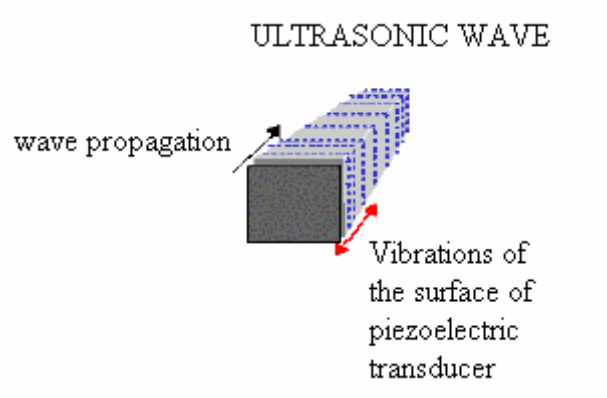

Fig.13 *The general principles of propagation of ultrasonic wave.*

The generated electronic signal is transferred by the piezotransducer into the ultrasonic wave traveling through the sample. Another piezotransducer transfers the received ultrasonic wave into an electronic signal for subsequent analyses (Fig 14).

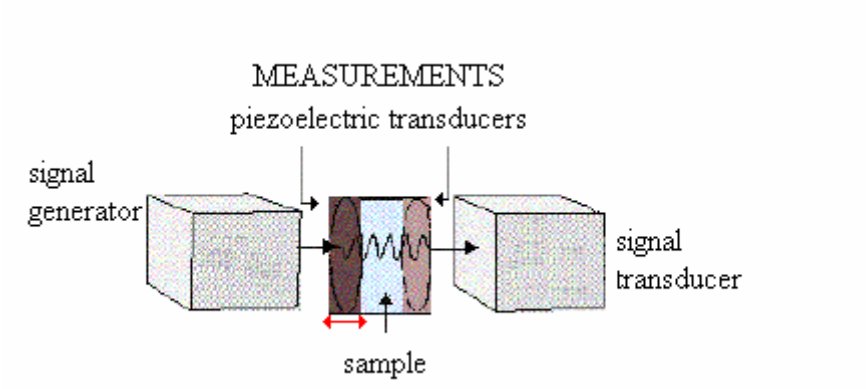

Fig. 14 *Passing wave through the sample.*

The wave probes intermolecular forces in materials. This method is fast and non-destructive. It is possible to use it for a wide spectrum of properties of materials [47].

Ultrasonic wave can caused compression and decompression in the sample. In the phase of compression, molecules are compressed which causes repulsion among them and vice versa. (Fig. 15)

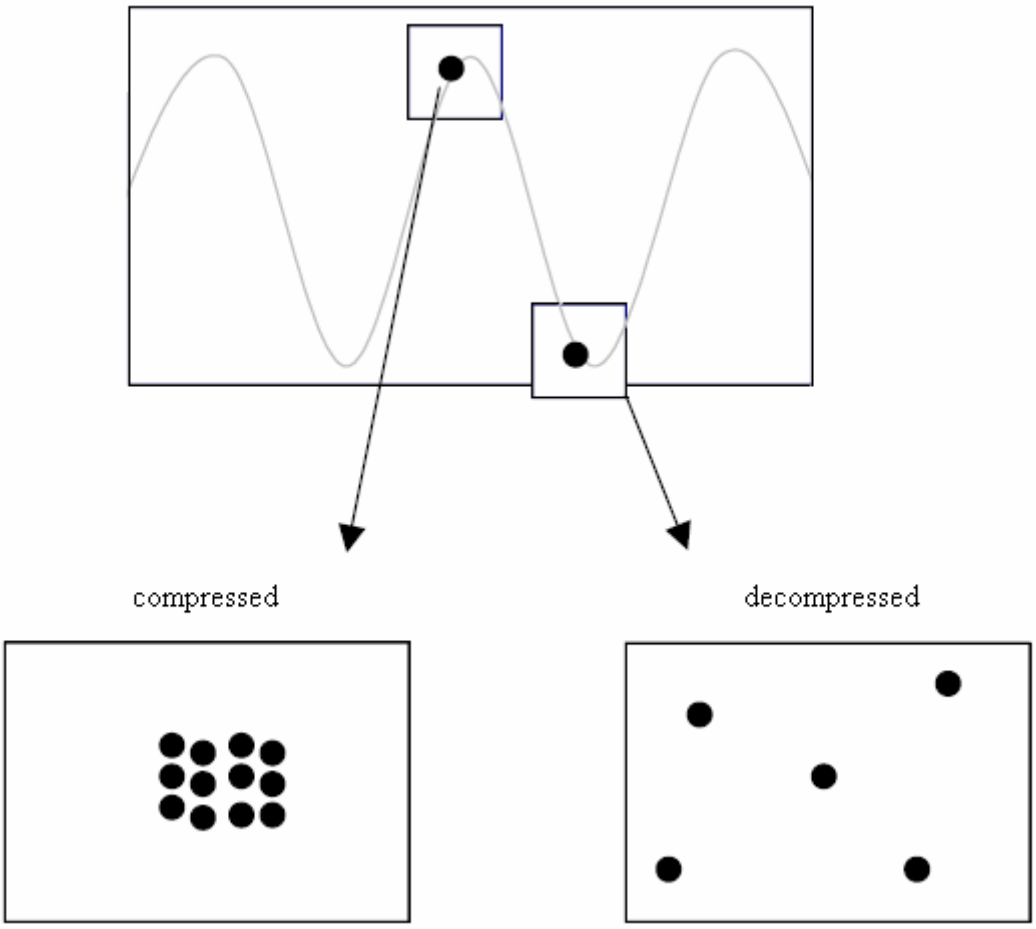

Fig. 15 *The behavior of molecules during the passing of ultrasonic wave.*

The two major parameters measured in HRUS are the attenuation and the velocity of the ultrasonic waves. The ultrasonic attenuation is determined by the energy losses in the ultrasonic propagating through the sample (Fig. 16). The peak produced is what is analyzed. The ultrasonic attenuation is calculated from the bandwidth (the width of the peak, measured across a point equal to the maximum amplitude divided by the square root of 2) at which this peak occurs. Ultrasonic attenuation characterizes the ultrasonic transparency of the analyzed sample and can be seen as a reduction of the amplitude of the wave.

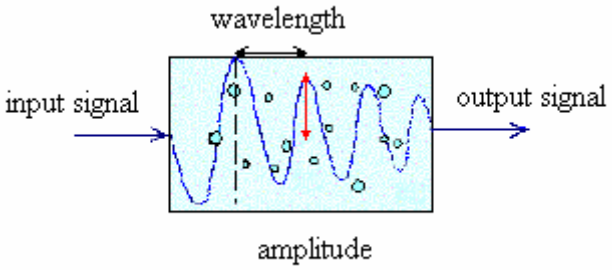

Fig. 16 *The parameters of ultrasonic wave.*

Ultrasonic velocity is determined by the density and the elasticity of the medium. This is extremely sensitive to the molecular organization and intermolecular interactions in the sample. The peak which is produced is again analyzed. The ultrasonic velocity is calculated from the frequency at which this peak occurs.

How it was mentioned above, the ultrasonic velocity depends on density and elasticity of sample. For example solids have the strongest interaction between the molecules, followed by liquids and gases. Solids are more rigid compared with liquids and gases, for this reason the sound travels faster in solids than in liquid and gases. There are big differences in density of solids, liquids and gases but the same principle is valid in liquids with different density. The only divergence from previous example is smaller differences in ultrasonic velocity (Fig. 17).

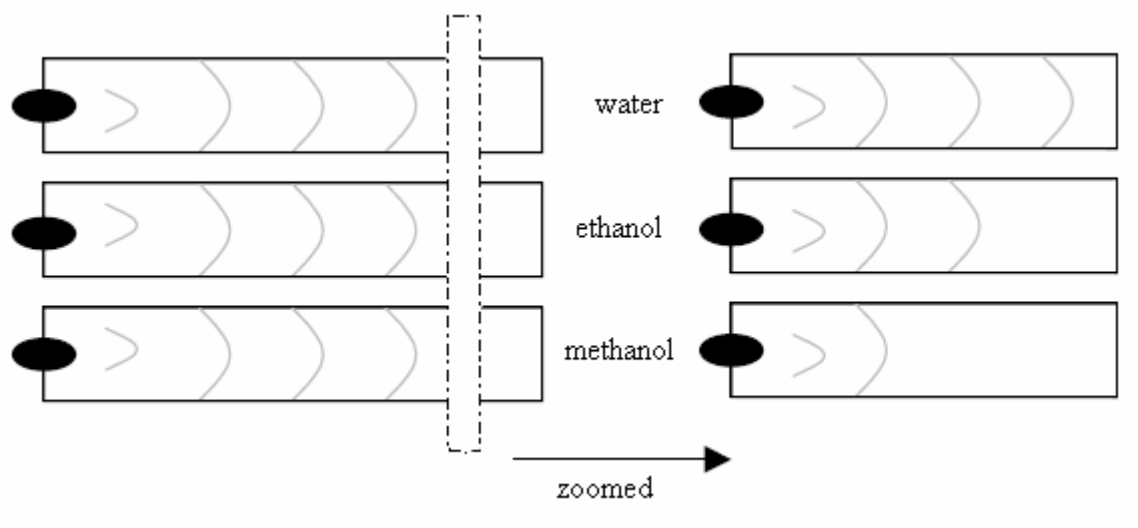

Fig. 17 *Different liquids have a characteristic ultrasonic velocity.*

HRUS can be use also for recognition of formation of gel or micelle because change in ultrasonic velocity detects the formation of a micelle because of highly compressible micellar hydrophobic core and a change in velocity detects the formation of the gel because of the rigidity of the network (Fig. 18).

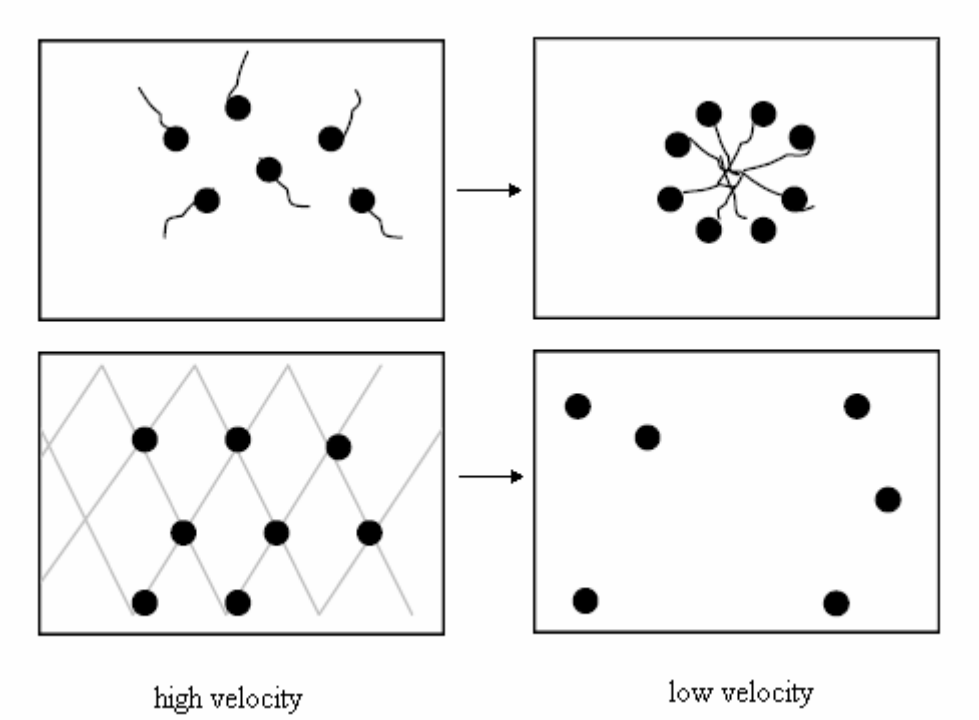

Fig.18 *Mmicelle and gel formation* [47]

3.2.1 (HR)US in evaluation of biomolecules hydration

Ultrasonic velocity and density measurement has been already used to study hyaluronan of hyaluronan solution. It was measured interferometrically relative to the velocity of sound through water at 25°C, i.e. 1496.58 + 0.04 m s^{-1}. Ultrasonic velocity was measured at 2, 3 and 4 MHz, and then averaged. A sound-velocity-temperature profile of water in the range 20–50°C was obtained [48].

US has also been used in wide range of biomolecules investigation. For example Hickey S. applied US to analyze of a pseudoternary phase diagram for mixtures consisting of water/isopropyl myristate/Epikuron 200 and a cosurfactant (n-propanol) [49]. Furthemore Kharakoz D.P. [50] and Buckin V.A. [51] have analyzed the physical nature of changes in the compressibility in the hydration shell of charged, polar and hydrophobic functional groups of biopolymers and low-molecular-weight solutes. Furthermore data on the density and compressibility of solutions and apparent volumes of biological and related organic solutes are discussed in many scientific journals [52], [53], [54].

Recently HRUS was used for real-time ultrasonic method for prion protein detection using plasminogen as a capture molecule. It was found out that the plasminogen coated beads bind selectively to prion proteins and HRUS system can discriminate between scrapie affected and nonaffected samples and thus has potential as a tool for the rapid diagnosis for prion diseases. [55].

4 THE AIM OF THE WORK

The aim of this work was to study the hydration of hyaluronan using different approaches and techniques, including DSC and HRUS. That generally means to verify and to try out couple of physical-chemical methods which seem to be, from different points of view, useful for the determination and enumeration of different types of water which are affected by the presence of hyaluronan molecules in a water solution. For this purpose five different molecular weights of hyaluronan were studied under different conditions. Such approach should shed light on the hydration aspects of hyaluronan, potential interrelationships and problems appearing when the only analytical method is used.

5 EXPERIMENTAL PART

5.1 Samples

Hyaluronan, isolated from Streptococcus zooepidemicus, was obtained from CPN Company (Dolní Dobrouč, Czech Republic). Five molecular weight of hyaluronan were used as follows: 100.1 kDa, 253.9 kDa, 522.1 kDa, 740 kDa and 1390 kDa. These molecular weight fractions were obtained after acid hydrolyses which were carried out in the microwave reactor.

The above mentioned molecular weights were collected employing the High Performance Size Exclusion Chromatography followed by infra red drying. By means of thermogravimetry (TA Instruments, Q5000IR) it was determined an equilibrium moisture content to obtain more precise results.

5.1.1 Low water content

Hyaluronan was placed in an aluminum pan. Excess of water was added to hyaluronan samples. Surplus water was allowed to evaporate slowly until the desired water content was obtained at room temperature. The pans were subsequently hermetically sealed and left to equilibrate at room temperature overnight.

Water content (W_c) was defined as follows: $W_c = \frac{\text{grams of water}}{\text{grams of dry sample}}$ (g/g) the obtained W_c were: 0.5, 0.75, 1.0, 1.5, 2.0, 2.5, 3.0 (g/g).

5.1.2 High water content

Hyaluronan samples were dissolved in milli-Q water. The hyaluronan concentrations was 0.1 %, 0.5 %, 1 %, 1.5 %, 2 %, 2.5 %, 3 % (w/w). The solutions were slowly mixed by a magnetic laboratory stirrer over a period of 24 hours to obtain perfectly dissolved and homogeneous hyaluronan sample.

5.2 DSC measurement

Differential scanning calorimetry was performed using the TA Instruments DSC Q200, equipped with a cooling accessory, and TA Universal Analysis 2000 software. Samples of approximately 10 mg (weighted to an accuracy of ± 0.01mg) were placed in hermetically sealed aluminum sample pans (TA Instruments, T-zero technology).

High water content samples were measured immediately, to avoid condensation of water on the pan lid, which can occur if the sealed samples are stored in the cold before use. Low water content samples were measured the next day after the preparation. The thermal protocols used were as follows: equilibrate at 40.0°C; isothermal at 40.0°C for 2 min; cooling from 40.0°C to –90.0°C at 3.0°C min^{-1}; isothermal at –90.0°C for 2.0 min; heating from –90.0°C to 30°C at 3.0°C min^{-1}. The lower temperature –90.0°C was chosen to ensure that all freezable water was frozen.

5.3 HRUS measurement

For monitoring of ultrasonic velocity HRUS 102 device (Ultrasonic-Scientific, Dublin, Ireland) was employed. It consists of two independent quartz cells tempered by a water bath; cell 1 serves as a sample cell and cell 2 as a reference. Measurements were set up at 25°C ± 0.02°C. The temperature ramp from 2°C up to 60°C, heating rate was 0.25°C min^{-1}under constant stirring (600 rpm) and at ultrasound frequencies of 5.478, 7.850, 8.219 and 12.196 MHz was used. This measurement arrangement was used for samples with high water content.

6 RESULTS AND DISCUSSION

6.1 Low water content

Representative DSC cooling and heating curves of hyaluronan hydrogels with different W_c are given in Fig.19 (for further concentrations reported in Fig.20–Fig.25 see appendix). The sample shown is 253 kDa hyaluronan with W_c 0.5–3.0 (g/g).

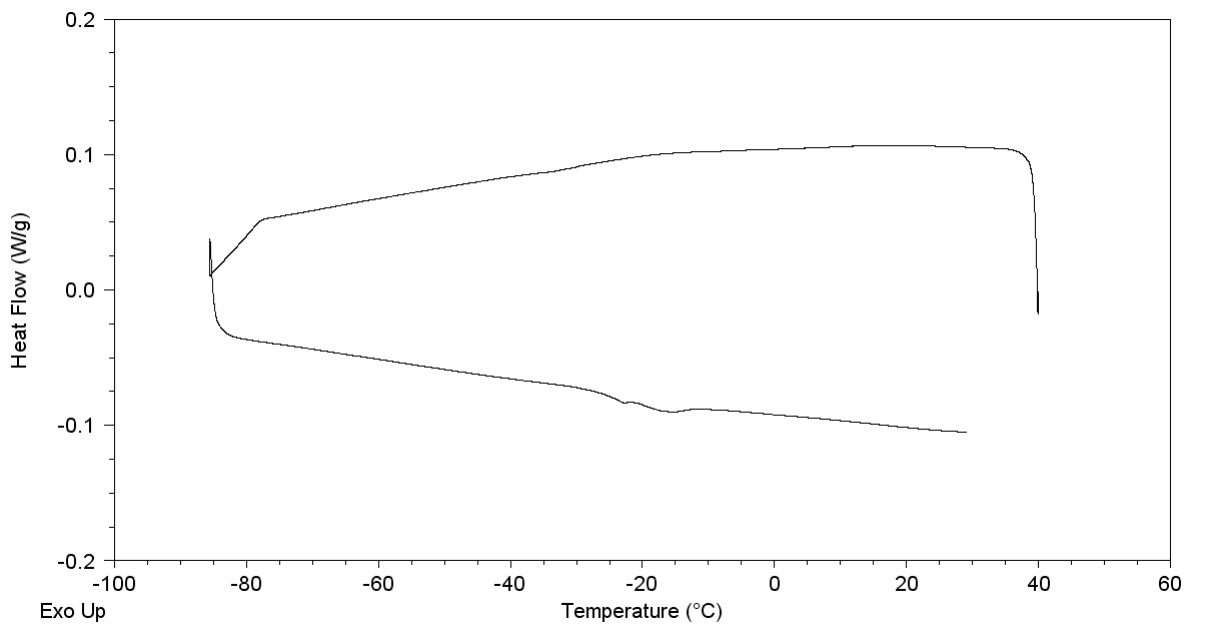

Fig. 19 *a) Cooling and heating curves for hyaluronan hydrogel of W_c 0.5.*

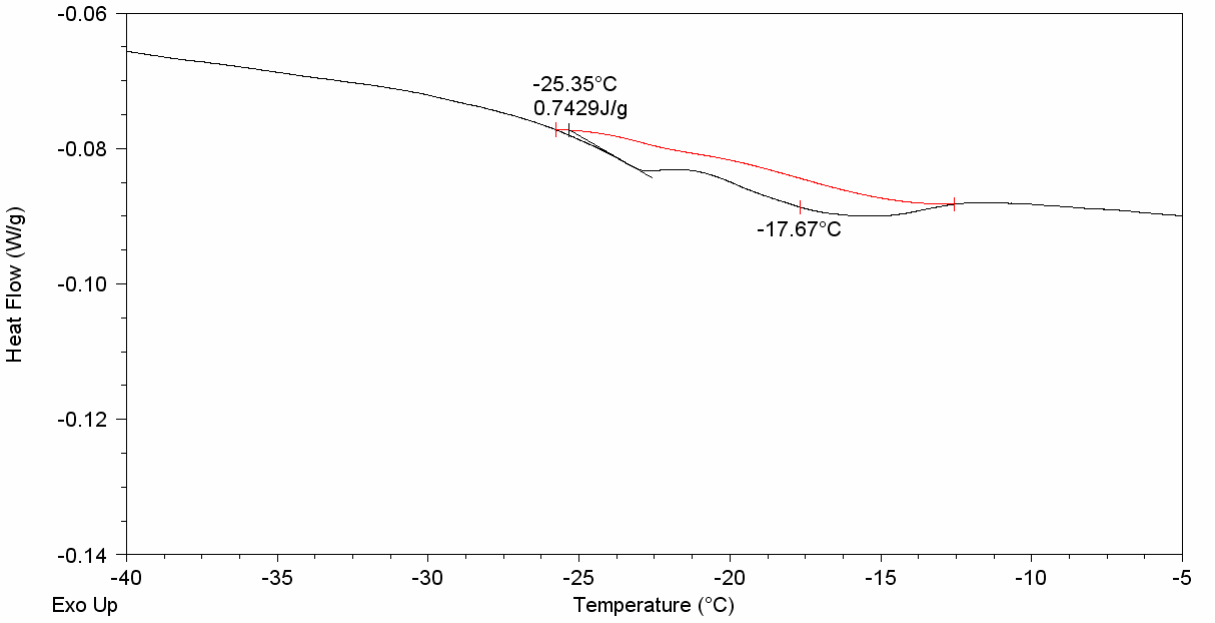

Fig. 19 *b) Expanded view of the melting endotherm portion of the curves shown above. The transition temperatures and enthalpy are as shown.*

Hyaluronan hydrogels with W_c 0.5 (Fig. 19), which after preparation looked like a stiff sheet, showed almost infinitesimal fusion endothermic peak on heating curves. Nearly all water molecules are present in the form of non-freezing water in this system, and a slight amount of water molecules are present in the form of freezing-bound water which caused the observed endothermic fusion peak. Hyaluronan hydrogels with W_c 0.75 showed more distinct endothermic fusion peak on heating curves. Shoulders which can be identified in this peak are possibly caused by the overlapping of different peaks which reflects the presence of several different types of freezing-bound water. Since cubic structure of freezing-bound water is thermodynamically metastable [56] such assumption is highly probable.

For hyaluronan hydrogels with W_c 1.0 there can be seen a small crystallization exothermic peak on cooling curve, and consequently, on the heating curve presence of overlapped endothermic fusion peaks. Enlarged peak area is caused by larger amount of freezing and freezing-bound water. Hyaluronan hydrogels with W_c 1.5 showed a distinct and sharp crystallization exothermic peak on the cooling curve. On heating curve there is a broad cold crystallization exothermic peak (exothermic peak below melting temperature and above temperature of glass transition caused by the presence of so-called glassy water), and a fusion endothermic peak. Again there can be seen an overlapped endothermic fusion peak. As demonstrated later, that disappeared with increasing W_c (see Fig. 23–25). W_c 2.0 shows an abnormally shaped crystallization exothermic peak on cooling curve which is caused by the super-cooling effect (explanation see in 6.2.1). Super cooling-effect is more obvious with increasing W_c which can be identified in Figs. 24 and 25. Further, on the heating curve there is an endothermic fusion peak. The DSC data records for W_c 2.5 and W_c 3.0 look like previous DSC records plus an increasing tendency as mentioned above.

As stated earlier, melting enthalpy of ice present in the hyaluronan system depends on the W_c [56]. There is an assumption: $W_{nf} = W_c - W_f$ and $W_f = W_{free} + W_{freezing\ bound}$ (for details consult chapter 6.2.2). Thus the total amount of freezing water in hyaluronan hydrogels was calculated from the area of endothermic melting peak as follows: obtained heat of ice melting (ΔH) calculated from DSC heating curves was normalized dividing by the weight of the dry hyaluronan. The obtained values for specific concentration in hydrogels were plotted against the respective W_c. The content of non-freezing water per gram of dry hyaluronan was directly determined from the x-intercept (see information in sec. 6.2).

It has been state previously that the water-binding capacity is directly related to the molecular weight of the molecule [4]. In principle, water binding capacity is related to the sum of non-freezing and freezing-bond water. One can suppose that the amount of non-freezing water should be constant since it is defined as an amount of water per the amount of hyaluronan weight. Conversely, Table II reporting the dependency of non-freezing water content to the molecular weight of hyaluronan reveals, although small, but evident trend of increasing number of non-freezing water with increasing molecular weight of hyaluronan. While molecular weight in the interval from 100 to 253 kDa showed similar values, there was determined a significant increase for 1390 kDa. In fact, more than ten-fold increase in molecular weight increased the non-freezing water content of about 40 %. We hypothesize that it is caused by the tertiary structure of hyaluronan and by the mutual approaching of its chains to the closer proximity. As a result the water located between two non-freezing layers

surrounding approaching chains can affect the freezing bound water molecules and bring about the change of their physical properties to be similar to the non-freezing water. It is also our hypothesis that this trend should not necessarily increase also with further progressive increase in molecular weight of hyaluronan than that used in this work. Instead, we expect the reaching a constant value at which the spherical effect of secondary structure would play role. Possibly, further increasing of molecular dimension can result in a decrease in the number of non-freezing water.

Tab. II The weight of non-freezing water for different molecular weight

M_W **(kDa)**	**non-freezing water (g)**
100.1	0.59
253.9	0.58
522.1	0.65
740.0	0.57
1390	0.81

The results from this part of experiment are the quantity of non-freezing water and are used for calculations in the next chapter.

6.2 High water content

Fig. 26 shows record of a representative DSC cooling and heating curve for hyaluronan dissolved in water. The sample shown is 1390 kDa hyaluronan at a concentration of 3 % (w/w) in water.

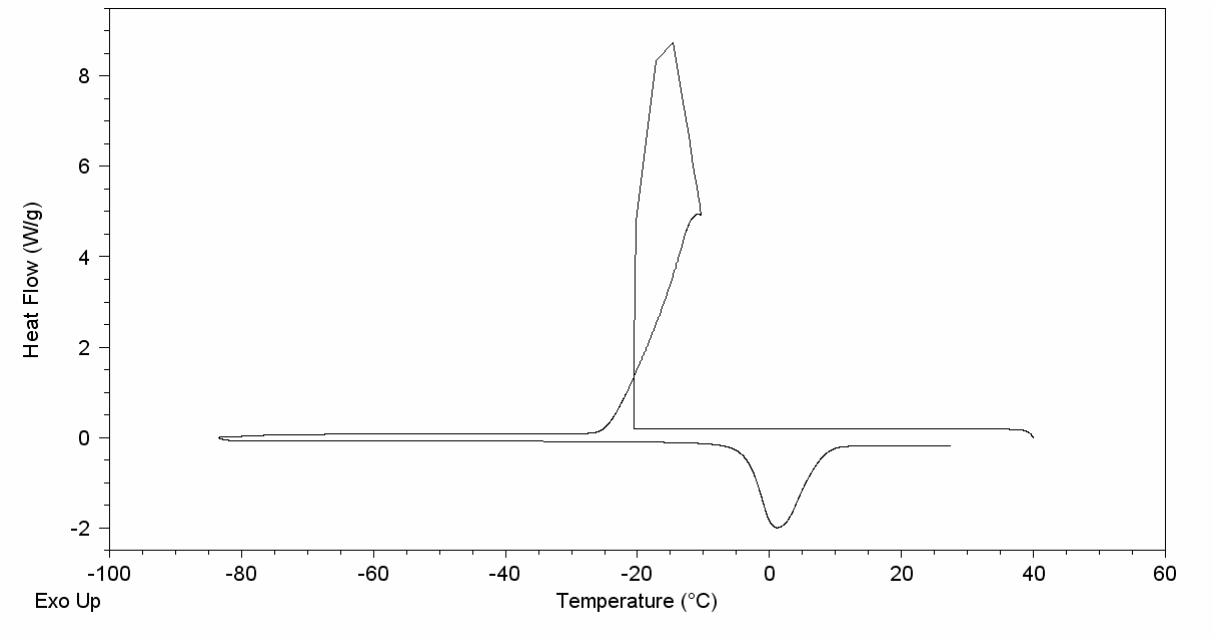

Fig. 26 *a) Representative cooling and heating curves for hyaluronan solutions.*

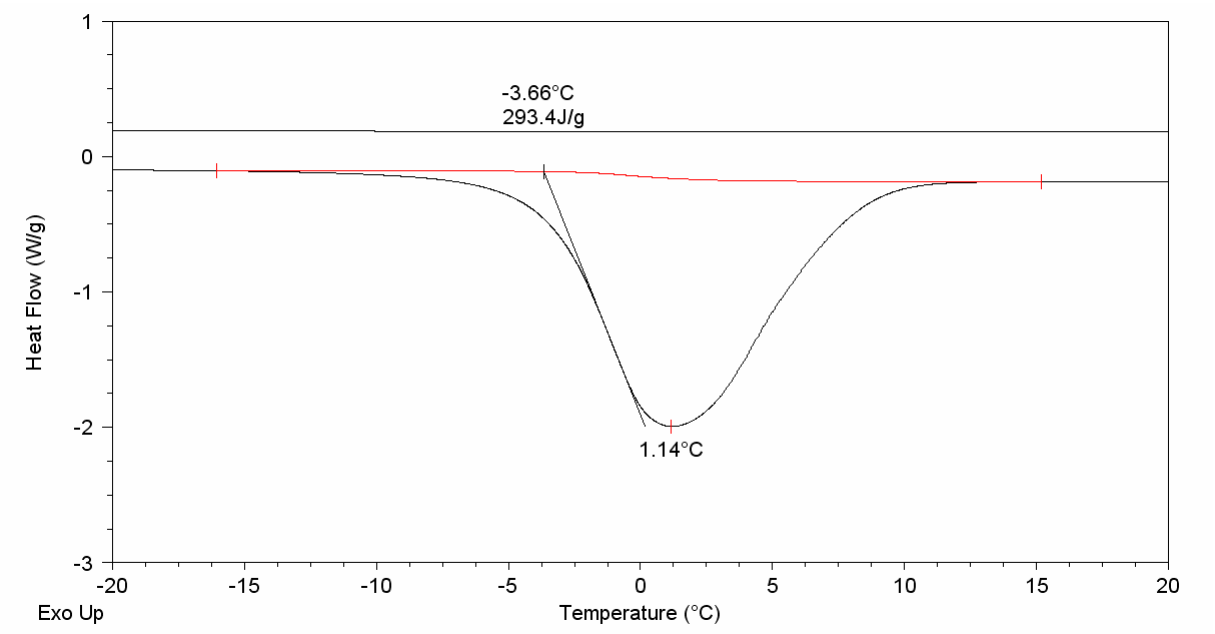

Fig. 26 *b) Expanded view of the melting endotherm portion of the curves shown above. The transition temperatures and enthalpy are as shown.*

6.2.1 Effect of hyaluronan on enthalpy change associated with the cooling curve

The exothermic transition due to the freezing of water in the cooling curve does not look like a typical exothermic peak because of so-called super-cooling effect (a process of chilling a liquid below its freezing point without it becoming solid). When the system started to crystallize, the temperatutr increased because of heat evolved in the course of the process. After the finishing of crystallization, the temperature further decreased to follow the chosen DSC temperature program. Further the exothermic transition due to the freezing of water in the cooling curve began at lower temperature in the hyaluronan solution than it is typically observed for pure water (under our conditions of cooling at 3.0°C min^{-1}, ice formation began at approximately –20°C for hyaluronan solution). This effect of ice nucleation inhibition by the presence of hyaluronan in water solution has been previously reported [57]. The larger molecular weight hyaluronan has a stronger anti-nucleation effect. It was attributed to the anti-nucleation effect and to the existence of the hyaluronan network. The latter is less well-established for the smaller molecular weight hyaluronan, and its ability to inhibit formation and growth of ice nuclei. Further a possible specific binding of hyaluronan to nascent nuclei limiting their growth is also probable [6]. The exothermic transition due to the nucleation and growth of ice in under-cooled hyaluronan solution is not an equilibrium transition, and the enthalpy change is too variable to use it in determining the amount of water freezing. The enthalpy change associated with the cooling curve was always less than the associated with the heating curve. This is also true for pure water, and reflects the difference in heat capacity of liquid water and ice [6].

6.2.2 Effect of hyaluronan on enthalpy change associated with the heating curve

The heating curve shows a single endothermic transition due to the melting of ice. The onset of melting occurs at a lower temperature in hyaluronan solution than in pure water (under our conditions of heating at 3.0°C min^{-1} ice melting begins at approximately –1.3°C for pure water). Table III lists the melting temperature and enthalpy change seen in a series of hyaluronan solutions. The magnitude of the melting temperature reduction increases as hyaluronan concentration increases, but does not appear to depend on hyaluronan molecular weight. The enthalpy change associated with the heating curve is a more accurate reflection of the state of water in the hyaluronan solution than with the cooling curve. The observed enthalpy change associated with melting contains no significant contribution from the heat of dilution (the increase in enthalpy accompanying the addition of a specified amount of solvent to a solution of constant pressure) of hyaluronan. The reported heat of dilution [58] for hyaluronan in water is very small in comparison with the enthalpy change we have recorded.

Table III shows that the enthalpy change for melting decreases with increasing hyaluronan concentration. From the obtained data it can be considered that there are two states for water in the sample of hyaluronan solution: free water and non-freezing (nf) water. Only the free water contributes to the observed enthalpy change. Assuming that the weight of free water is equal to the total water weight less the non-freezing water, the following expression holds:

$$\frac{\Delta H_{\text{obs}}}{g_{\text{HYA}}} = \frac{\Delta H_{\text{free wate}}}{g_{\text{free water}}}\left(\frac{g_{\text{total water}}}{g_{\text{HYA}}}\right) - \frac{\Delta H_{\text{free water}}}{g_{\text{free water}}}\left(\frac{g_{\text{nf water}}}{g_{\text{HYA}}}\right) \quad (1)$$

Table III Thermal properties of hyaluronan solutions

Molecular Weight (kDa)	Concentration % (w/w)	Temperature of melting (°C)	Enthalpy change ΔH_{obs}/g solution (J/g)	Enthalpy change ΔH_{obs}/g HYA (J/g)
100	0.10	-3.86	324.8	342076
	0.50	-4.00	322.9	64337
	1.00	-4.06	311,1	31775
	1.50	-4.17	316.5	24773
	2.00	-4.25	313.0	18169
	2.50	-4.36	313.7	15241
	3.00	-4.26	274.9	10721
253	0.10	-3.70	332.4	391992
	0.50	-3.97	323.2	73062
	1.00	-4.12	326.7	32855
	1.50	-4.15	322.2	24204
	2.00	-4.25	311.0	17011
	2.50	-4.24	303.8	13720
	3.00	-4.27	285.0	9901
522	0.10	-3.82	332.7	462396
	0.50	-3.96	327.6	64268
	1.00	-4.12	328.7	35770
	1.50	-4.20	325.0	23555
	2.00	-4.29	323.4	18350
	2.50	-4.36	319.4	14284
	3.00	-4.46	315.2	11718
740	0.10	-3.91	336.2	67430
	0.50	-4.03	330.5	15204
	1.00	-4.11	320.0	8646
	1.50	-4.17	324.9	7959
	2.00	-4.28	310.9	3870
	2.50	-4.40	317.3	3407
	3.00	-4.46	308.8	2699
1390	0.10	-3.86	329.9	300057
	0.50	-4.00	325.6	71858
	1.00	-4.07	298.7	34255
	1.50	-3.22	291.9	20110
	2.00	-4.28	307.2	16796
	2.50	-3.41	281.9	12812
	3.00	-3.66	293.4	11151

Thus a plot of the enthalpy change, normalized to the hyaluronan weight, as a function of the total water content of the sample will yield the enthalpy change for the free water as a slope. The x-intercept is the point at which the total water content is equal to the amount of non-freezing water, and zero enthalpy change is observed. Thus the x-intercept provided following information: 3.03 g water/g of hyaluronan for 100.1 kDa hyaluronan, 2.99 g water/g of hyaluronan for 253.9 kDa hyaluronan, 2.49 g water/g of hyaluronan for 522.1 kDa hyaluronan, 5.03 g water/g of hyaluronan for 740 kDa hyaluronan and 5.66 g water/g of hyaluronan for 1390 kDa hyaluronan. The interpretation of these results would be that there is 3.03 g non-freezing water per g of 100kDa molecular weight hyaluronan and so on. But this interpretation is inconsistent with the results of low water content (see 6.1) and of similar analyses [56] of DSC data for hydrated hyaluronan at low water content, which gave an x-intercept about 0.5 g water/g hyaluronan. It was described a third type of water in hyaluronan solution [56], [59], [60] which is called freezing-bound water. It is characterized by the lower melting temperature and a lower melting enthalpy than that of free water. Presence of the freezing-bound water shows that hyaluronan can affect the thermodynamic behavior of several hydration layers of water.

Therefore, there is consideration of existence tree different types of water in hyaluronan solution. These types of water are 'free (bulk) water' which freezes as normal water it means that this water melts, crystallized around 0°C and enthalpy of fusion is 333.56 J/g further 'freezing-bound water' (fb) which freezes at lower temperature than normal water but it freezes and it also exhibits a reduced enthalpy of fusion. Finally 'non-freezing water' (nf) which does not freeze even at low temperature which was used in this work, i.e. –90°C. With regards of consideration above-mentioned an alternative expression for quantitative analyses of the enthalpy data can be developed as follows:

$$\frac{\Delta H_{\text{obs}}}{g_{\text{total water}}} = \frac{\Delta H_{\text{free water}}}{g_{\text{free water}}}\left(\frac{g_{\text{free water}}}{g_{\text{total water}}}\right) + \frac{\Delta H_{\text{fb water}}}{g_{\text{fb water}}}\left(\frac{g_{\text{fb water}}}{g_{\text{total water}}}\right) \tag{2}$$

This equation states that only the free water and freezing-bound water contributes to the observed enthalpy change. The enthalpy change may be related to the solute concentration by multiplying both sides of the equation by the water content, in g total water/g hyaluronan.

$$\frac{\Delta H_{\text{obs}}}{g_{\text{HYA}}} = \frac{\Delta H_{\text{free water}}}{g_{\text{free water}}}\left(\frac{g_{\text{free water}}}{g_{\text{HYA}}}\right) + \frac{\Delta H_{\text{fb water}}}{g_{\text{fb water}}}\left(\frac{g_{\text{fb water}}}{g_{\text{HYA}}}\right) \tag{3}$$

Expressing the weight of free water in terms of total water, freezing-bound water, and non-freezing water, one can obtain:

$$\frac{\Delta H_{\text{obs}}}{g_{\text{HYA}}} = \frac{\Delta H_{\text{free water}}}{g_{\text{free water}}}\left(\frac{g_{\text{total water}}}{g_{\text{HYA}}}\right) + \left(\frac{\Delta H_{\text{fb water}}}{g_{\text{fb water}}} - \frac{\Delta H_{\text{free water}}}{g_{\text{free water}}}\right)\left(\frac{g_{\text{fb water}}}{g_{\text{HYA}}}\right) - \frac{\Delta H_{\text{free water}}}{g_{\text{free water}}}\left(\frac{g_{\text{nf water}}}{g_{\text{HYA}}}\right) \tag{4}$$

After the plotting the observed enthalpy change, normalized to the polymer weight, as a function of the total water content of the sample again, the enthalpy change for the free

water can be obtained from the slope. The x-intercept now includes terms for both the freezing-bound water and the non-freezing water:

$$\frac{g_{\text{nf water}}}{g_{\text{HYA}}} + \left(1 - \frac{\Delta H_{\text{fb water}}}{g_{\text{fb water}}} \frac{g_{\text{free water}}}{\Delta H_{\text{free water}}}\right)\left(\frac{g_{\text{fb water}}}{g_{\text{HYA}}}\right) \tag{5}$$

Hence, the x-intercept (see Fig. 27) reflects the non-freezing water content, added to the fractional contribution of the freezing-bound water, the magnitude of which reflects the reduction in enthalpy change associated with melting of this water [6].

Now one can estimate the minimum amount of freezing-bound water per gram of hyaluronan in diluted and semi-diluted solutions by combination of data obtained in this part, high water content, with the data analysis from the part concerning the determination of low water content (6.1). Thus the content of non-freezing water was adopted from the table reporting the low water content for specific hyaluronan molecular weight (see 6.1–Tab. II). The minimum value for the enthalpy change associated with melting of the freezing-bound water was used 312 J/g [56].

Obtained values of freezing-bound water, summarized in Tab. IV exhibit no obvious dependency. For the first three value (100.1 kDa; 253.9 kDa; 522.1 kDa), there is decrease but for the next two values (740.0 kDa; 1390 kDa) there is increase of the values.

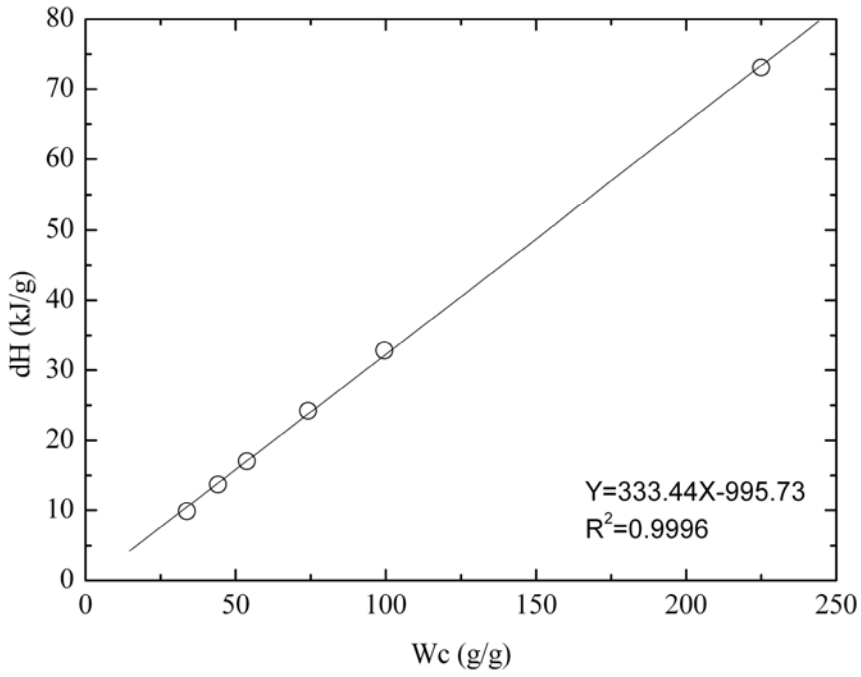

Fig. 27 *Normalized melting enthalpy versus W_c for the sample with M_w 253.9 kDa.*

Tab.IV The weight of freezing-bound water per g of hyaluronan for different M_W

M_W (kDa)	Freezing-bound water (g)/1g HYA
100.1	38.7
253.9	38.2
522.1	29.2
740.0	70.7
1390.0	76.9

A perusal of literature provides rather confusing information on the physical meaning of the slope obtained from above-mentioned linearized plot. Liu and Cowman stated [6] that the number value of the slope is equal to the free water heat of melting, i.e. 333.56 J g^{-1}. In contrast, Yoshida et al. [56] reported rather lower values for low water content and did not any conclusion concerning the point. In this work, the slope showed value around such number which verifies the statement of Liu and Cowman.

This value of enthalpy change is not accurate since value 312 J/g was used for the determination of freezing-bound water amount [56]. In fact, it represents the minimal value obtained by measurement of low water content samples. To improve the enumeration of individual different freezing-bound water types, the separation of individual peaks and attribution of exact enthalpies of melting to specific freezing-bound water should be carried out. The separation of peaks can be done either by the peak deconvolution or by techniques suggested for the determination of pharmaceutical substances purity. Nevertheless, such exact enumeration of freezing-bound water is beyond the scope of this work.

The estimation of the physical dimensions of the freezing-bound water layer surrounding the hyaluronan chain can be considered as follows. The volume of a disaccharide residue of hyaluronan can be determined by considering the partial specific volume of hyaluronan (about 0.56 cm^3g^{-1}) [61], and the disaccharide residue molecular weight of 401 Da [6] for the sodium salt form, yielding 0.37 nm^3 as the volume of one disaccharide. The water layer, containing 38.7 g water/g hyaluronan (for sample 100.1 kDa), contains approximately 826 water molecules per disaccharide (for other M_W see Tab. V).

Table V Estimation of the number of water molecules surrounding dissacharide units for various molecular weights of hyaluronan

M_W HYA (kDa)	Molecules of water per disaccharide unit
100.1	826
253.9	851
522.1	650
740.0	1 575
1390	1 712

The data in the table V are valid only for an ideal case when the disaccharide is in its most extended conformation and the length is approximately 1nm. However, in agreement with the statement about the mutual influence of the hyaluronan chains and formation of the secondary and tertiary structure, such considerations should be taken as indicative. Nevertheless, the principle and consideration mentioned above are still relevant.

6.3 HRUS-high water content

Fig. 30 shows HRUS records of 1390 kDa hyaluronan dissolved in water. As can be seen the elevated temperatures caused a monotonous decrease in U12 which is caused by the decrease in hydration of hyaluronan molecules (U12 means difference of ultrasonic velocity between cell 1 with a sample and cell 2 filled with water). The steep decrease of U12 at low temperatures was caused by the change in temperature programme, and therefore, it is considered as an artifact and it was not taken into consideration. Basically, the larger number of molecules in hydration shell the larger U12 parameter is. That is caused by the increase in density of water in the close vicinity of a hydrophilic molecule; it is reported to be 10–20 % denser than those of bulk water [63]. In fact, there is a progressive decrease of values U12 reported in Fig. 28 with decreasing concentration. The elevated temperatures are responsible for the decrease in dipole moment of water which consequently leads to the decrease of strength of water H-bonds responsible for water structures formation and thus weakening of hydration shell. Basically, there is a decrease in number of water molecules surrounding the hyaluronan molecules.

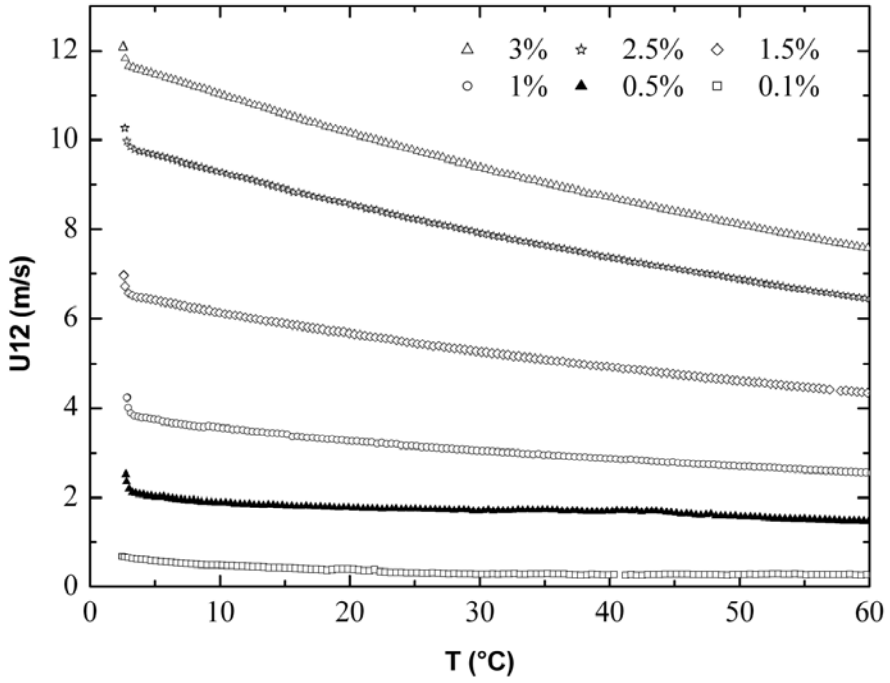

Fig. 28 *Thermal behavior of the U12 by different concentrations.*

Fig. 29 reports the values of U12 vs. concentration at constant temperature for 1390 kDa hyaluronan; it can be seen that dependence is linear which implies that there are not changes in the secondary hyaluronan structure caused either by applied frequency or by the temperature. Together with results obtained for higher ultrasonic frequencies i.e. at 8.219 and 12.196 MHz resulting in an equal ultrasonic velocity as for 5.478 MHz reported above, it is an indicator of incompressibility of hyaluronan secondary structure. Such behavior was similar also for other samples except low concentrated sample (0.1 and 0.5 %) of molecular weight 100.1 kDa.

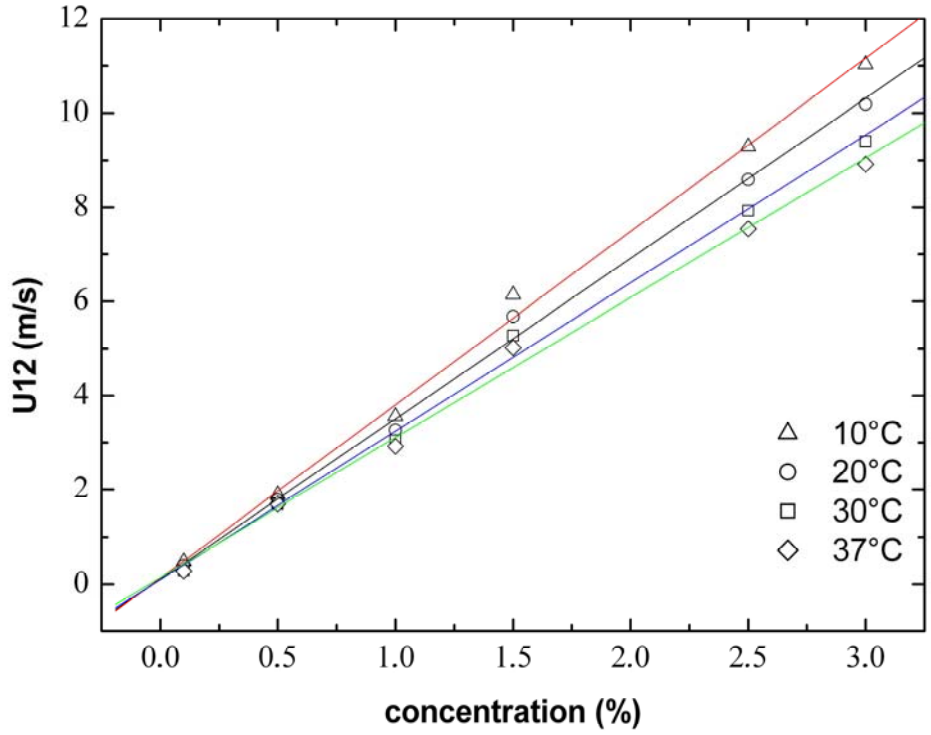

Fig. 29 *U12 vs. concentration at constant temperature.*

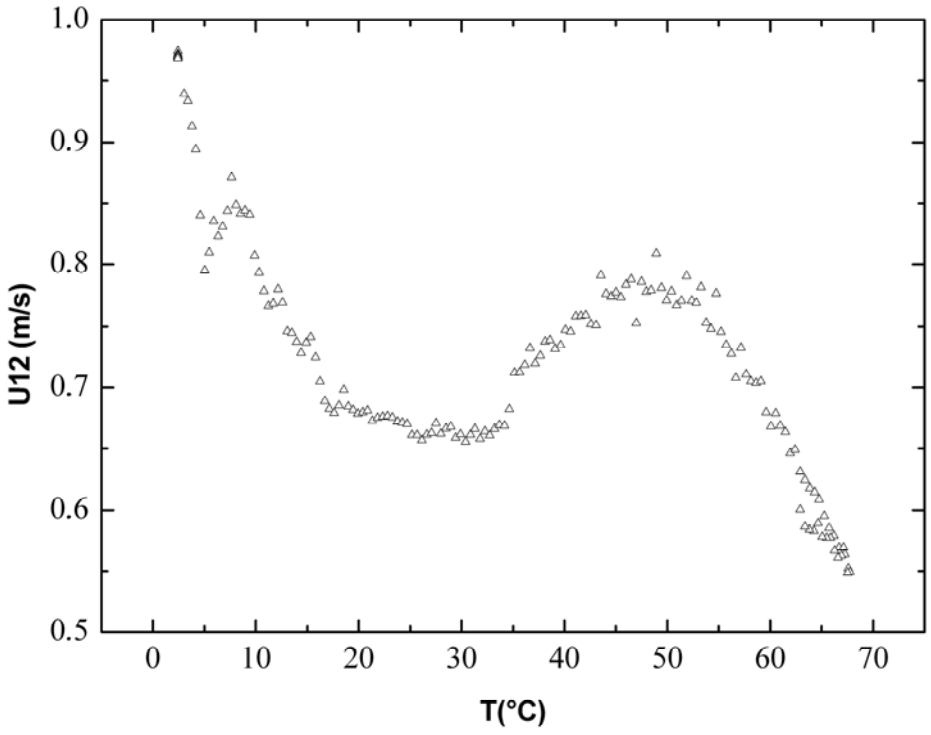

Fig. 30 *U12 vs. temperature 100.1 kDa, concentration 0.1 %.*

The record reported in Fig. 30 shows a completely different behavior of hyaluronan sample. First, in the temperature interval 20 to 30°C there is the progressive decrease interrupted by a plateau followed by a small increase in U12. At 50°C the U12 parameter decreased again. In line with the previously reported results describing the behavior of carrageenan [64] such behavior can be attributed to the progressive unfolding of α-helix structure of hyaluronan. The small increase is caused by the increase in hydration of unfolded chains. The reason, why such phenomena can be seen only for low concentrated solutions and low molecular weigh samples can be explained as the fact that molecules under such conditions are not in the close proximity to influence mutually each other. Therefore, the hyaluronan gel-like structure is not stable any longer and in the solution there is enough room for disruption or better unfolding of hyaluronan secondary structure.

As mentioned above, hyaluronan represents an incompressible system under ultrasonic frequencies employed for the measurement. Principally, it means that there is present no structure formed by hyaluronan which exhibits any relaxation time contributing to the decrease in ultrasonic velocity after compression. Thus there is a possibility to calculate the amount of non-freezing water in the hydration shell of hyaluronan using simple considerations and equations. Calculation can be done as described in Equations (6)–(8). Briefly, in the observed system the propagation of ultrasonic wave through a liquid phase is described by:

$$u^2 = \frac{1}{d\beta} \tag{6}$$

Where u is the measured ultrasound velocity; β is the adiabatic compressibility of the observed system and hydrated counterion can be regarded as incompressible in comparison to the bulk solvent then it can be readily shown:

$$V_{0,H_2O} = \frac{\beta_{soln}}{\beta_{solv}} \tag{7}$$

Where V_{0,H_2O} is the experimentally determined volume fraction of non-interacting solvent (free water) β_{soln} and β_{solv} are the respective solution and solvent compressibilities determined from ultrasonic velocity and density data. The mass of water interacting with sodium hyaluronate m'_{H_2O} is given by:

$$m'_{H_2O} = (d - c) - \frac{\beta_{soln}}{\beta_{solv}} \; d_0 \tag{8}$$

[61]

Obviously for precise determination of hydration shell, the ultrasonic data should be completed by the values of density of the observed systems. Therefore, in case of possessing of a precise densitometer with resolution approximately 10^{-5} g cm^{-3} such equations can be simply used for the enumeration of hydration shell. It is our hypothesis that such water shell corresponds roughly to the non-freezing water as evaluated by DSC measurement. It is likely that using ultrasonic approach the results would not provide exactly the same values as DSC

and freezing-bound water would significantly contribute to the determined value. Anyway in comparison with DSC measurement, such approach exhibits the enlarged application capability, especially for solutions with higher ionic strength and for significantly broader range of temperatures.

7 CONCLUSION

Semi-diluted hyaluronan solutions have significantly altered freezing and melting transitions of water. The results are affected by the presence of freezing-bound and of a small amount of non-freezing water strongly bound to the polymer. Those have slightly altered thermodynamic properties which were used for the enumeration of such types of water.

Experimental data also confirmed that hyaluronan is an incompressible molecule and water enumeration is possible using additional densitometry measurement.

Measurement of diluted solutions of low molecular hyaluronan showed the molecular unfolding at 20°C associated with local increase in hydration. It is obvious that such phenomena together with knowledge of hyaluronan interactions bear a great potential in development of so-called thermo-responsible polymers. Those can be aimed to transport a specific substance into human body, where, as a response to the increased temperature unfold and release a transported molecule.

8 REFERENCES

[1] Hascall V. C.: Hyaluronan: Structure and physical properties*, Glycoforum,* Cited. 15 Dec, 1997.
Available at http://www.glycoforum.gr.jp/science/hyaluronan/HA01/HA01E.html

[2] Jouon N., Rinaudo M., Milas M., Desbrieres J.: Hydravion of hyaluronic acid as a function of the counterion type and relative humidity. *Carbohydrate Polymers,* 1995, vol. 26, pp. 69–73.

[3] Hatakeyama H., Hatakeyama T.: Interaction between water and hydrophilic polymers. *Thermochimica Acta,* 1998, vol. 308, pp. 3–22.

[4] Sutherland W.: Novel and established applications of microbial polysaccharides. *Institute of cell and molecular biology, Edinburgh University,* 1998, vol.16.

[5] Kogan G., Šoltéz L., Stern R., Gemener P.: Hyaluronic acid: a natural biopolymer with a broad range of biomedical and industrial applications. *Biotechnology Letters,* 2007, vol. 29, pp. 17–25.

[6] Lui J., Cowman M.K.: Thermal analysis of semi-diluted hyaluronan solutions. *Journal of thermal analysis and calorimetry*, 2000, vol. 59, pp. 547–557.

[7] Stern R.: Hyaluronan catabolism: a new metabolic pathway. *European Journal of Cell Biology*, 2004, vol. 83, no 7, pp. 317–325.

[8] Lapčík L.Jr., Lapčík L., De Smedt S., Demeester J., Chabreček P.: Hyaluronan: Preparation, Structure, Properties and Applications. *Chemical reviews*, 1998, vol.8, pp. 2664–2683.

[9] Ponnuraj K., Jedrzejas M.J.: Mechanism of hyaluronan binding and degradation. *Journal of Molecular Biology,* 2000, pp. 885–895.

[10] Scott JE: Secondary structures in hyaluronan solutions: chemical and biological implications. The Biology of Hyaluronan. *Ciba Foundation Symposium*, 1989, No.143 pp. 6–14.

[11] Scott JE, Cummings C, Brass A, Chen Y: Secondary and tertiary structures of hyaluronan in aqueous solution, investigated by rotary shadowing-electron microscopy and computer simulation. Hyaluronan is a very efficient network-forming polymer. *Biochemical Journal,* 1991, vol. 274; pp. 699–705.

[12] Scott JE: Supramolecular organization of extracellular matrix glycosaminoglycans, in vitro and in the tissues. *FASEB Journal*, 1992, vol. 6, pp. 2639–2645.

[13] Chang N.S, Boackle R.J, Armand G: Hyaluronic acid-complement interactions. I. Reversible heat-induced anticomplementary activity, *Molecular Immunology,* 1985, vol. 22, pp. 391–397.

[14] Evanko S., Wight T.: Intracellular hyaluronan, In:Hyaluronan: synthesis, function, catabolism, *Glycoforum gr*., Cited 30 Jul, 2001.
Available at http://www.glycoforum.gr.jp/science/hyaluronan/HA20/HA20E.html.

[15] Hedman K., Kurkinen M., Alitalo K.., Veheri A., Johansson S., Hook M.: Isolation of the pericellular matrix of human fibroblast cultures. *Journal of Cell Biology*, 1979, vol. 81, pp. 83–91.

[16] Almond A.: Visions and reflections (minireview) Hyaluronan. *Cellular and Molecular life Sciences*, 2007, vol. 64, pp. 1591–1596.

[17] Block, A., and Bettelheim, F.: Water Vapor Sorption of Hyaluronic Acid, *Biochimica et Biophysica Acta,* 1970, vol. 69, pp.201.

[18] Maytin E.V., Chung H.H., Seetharaman V.M.: Hyaluronan participates in the epidermal response to disruption of the permeability barrier in vivo. *American Journal of Pathology*, 2004, vol. 165, pp. 1331–1341.

[19] Garg H.G., Hales Ch.A.: Chemistry and biology of hyaluronan, Harvard Medical School, Pulmonary and Critical Care Unit, Massachusetts General Hospital Boston, MA 02114-2969 U.S.A., 2004, 605p, ISBN 0 08 044382 6.

[20] O'Regan, M., Martini, I., Crescenzi, F., De Luca, C., Lansing M.: Molecular mechanisms and genetics of hyaluronan biosynthesis. *International Journal of Biological Macromolecules,* 1994, vol. 16, pp. 283–286.

[21] Armstrong, D.: The Molecular Weight Properties of Hyaluronic Acid produced Streptococcus zooepidemicus. *Chemical Engineering (Brisbane: University of Queensland)*, 1997.

[22] Goh, L.T.: Effect of culture conditions on rates of intrinsic hyaluronic acid production by Streptococcus equi subsp. zooepidemicus. *Chemical Engineering (Brisbane: University of Queensland)*, 1998.

[23] Chaplin, M. F.: Roles of water in biological recognition processes, *Wiley Encyclopedia of Chemical Biology*, Ed. T. P. Begley (John Wiley & Sons) Article in Press, 2008.

[24] Chaplin M. F. Available at: http://www.lsbu.ac.uk/water/chaplin.html

[25] Wolfe J., Bryant G., Koster K. L.: What is 'unfreezable water', how unfreezable is it and how much is there?, *Cryo-Letters*, 2002, vol. 23, pp. 157–166.

[26] Kirschner K. N., Woods R. J.: Solvent interactions determine carbohydrate conformation, Proc, *National Academic Science U.S.A.*, 2001, vol. 98, pp. 10541-10545.

[27] Wunderlich, B.: *Thermal analysis of Polymeric Materials.* Berlin: Springer-Verlag, 2005, ISBN 3-540-23629-5.

[28] Watson E. M., O'Neill M. J., Justin, J., Brenner, N.: A Differential Scanning Calorimeter for Quantitative Differential Thermal Analysis. *Analytical Chemistry,* 1964, vol. 36, pp.1233–1238.

[29] Ramachandran V.S. Paroli R.M., Beaudoin J.J., Degado A.H.:Handbook of thermal analysis of constuction materials. Institute for research in construction, National research souncil of Canada, Ottawa, Ontario, Canada, 2002, ISBN 0-8155-1487-5.

[30] Yoshida H., Hatakeyama T., Hatakeyama H.: Glass transition of hyaluronic acid hydrogel, *Kobunshi Ronbunshu*, 1989, vol. 46, issue 10, pp. 597–602.

[31] Takigam S., Takgami M., Phillips G.O., *Carbohydrate polymers*, 1993, vol. 22, pp. 153.

[32] Hatakeyama T., Yoshida H., Nakamura K., Hatakeyama H., Maeno N., Hondah T., Physics and Chemistry of Ice, Hokkaido University Press, Sapporo, 1992, p. 262.

[33] Yoshida H., Hatakeyama T., Hatakeyama H., Glasser W., Hatakeyama H., Viscoelasticity of Biomaterials, ACS Symp. Ser., 489, Amer. Chem. Soc., Wahington D.C., 1992, p. 385.

[34] Hatakeyama T., Hatakeyama H., *Koubunshi Ronbunshu (J.of High Polymers)*, 1996, in press.

[35] Yoshida H., Hatakeyama T., Hatakeyama H., Maeno N., Hondah T., Physics and Chemistry of Ice, *Hokkaido University Press*, 1992, pp. 282.

[36] Takigami S., Takigami M., Philips O.G., Hydration characteristics of the cross-linked hyaluronan derivative hylan. *Carbohydrate polymers,* 1993, vol. 22, pp. 153–160.

[37] Magne F.C., Portas H.J., Wakeham H.A.: A calorimetric investigation of moisture in textiles fibers. *Journal of the American Chemical Society*, 1947, vol. 69, issue 8, pp 1896–1902.

[38] Hatakeyama T., Hirose S., Hatakeyama H.: Differential scanning calorimetric studies on bound water in 1,4-dioxane acidolysis lignin, *Makromolekula Chemie-Macromolecular Chemistry and Physics*, 1983, vol. 184, pp. 1265–1274.

[39] Quinn E.X., Hatakeyama T., Yoshida H., Takahashi M., Hatakeyama H., *Polymer Gels and Network,* 1993, vol. 1, pp. 93.

[40] Quinn E.X., Hatakeyama T., Takahashi M., Hatakeyama H.: *Polymer* ,1994, vol. 35, pp. 1248.

[41] Nishinari K., Takaya T., Watase M., Kohyam K., Iida H., in:P.O. Williams, G.O. Phillips (Eds.), *Gum and Stabilizers forthe Food Industry*, 1994, p. 359.

[42] Takgami S., Takigami M., Phyllips G.O., *Carbohydrate Polymers*, 1995, vol. 26, pp.11.

[43] Takgami S., Takigami M., Phillips G.O., *Food Hydrocolloids*, 1996, vol. 10, pp. 11.

[44] Hatakeyama T., Hatakeyama H., Nakramura K.: Non-freezing water concent of monovalent and divalent cation salts of polyectrolyte water systems studied by DSC, *Thermochimica Acta*, 1995, vol. 253, pp. 137–148.

[45] Nakamura K., Hatakeyama T., Hatakeyama H., *Thermochimica Acta*, 1995, vol. 267, pp. 343.

[46] Hatakeyama T., Yamauchi A., Hatakeyama H.: Studies on bound water in polyvinyl-alcohol hydrogel by DSC and FT-NMR, *European Polymer Journal*, 1984, vol. 20, issue 1, pp. 61–64.

[47] HRUS Spectrometer User Guide

[48] Davies A., Gormally J., Wyn-Jones E., Wedlock D.J., Phyllips G.O.: A study of factors influencing hydravion of sodium hyaluronate from compressibility and high-precision densimetric measurements. *Biochemical Journal*, 1983, vol. 213, pp. 363–369 .

[49] Hickey S., Lawrence J.M., Hagan S.A., Buckin V.: Analyse of the phase diagram and microstructural transitions in phospholipid microemulsion systemes using high-resolution ultrasonic spectroscopy. *Langmuir*, 2006, vol. 22, pp. 5575–8863.

[50] Kharakoz D.P.: Acoustical study of compressibility of amino acid and protein solutions, PhD thesis, 1984, Pushchino: *Indy. Biol. Phys. Acad. Sci*. USSR. 240 pp

[51] Buckin V.A.: Acoustical ivestifation of nucleic acid hydration, PhD thesis, *Pushchino: Indy. Biol. Phys. Acad. Sci*. USSR, pp. 250, (In Russian)

[52] Buckin V.A., Kankiya B.I., Bulichov N.V., Lebedův A.V., Bukovský I.Y.: Measurement of anomalously high hydration of (DA)N. (DT)N double helices in dilute solution, *Nature,* 1989, vol. 340, issue 6231, pp. 321–322 .

[53] Buckin V.A., Kankiya B.I, Kazaryan R.L., *Biophysical Chemistr*, 1989, vol. 34, pp.211.

[54] Buckin V.A., Kankiya B.I, Sarvazyan A.P.,Uedaria H.,: Acoustical investigation of poly (DA). poly (DT), poly [D(A-T)]. poly [D(A-T)], poly (U) and DNA hydration in dilute aqueous solutions, *Nucleic Acids Res*earch, 1989, vol. 17, issue 11, pp. 4189–4203 .

[55] Negredo C., Monks E., Sweeney T.: A novel real-time ultrasonic method for prion protein detection using plasminogen as a capture molecule. *BMC Biotechnol*, 2007, vol. 7, pp. 43.

[56] Yoshida H., Hatakeyama T., Hatakeyama H.: Characterization of water in polysaccharide hydrogels by DSC. *Journal of Thermal Analyses*, 1992, vol. 40, pp. 483–489.

[57] Cowman M.K., Lui L., Li M., Bittner D.M., Kim J.S.: The Chemistry, Biology, and Medical Applications of Hyaluronan and its Derivatives. T.C.Laurent, Ed., Portaland Press, London 1998 pp. 17–24.

[58] Benegas J.C., Di Blas A., Paoletti S., Cesaro A.:Some aspects of the enthalpy of dilution of biological polyelectrolytes. *Journal of Thermal Anaysis*, 1992, vol. 38, pp. 2613–2620.

[59] Joshi N. H., Topp E.M.: Hydravion in hyaluronic acid and its esters using differential scanning calorimetry, *International Journal of Pharmaceutics*, 1992, vol. 80, issue 2-3, pp. 213–225.

[60] Jouon N., Rinaudo M., Milas M., Desbrieres J.: Hydration of hyaluronic acid as a function of the counterion type and relative humidity, *Carbohydrate Polymers*, 1995, vol. 26, issue 1, pp. 69–73.

[61] Davies A., Gormally J., Wyn-Jones E.: A study of hydration of sodium hyaluronate from compressibility and high precision densitometry measurements, *International Journal of Biological Macromolecules,* 1982, vol. 4, pp. 436–438.

[62] Cowman M.K., Li M., Balazs E.A.: Tapping mode atomic force microscopy of hyaluronan: Extended and intramolecularly interacting chains, *Biophysical Journal*, 1998, vol. 75, issue 4, pp. 2030–2037.

[63] Rowe A.J., *Biophysical Chemistry*, 2001, vol. 93, pp. 93–101.

[64] Ultrasonic scientific: Thermal transitions in aqueous carrageenan solution, 2002, available at: http://www.ultrasonic-scientific.com/Applications/Apps/conformation.htm

9 APPENDIX

9.1 DSC records for low water content

9.1.1 253.9 kDa hyaluronan

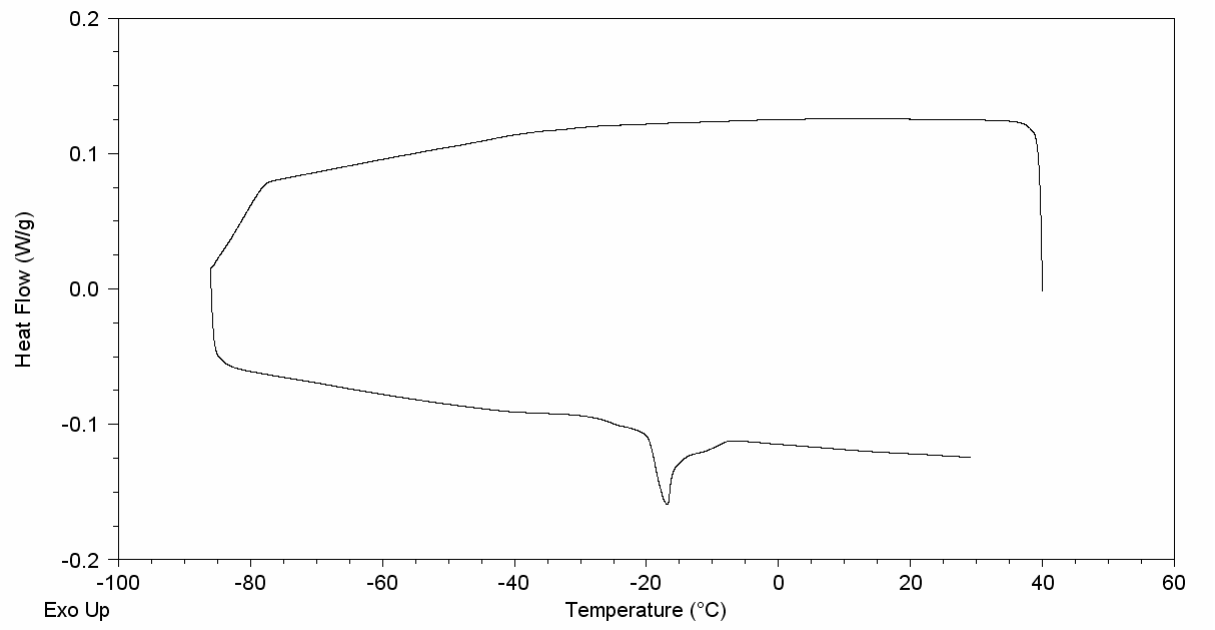

Fig. 20 *a) Cooling and heating curves for hyaluronan hydrogel of W_c 0.75.*

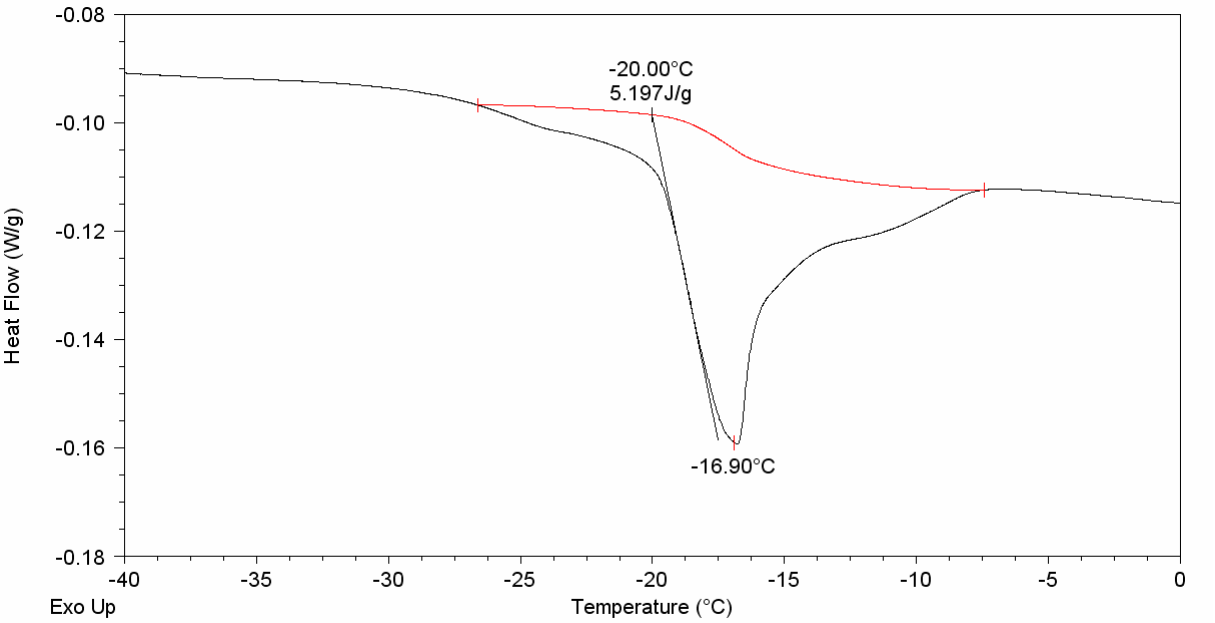

Fig. 20 *b) Expanded view of the melting endotherm portion of the curves shown above. The transition temperatures and enthalpy are as shown.*

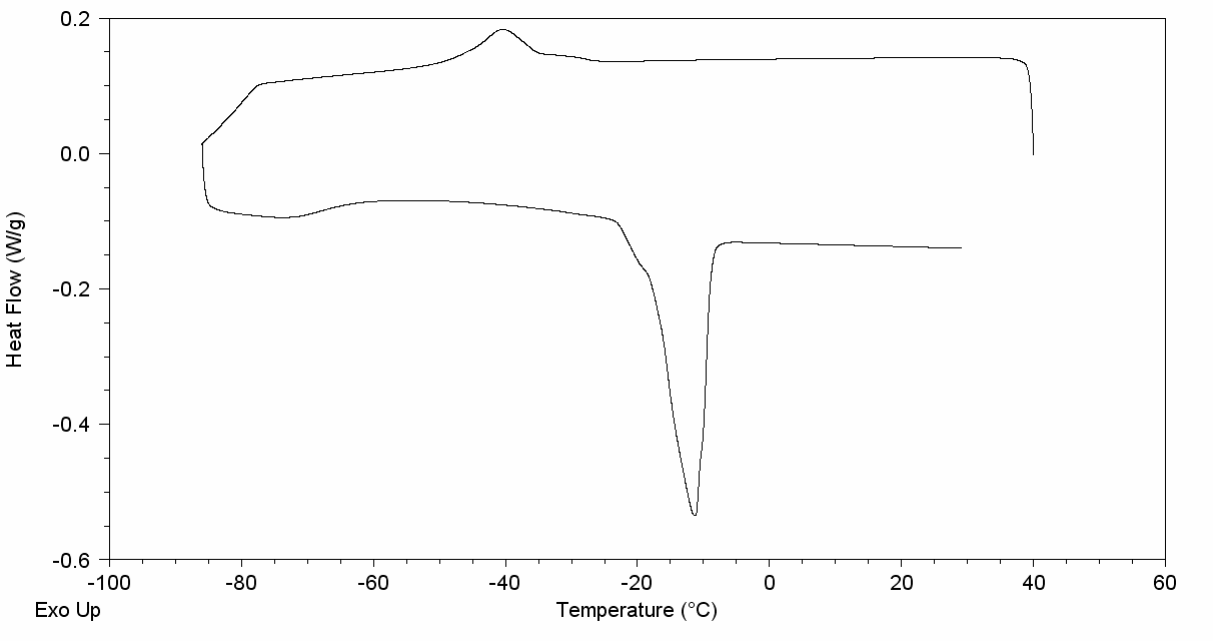

Fig. 21 *a) Cooling and heating curves for hyaluronan hydrogel of W_c 1.0.*

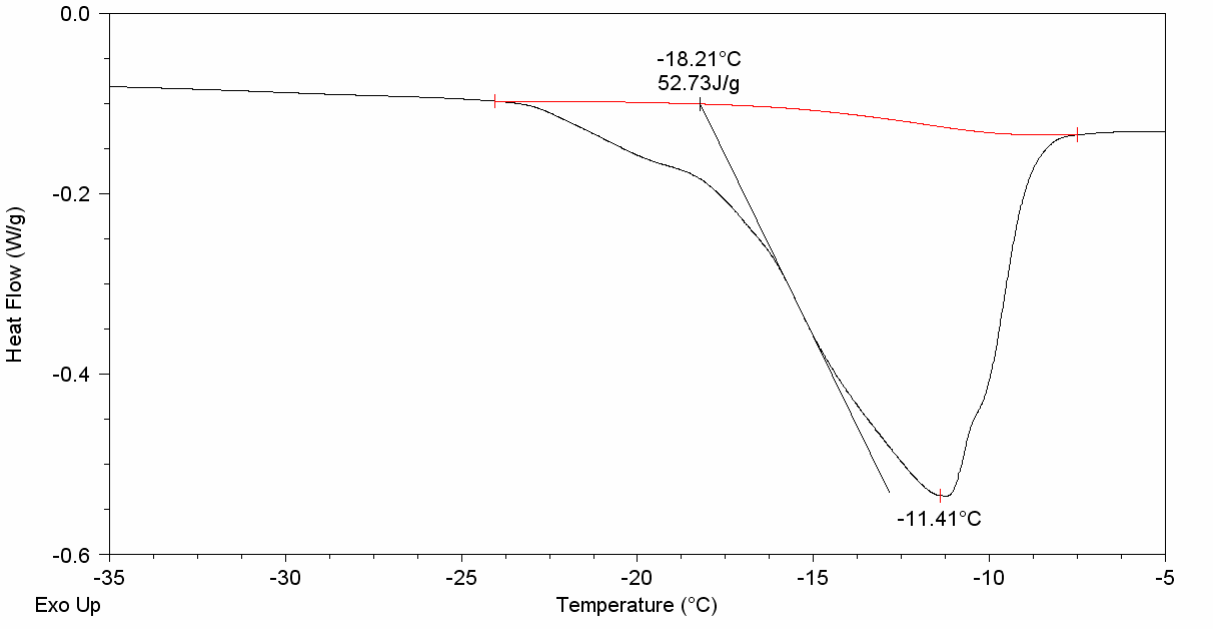

Fig. 21 *b) Expanded view of the melting endotherm portion of the curves shown above. The transition temperatures and enthalpy are as shown.*

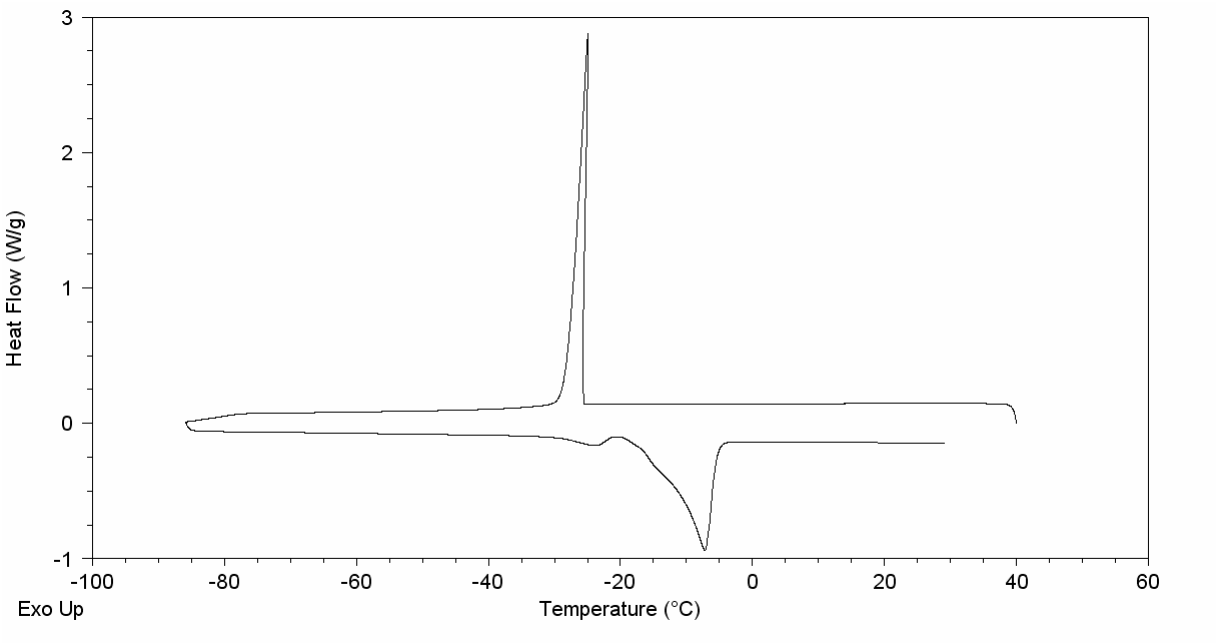

Fig. 22 *a) Cooling and heating curves for hyaluronan hydrogel of W_c 1.5.*

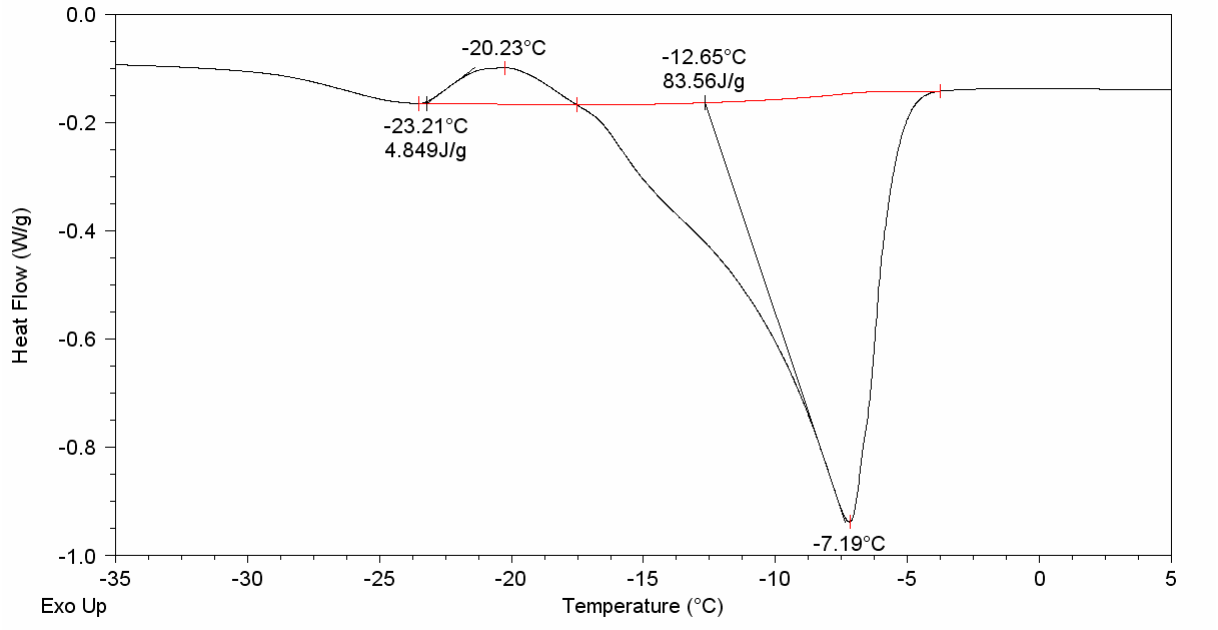

Fig. 22 *b) Expanded view of the melting endotherm portion of the curves shown above. The transition temperatures and enthalpy are as shown.*

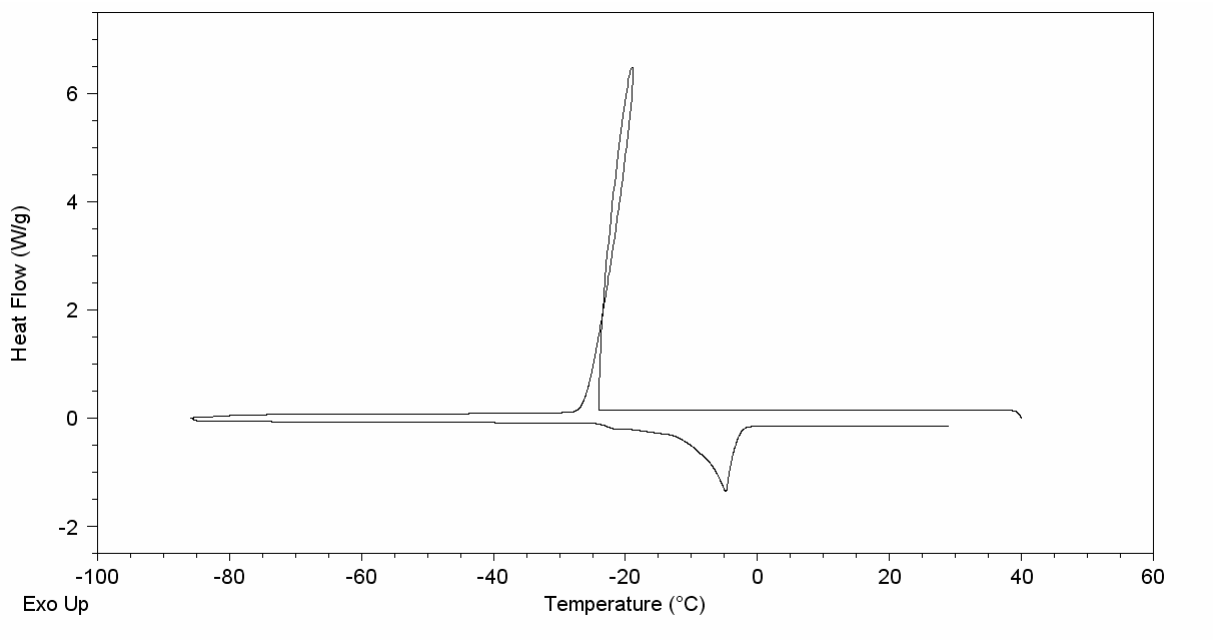

Fig.23 *a) Cooling and heating curves for hyaluronan hydrogel of W_c 2.0.*

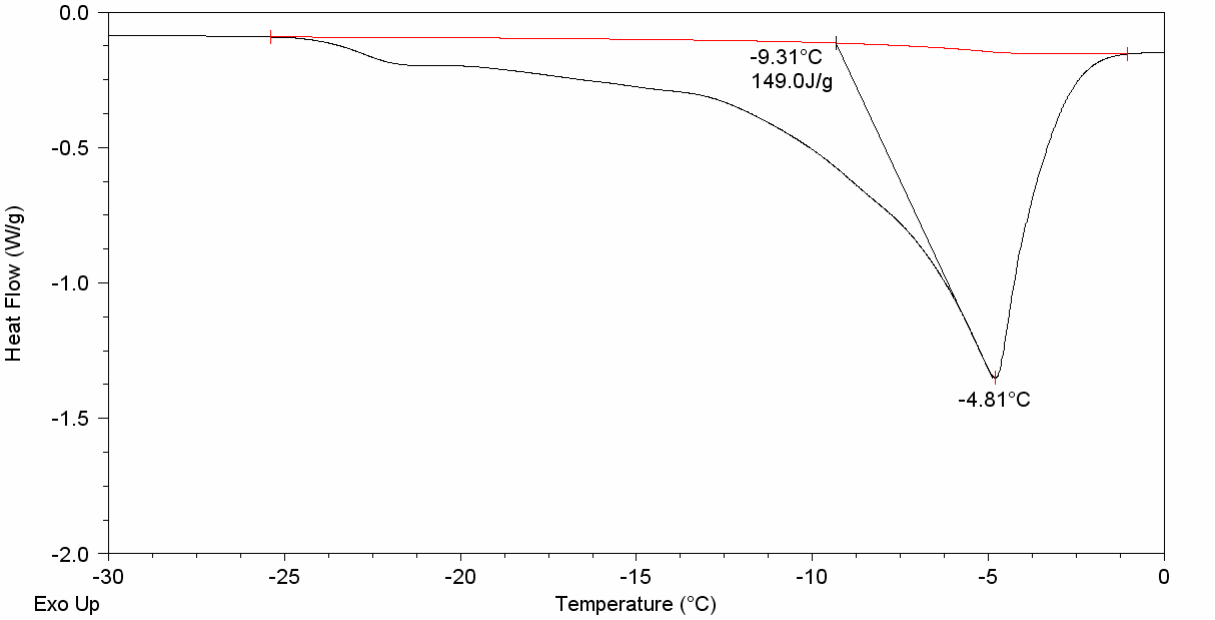

Fig. 23 *b) Expanded view of the melting endotherm portion of the curves shown above. The transition temperatures and enthalpy are as shown.*

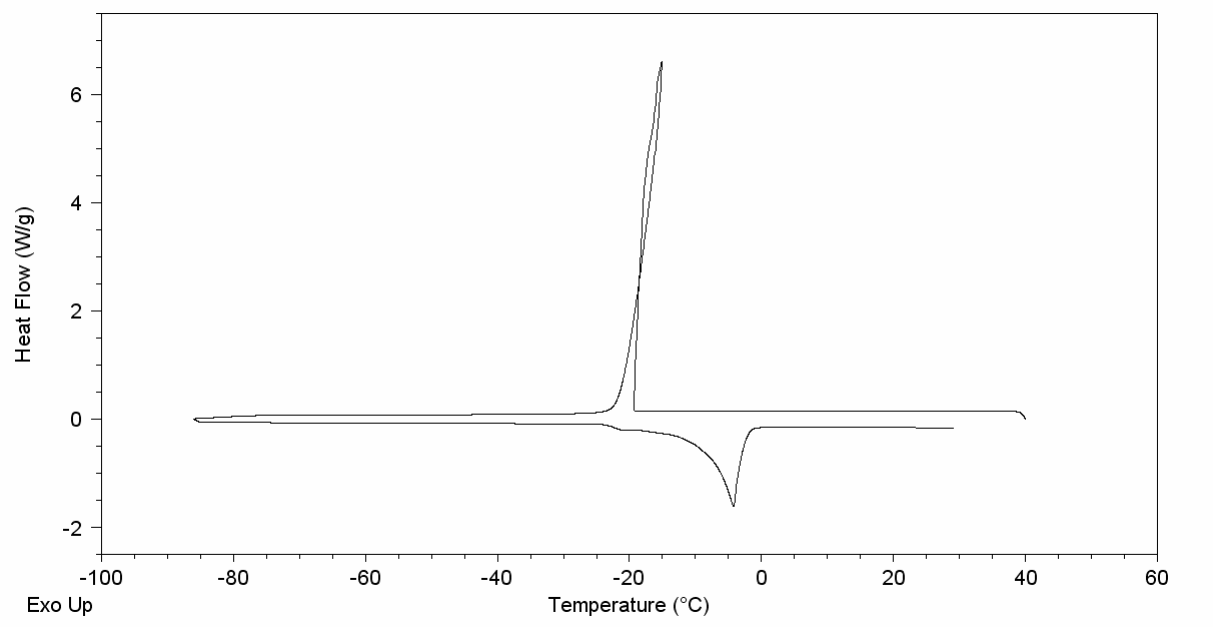

Fig.24 *a) Cooling and heating curves for hyaluronan hydrogel of W_c 2.5.*

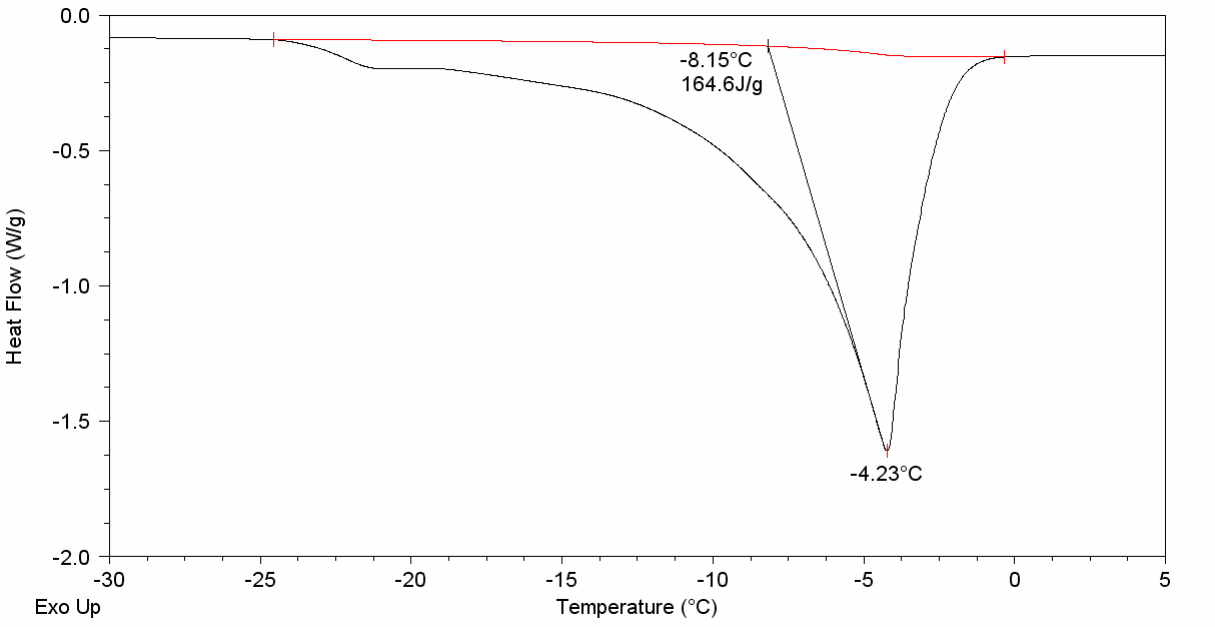

Fig. 24 *b) Expanded view of the melting endotherm portion of the curves shown above. The transition temperatures and enthalpy are as shown.*

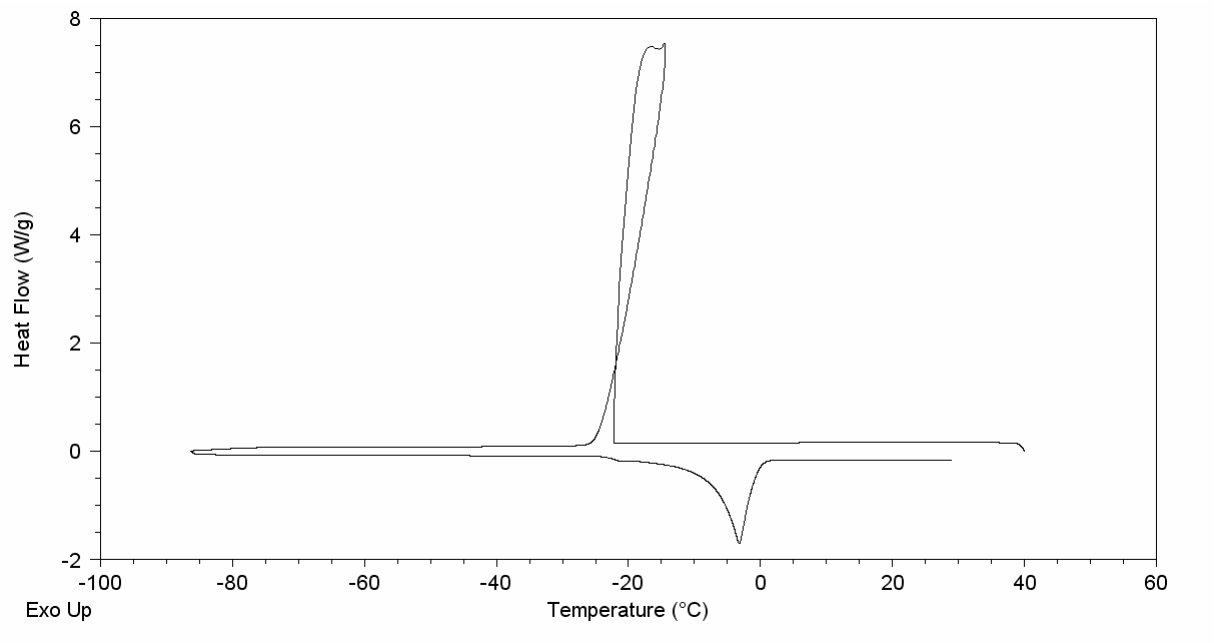

Fig.25 *a) Cooling and heating curves for hyaluronan hydrogel of W_c 3.0.*

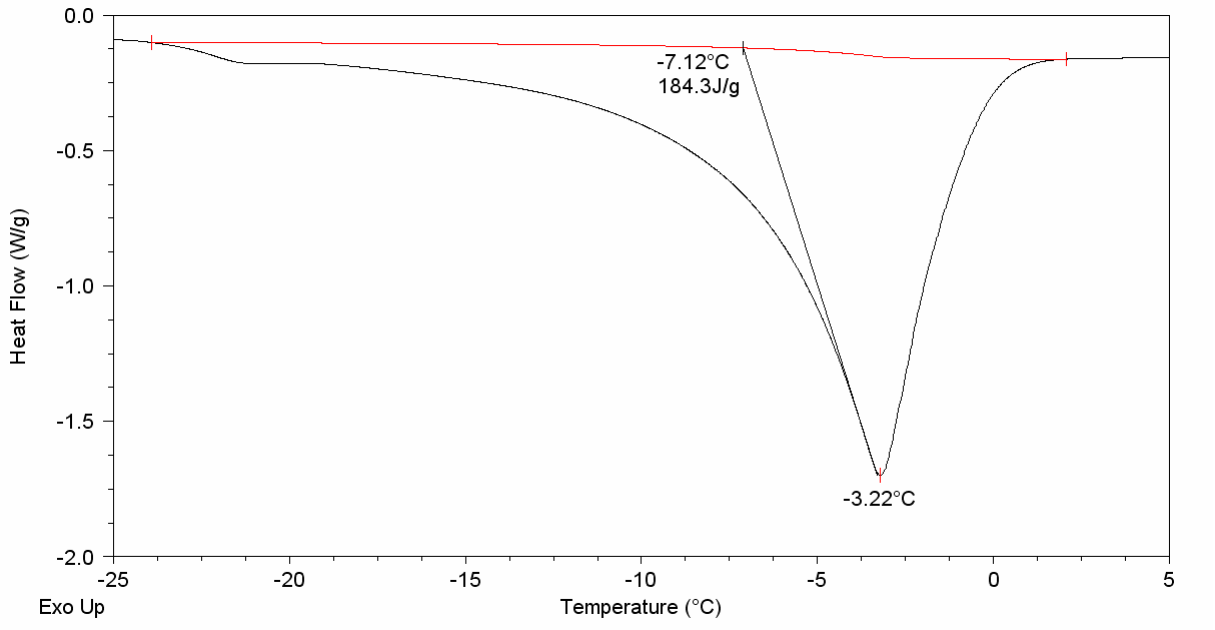

Fig. 25 *b) Expanded view of the melting endotherm portion of the curves shown above. The transition temperatures and enthalpy are as shown.*

9.1.2 100.1 kDa hyaluronan

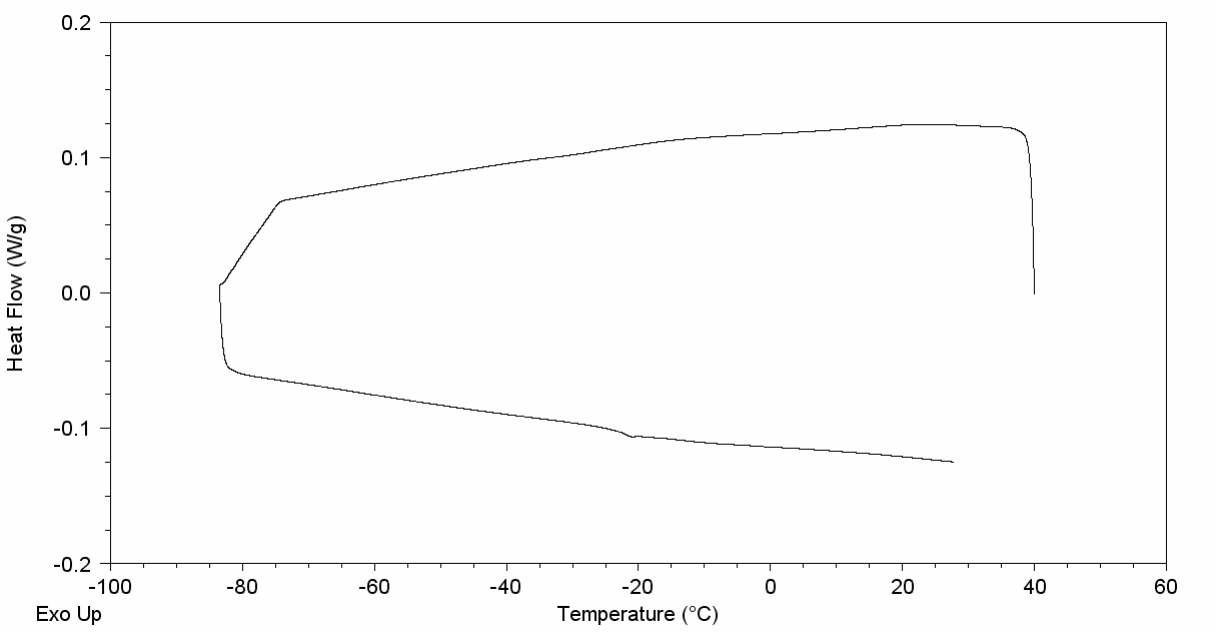

a) Cooling and heating curves for hyaluronan hydrogel of W_c 0.5.

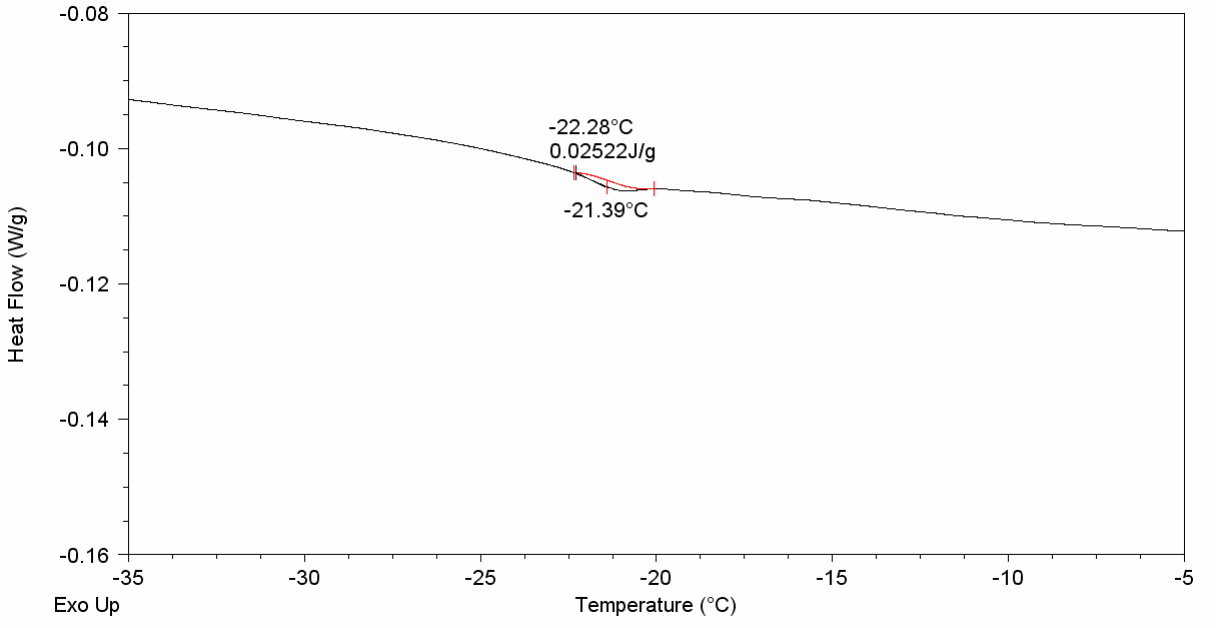

b) Expanded view of the melting endotherm portion of the curves shown above. The transition temperatures and enthalpy are as shown.

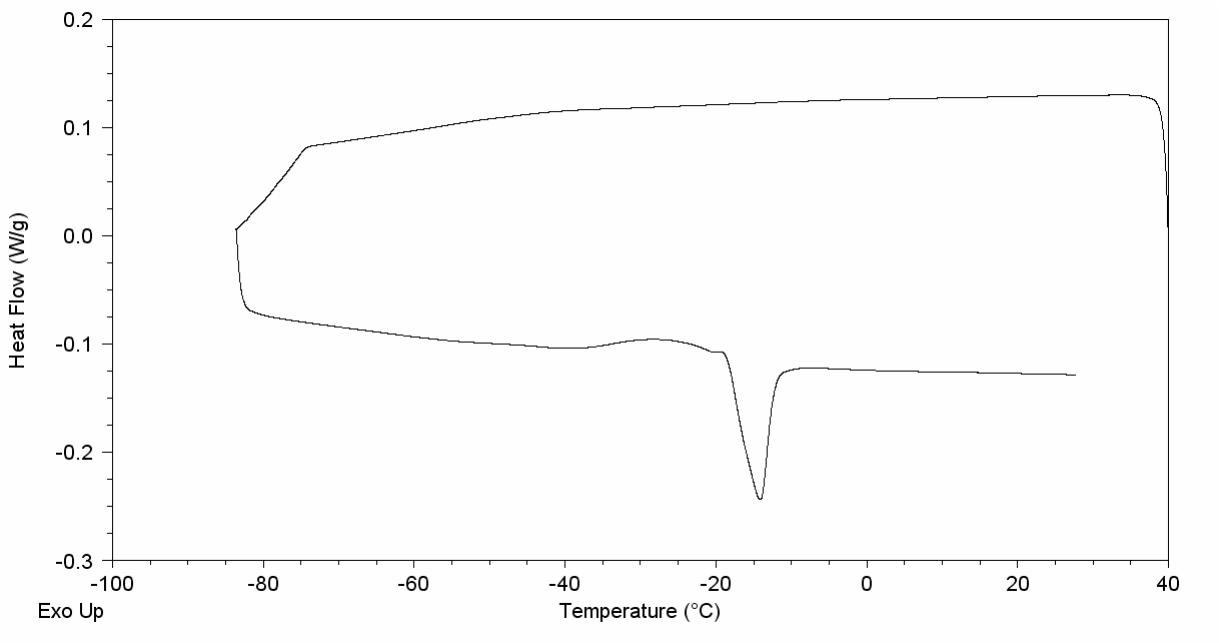

a) Cooling and heating curves for hyaluronan hydrogel of W_c 0.75.

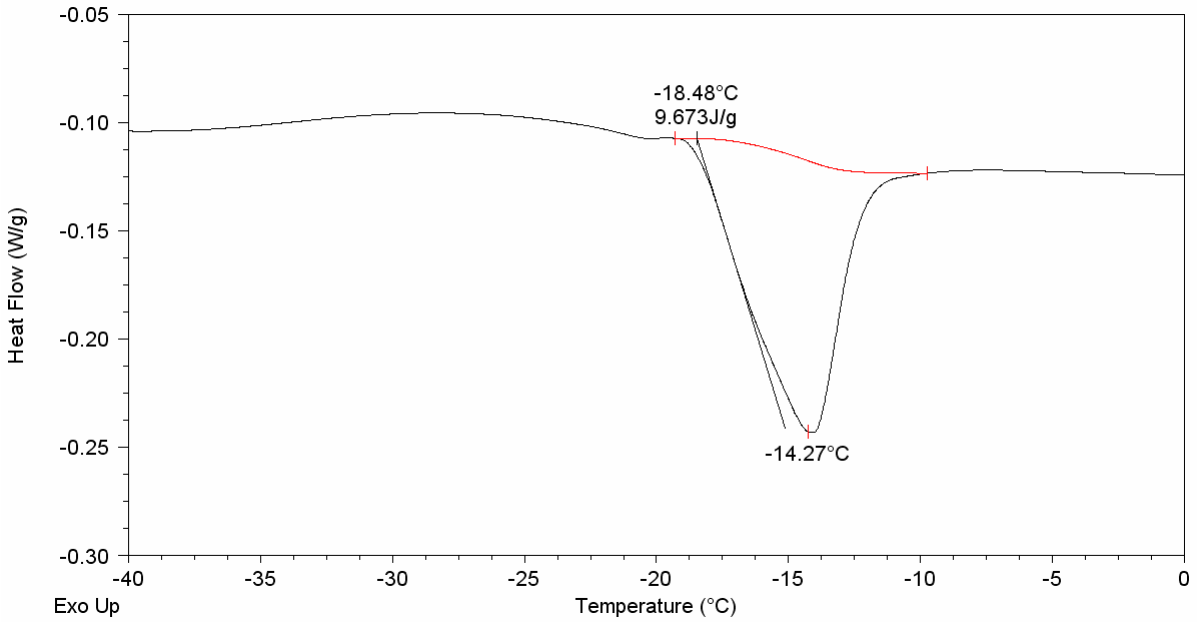

b) Expanded view of the melting endotherm portion of the curves shown above. The transition temperatures and enthalpy are as shown.

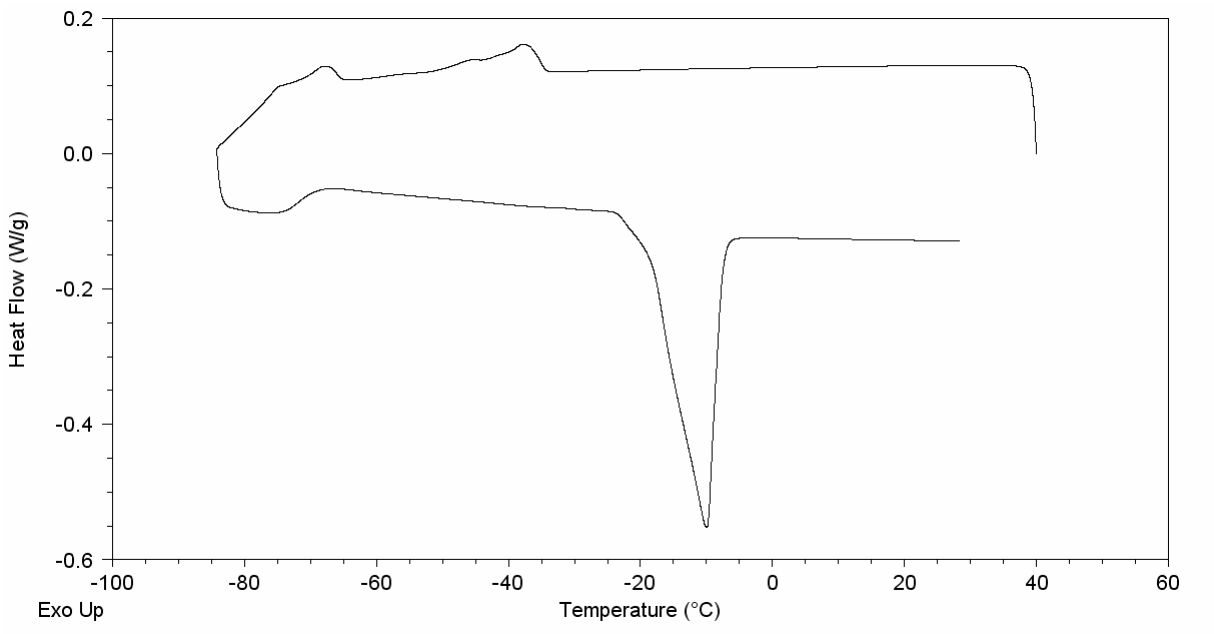

a) Cooling and heating curves for hyaluronan hydrogel of W_c 1.0.

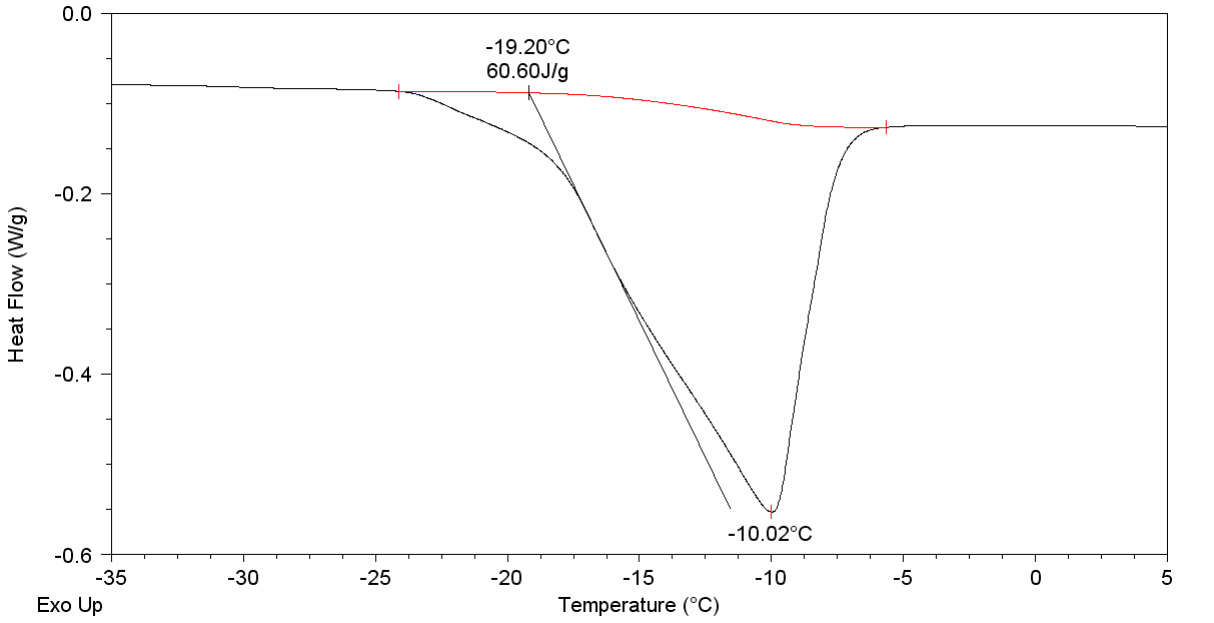

b) Expanded view of the melting endotherm portion of the curves shown above. The transition temperatures and enthalpy are as shown.

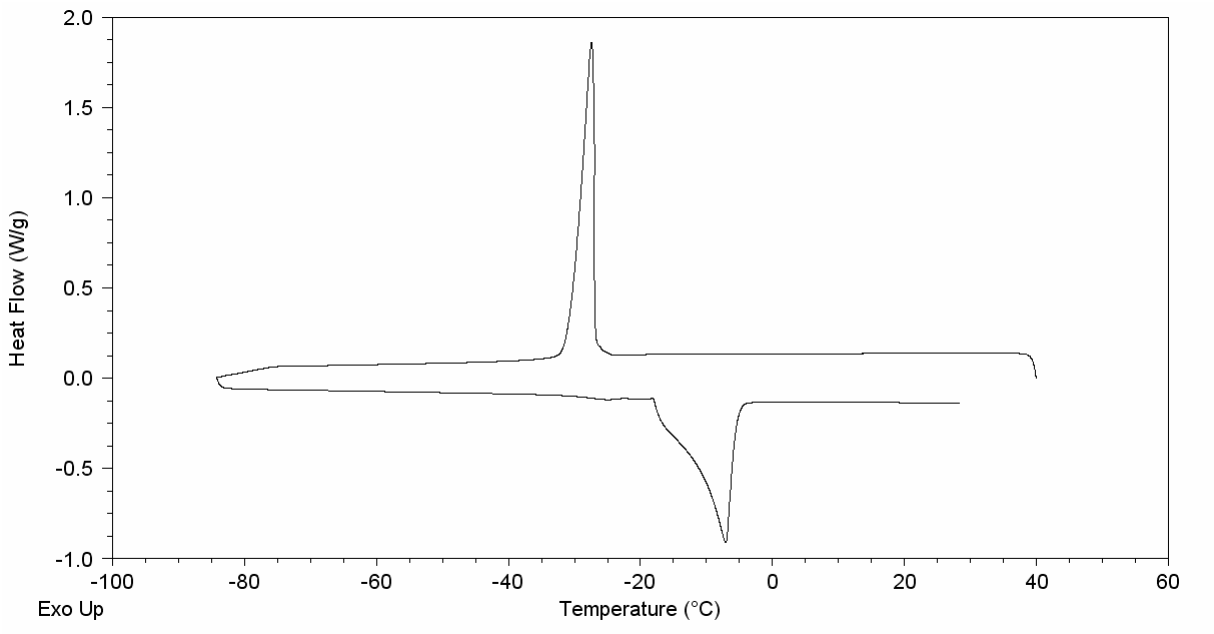

a) Cooling and heating curves for hyaluronan hydrogel of W_c 1.5.

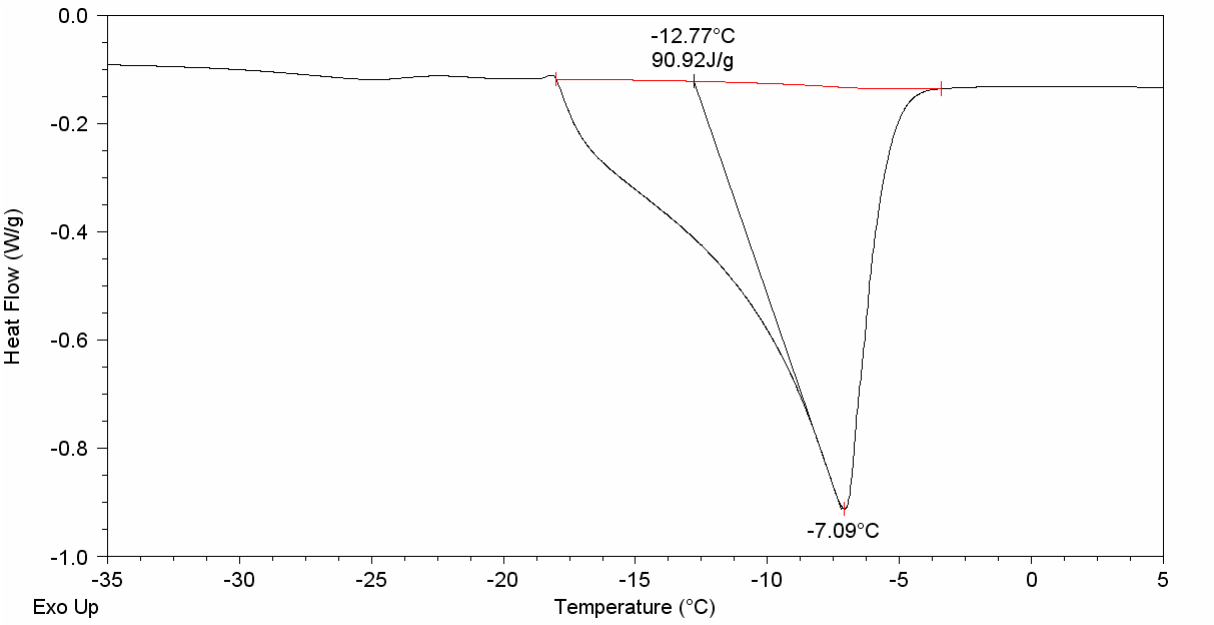

b) Expanded view of the melting endotherm portion of the curves shown above. The transition temperatures and enthalpy are as shown.

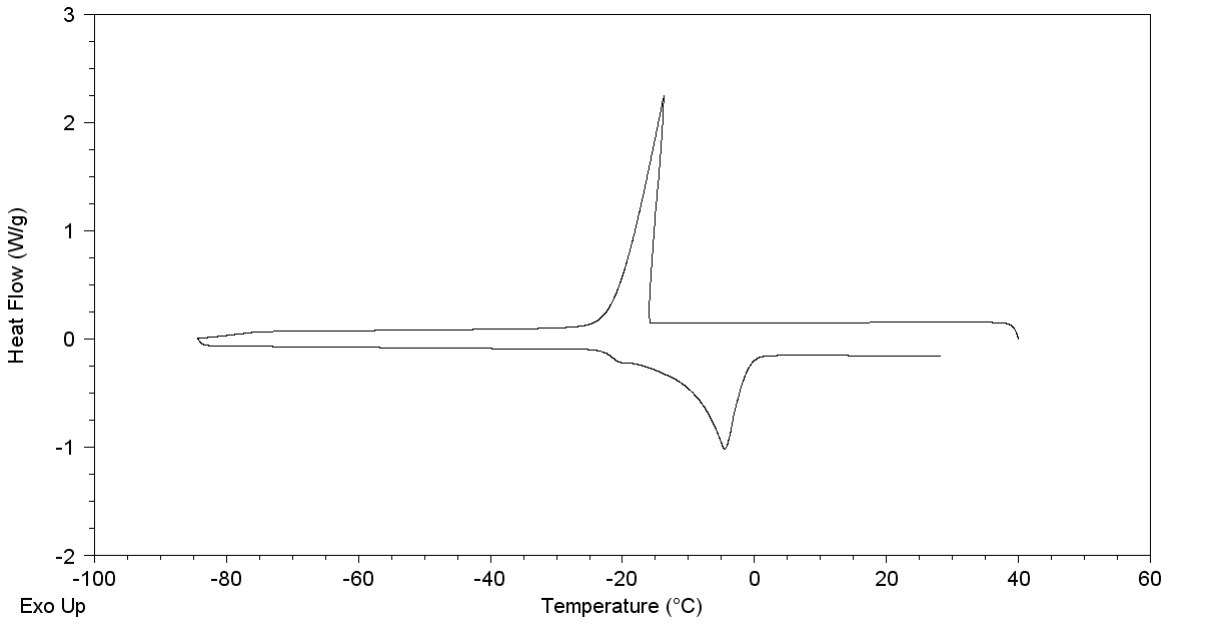

a) Cooling and heating curves for hyaluronan hydrogel of W_c 2.0.

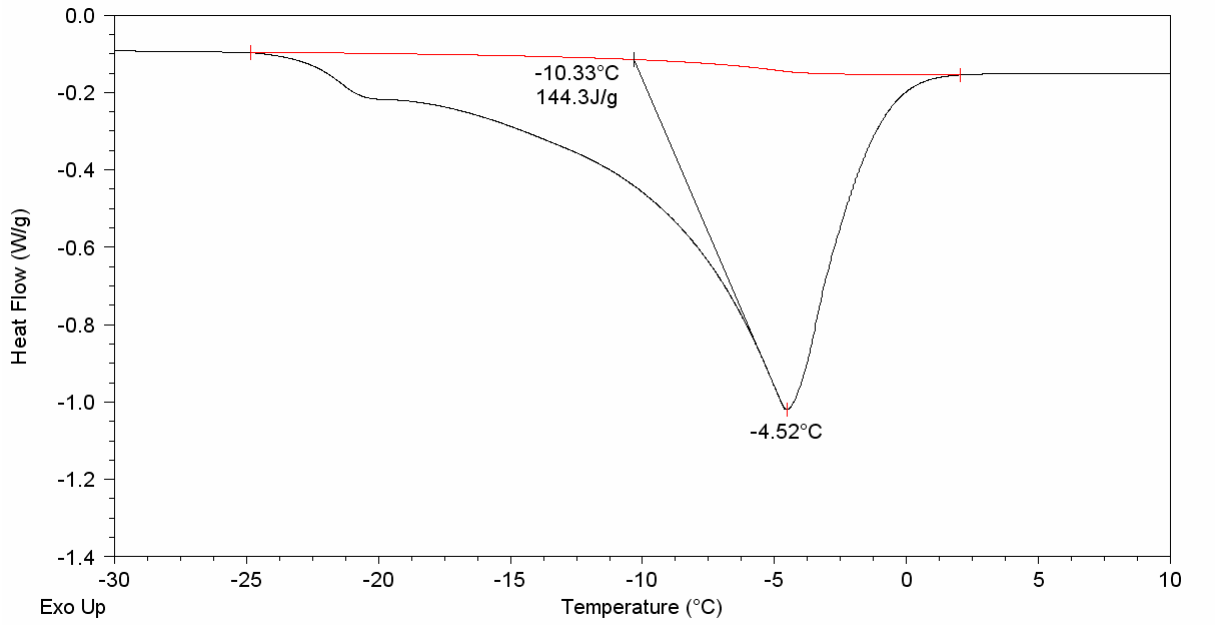

b) Expanded view of the melting endotherm portion of the curves shown above. The transition temperatures and enthalpy are as shown.

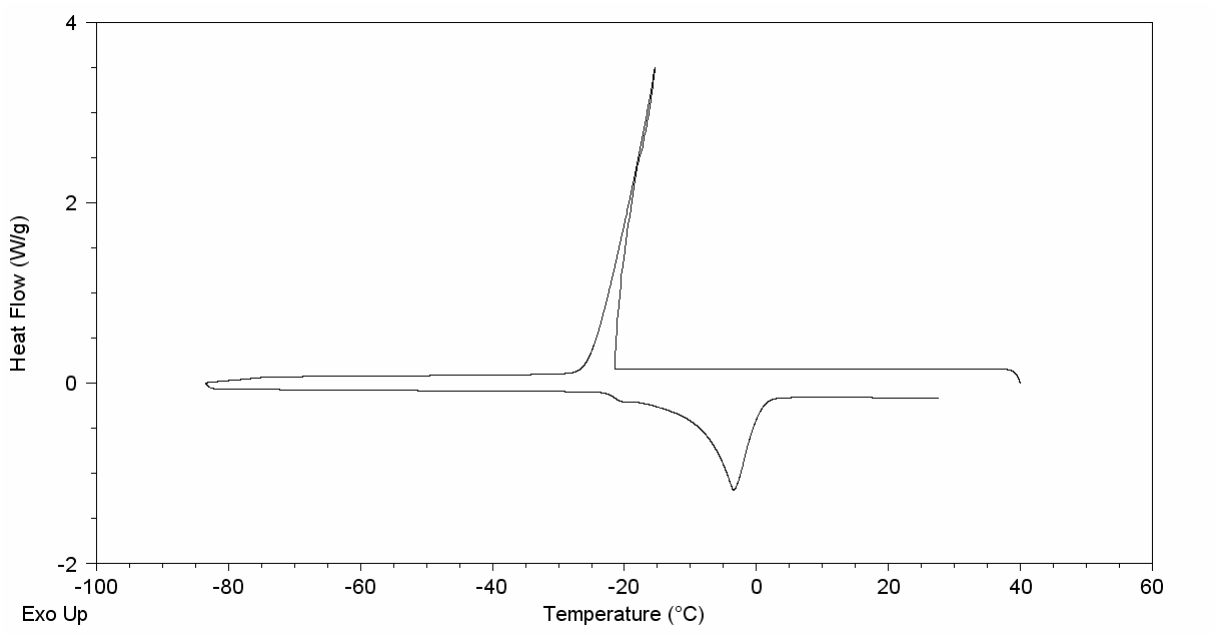

a) Cooling and heating curves for hyaluronan hydrogel of W_c 2.5.

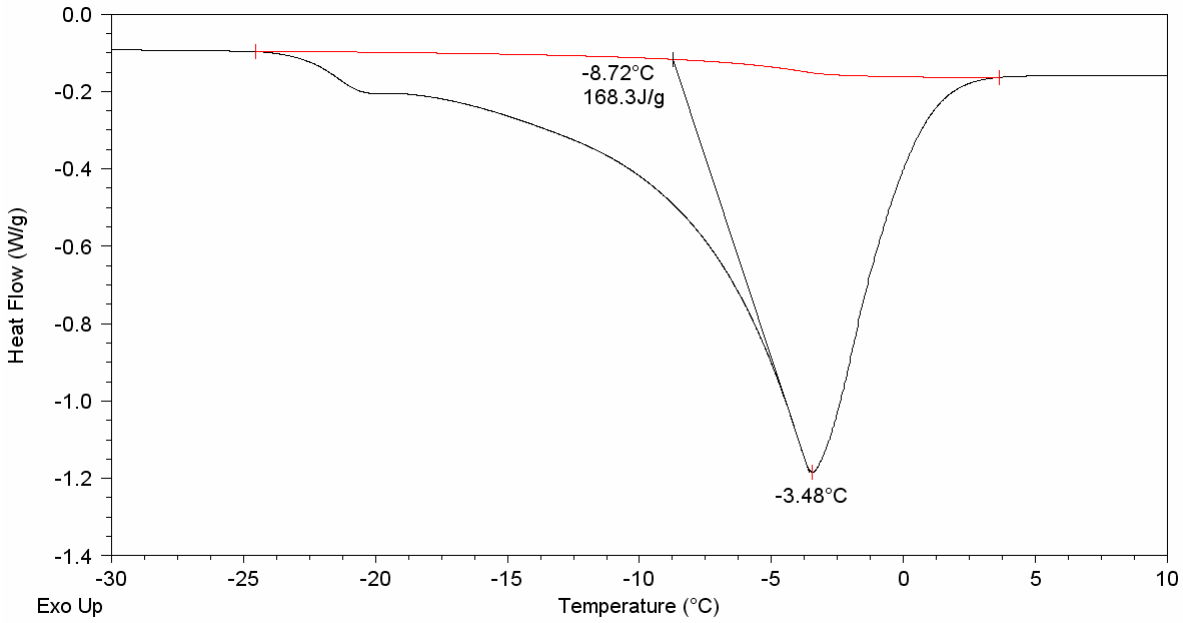

b) Expanded view of the melting endotherm portion of the curves shown above. The transition temperatures and enthalpy are as shown.

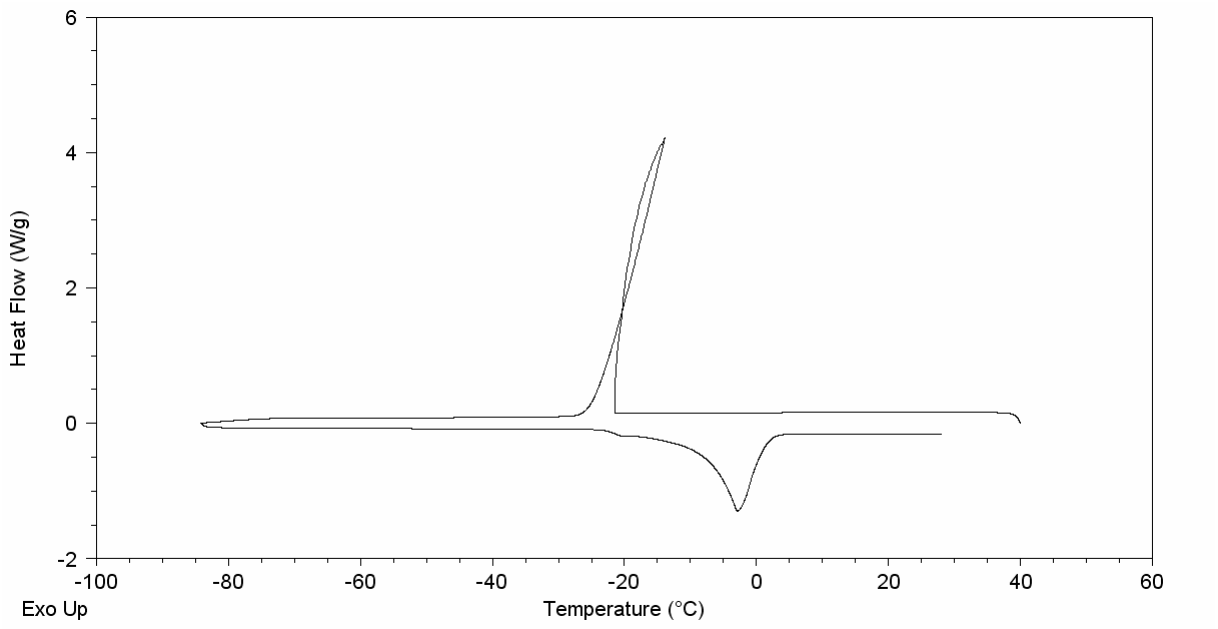

a) Cooling and heating curves for hyaluronan hydrogel of W_c 3.0.

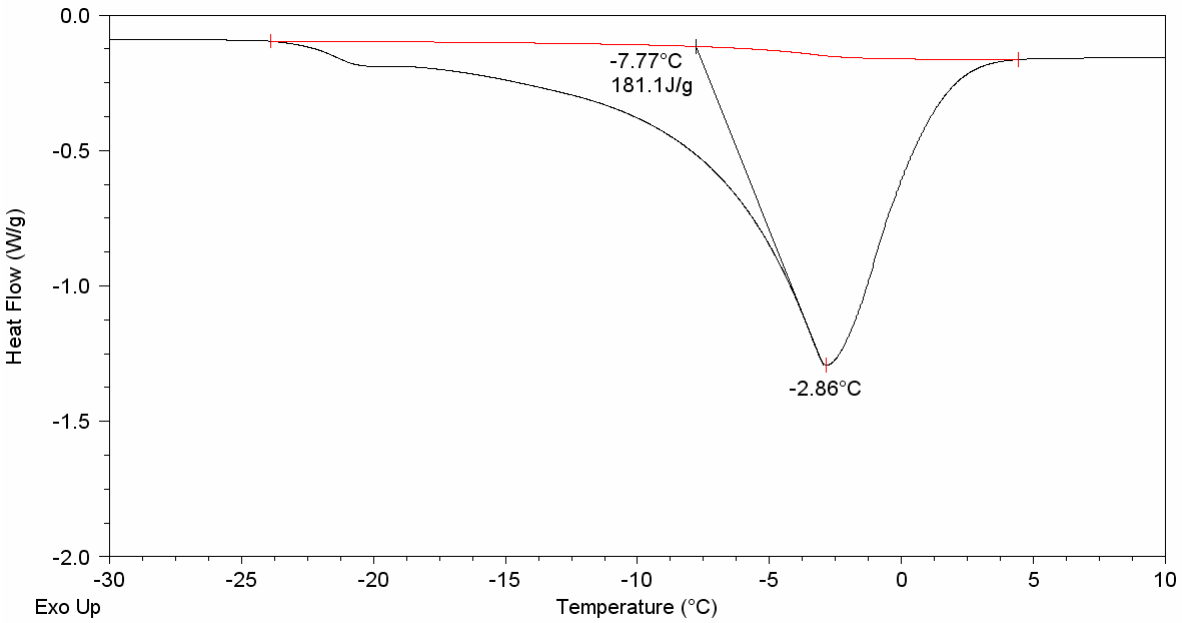

b) Expanded view of the melting endotherm portion of the curves shown above. The transition temperatures and enthalpy are as shown.

9.1.3 522.1 kDa hyaluronan

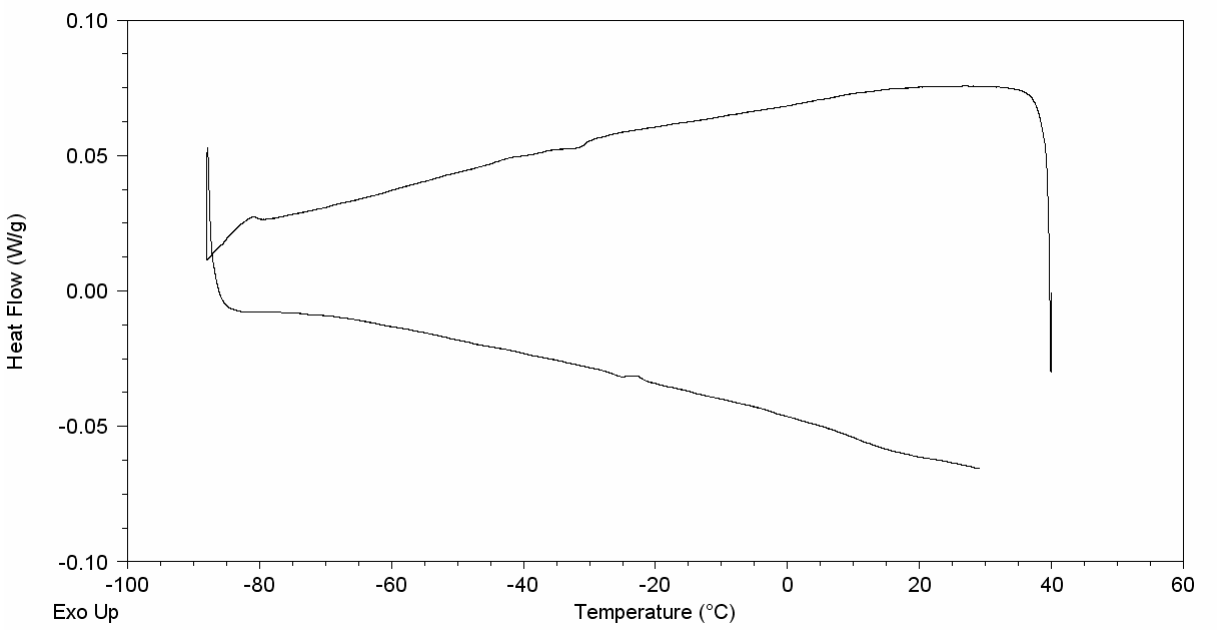

a) Cooling and heating curves for hyaluronan hydrogel of W_c 0.5.

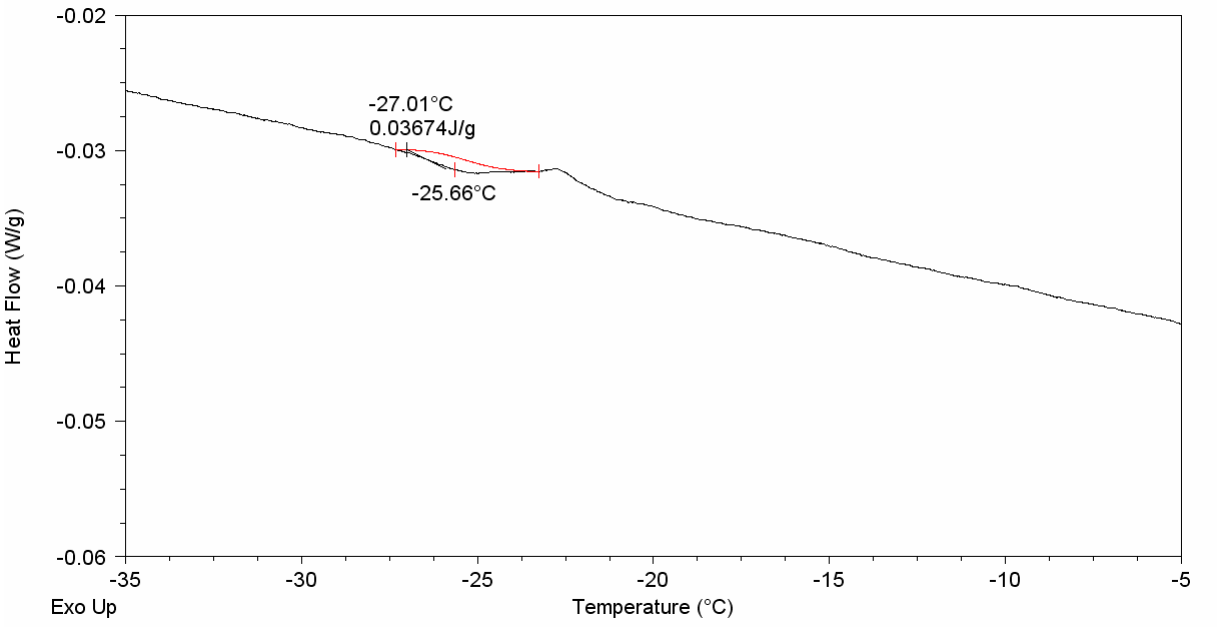

b) Expanded view of the melting endotherm portion of the curves shown above. The transition temperatures and enthalpy are as shown.

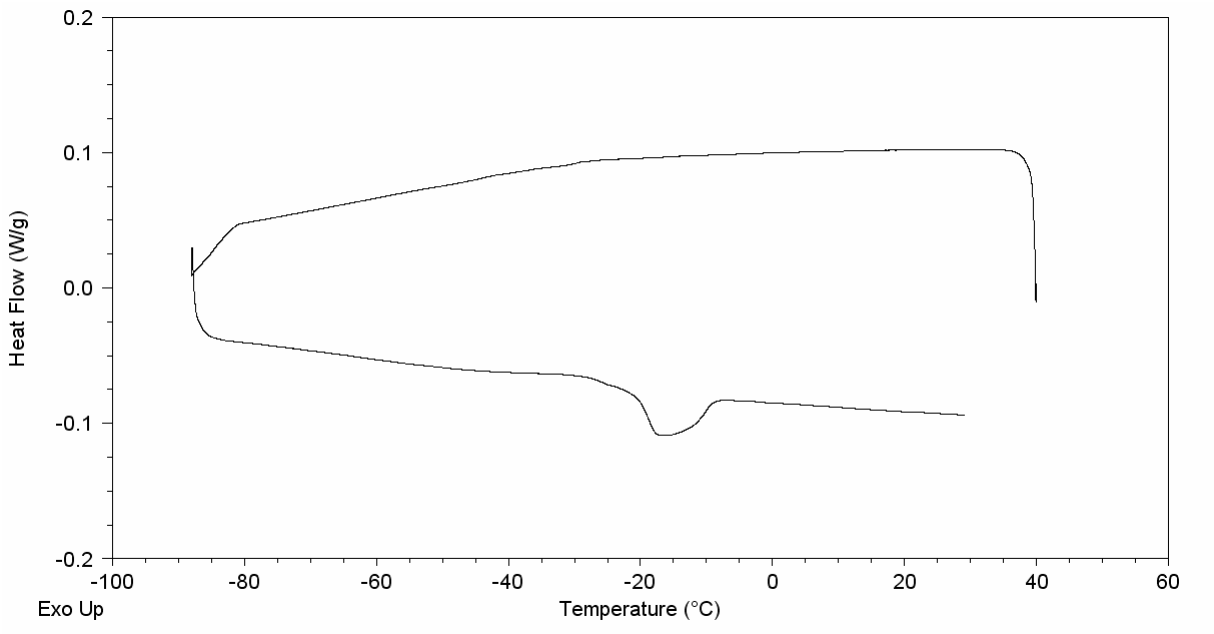

a) Cooling and heating curves for hyaluronan hydrogel of W_c 0.75.

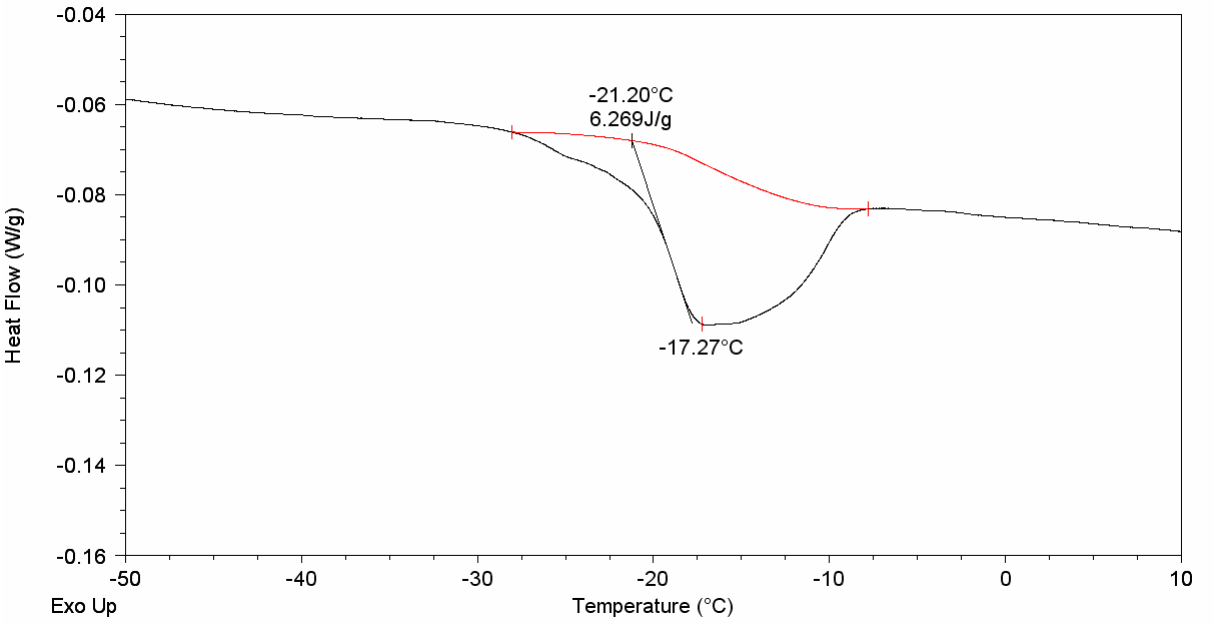

b) Expanded view of the melting endotherm portion of the curves shown above. The transition temperatures and enthalpy are as shown.

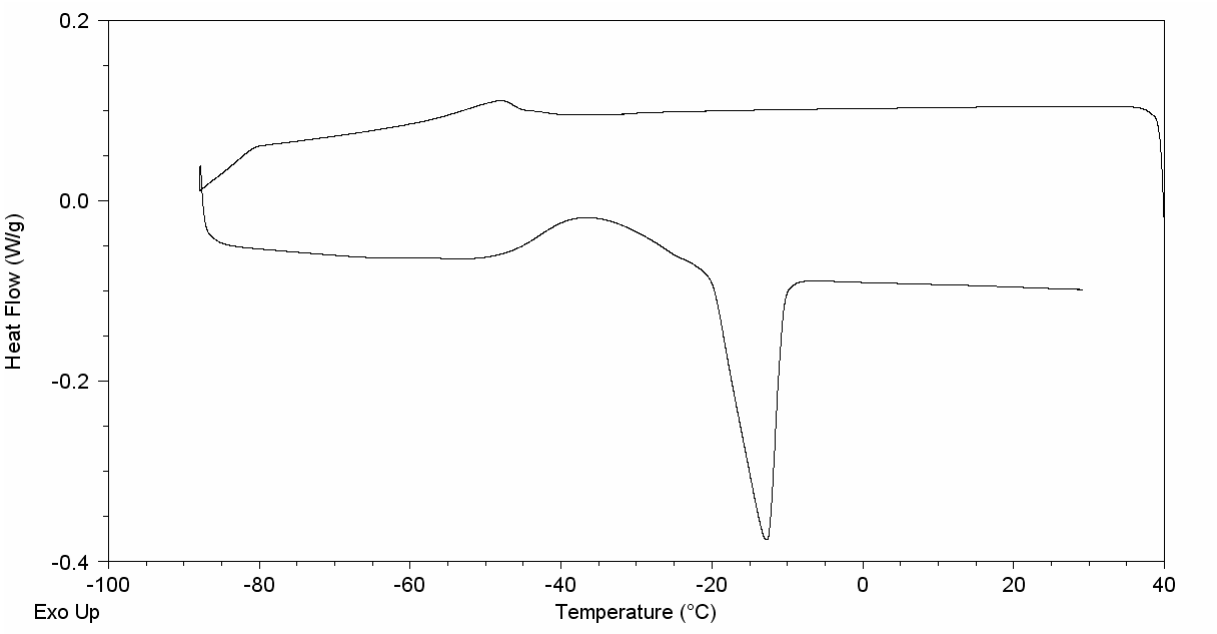

a) Cooling and heating curves for hyaluronan hydrogel of W_c 1.0.

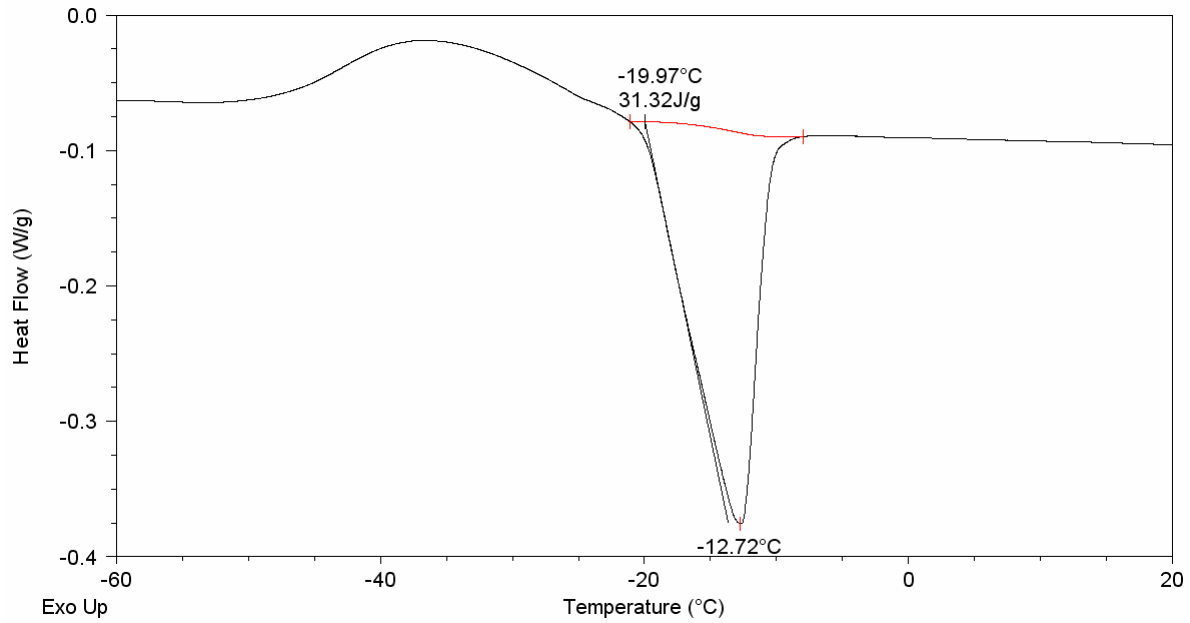

b) Expanded view of the melting endotherm portion of the curves shown above. The transition temperatures and enthalpy are as shown.

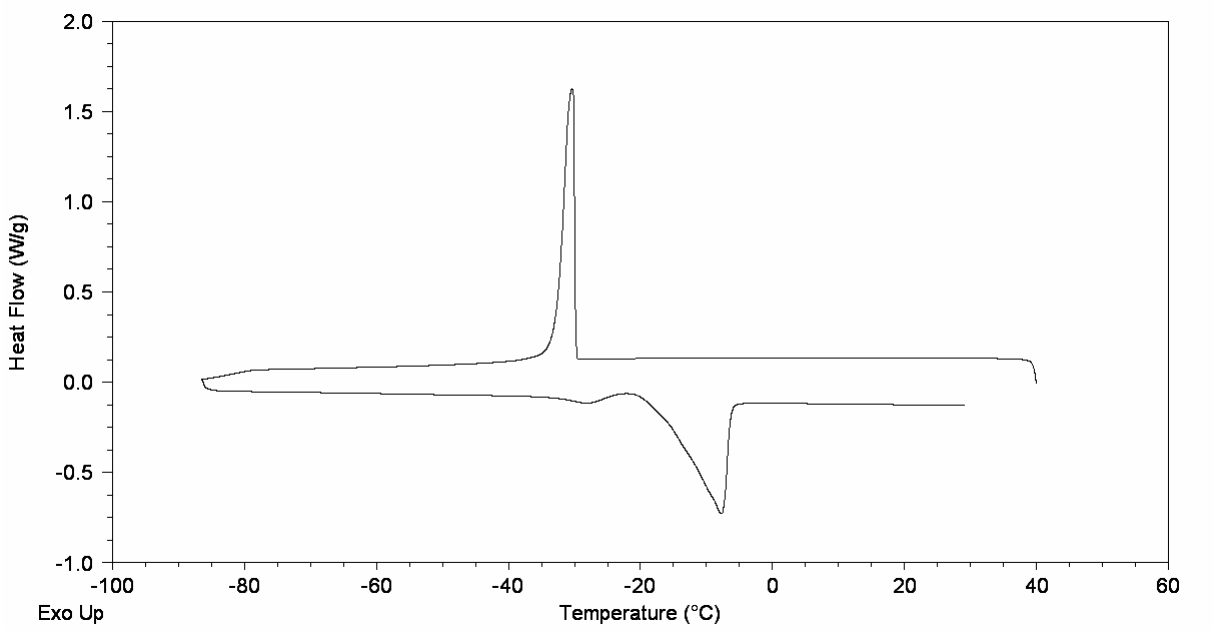

a) Cooling and heating curves for hyaluronan hydrogel of W_c 1.5.

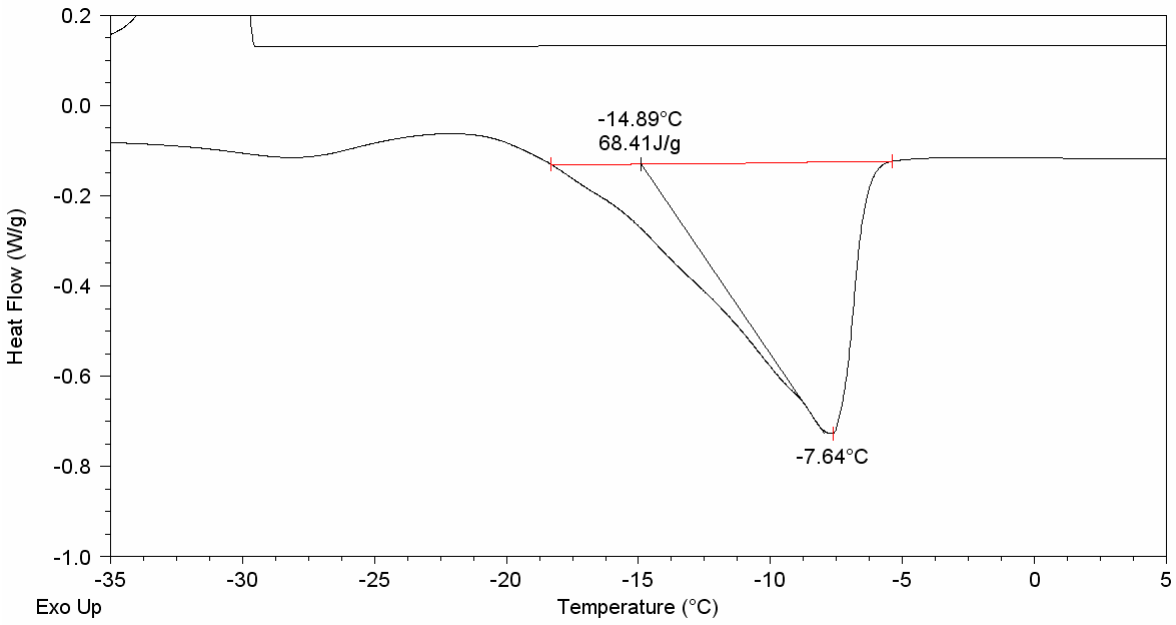

b) Expanded view of the melting endotherm portion of the curves shown above. The transition temperatures and enthalpy are as shown.

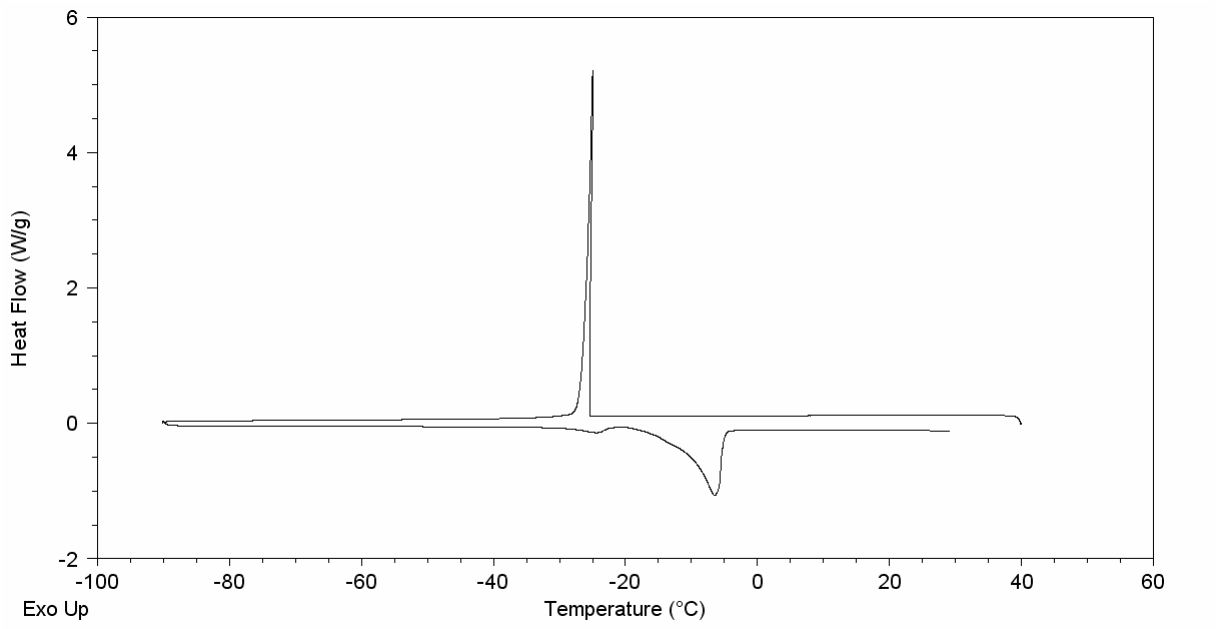

a) Cooling and heating curves for hyaluronan hydrogel of W_c 2.0.

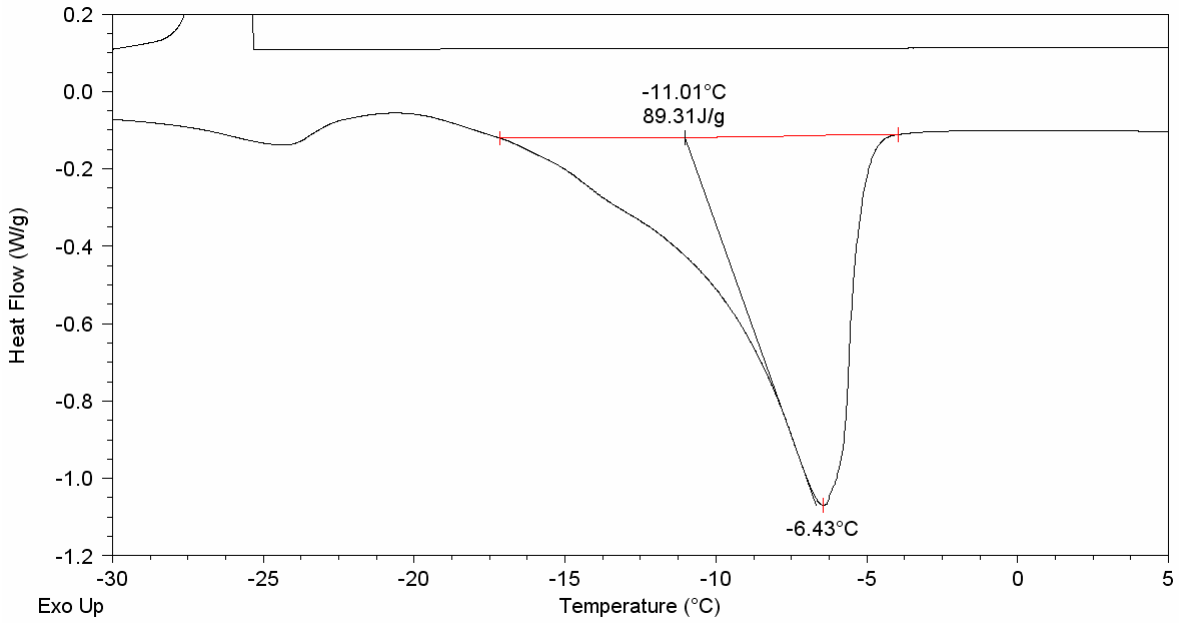

b) Expanded view of the melting endotherm portion of the curves shown above. The transition temperatures and enthalpy are as shown.

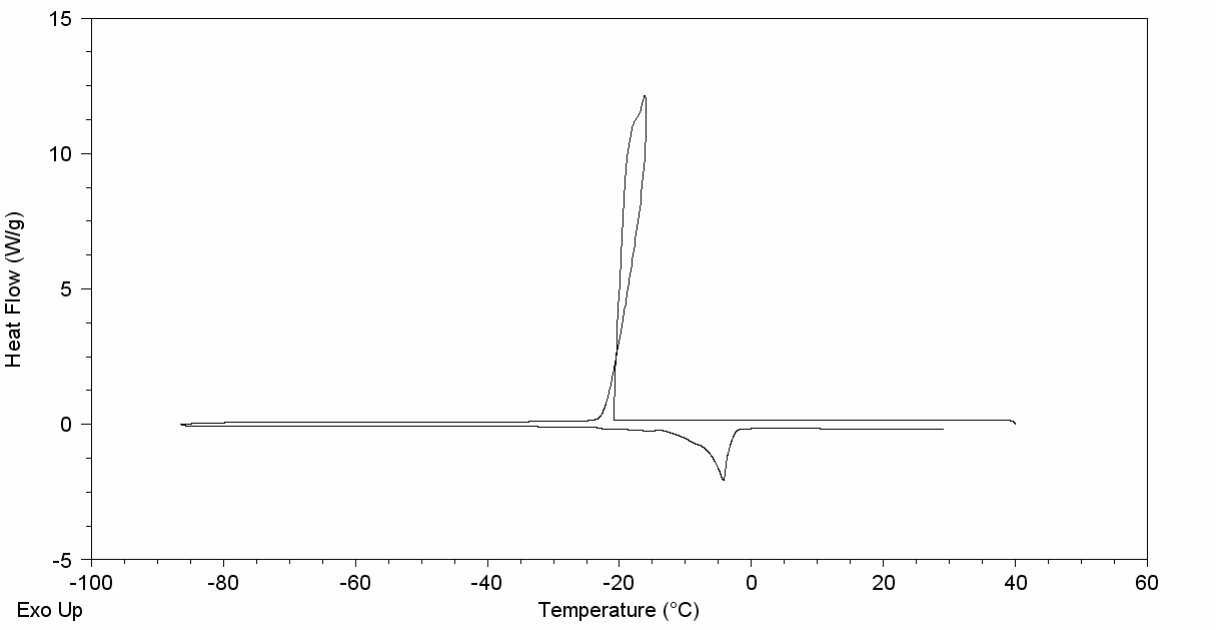

a) Cooling and heating curves for hyaluronan hydrogel of W_c 2.5.

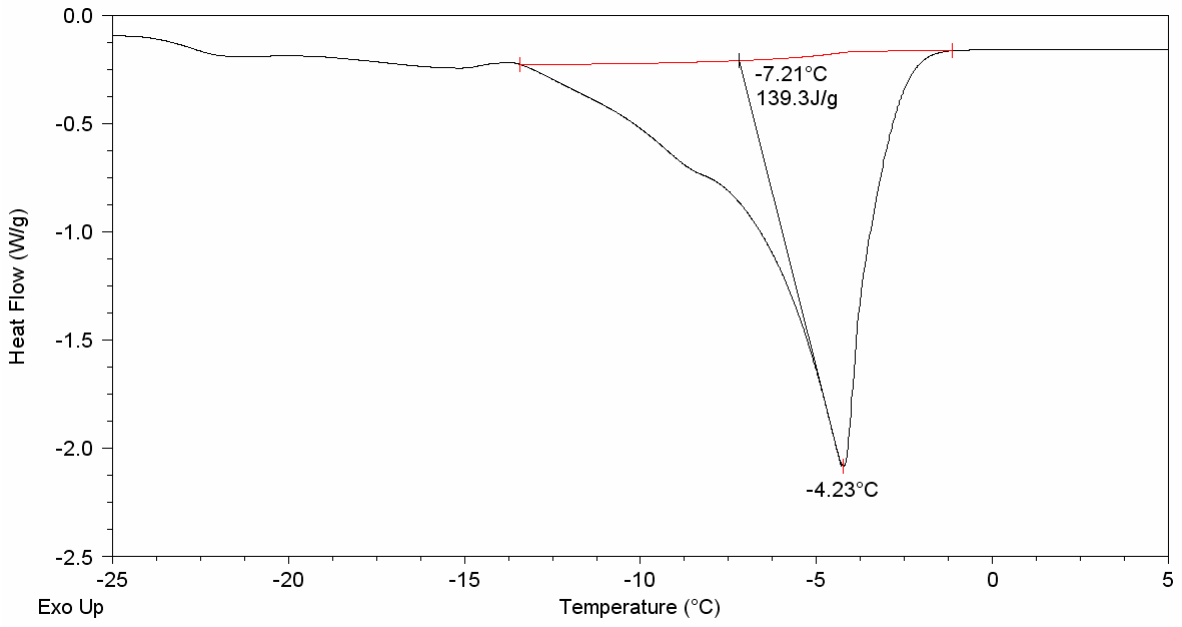

b) Expanded view of the melting endotherm portion of the curves shown above. The transition temperatures and enthalpy are as shown.

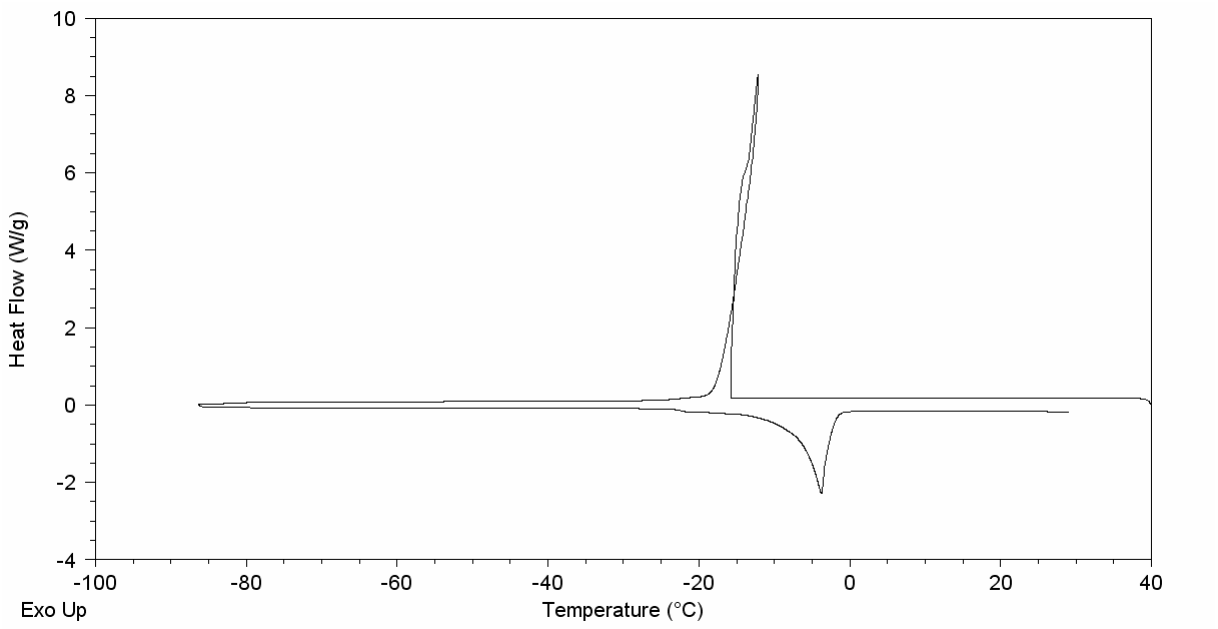

a) Cooling and heating curves for hyaluronan hydrogel of W_c 3.0.

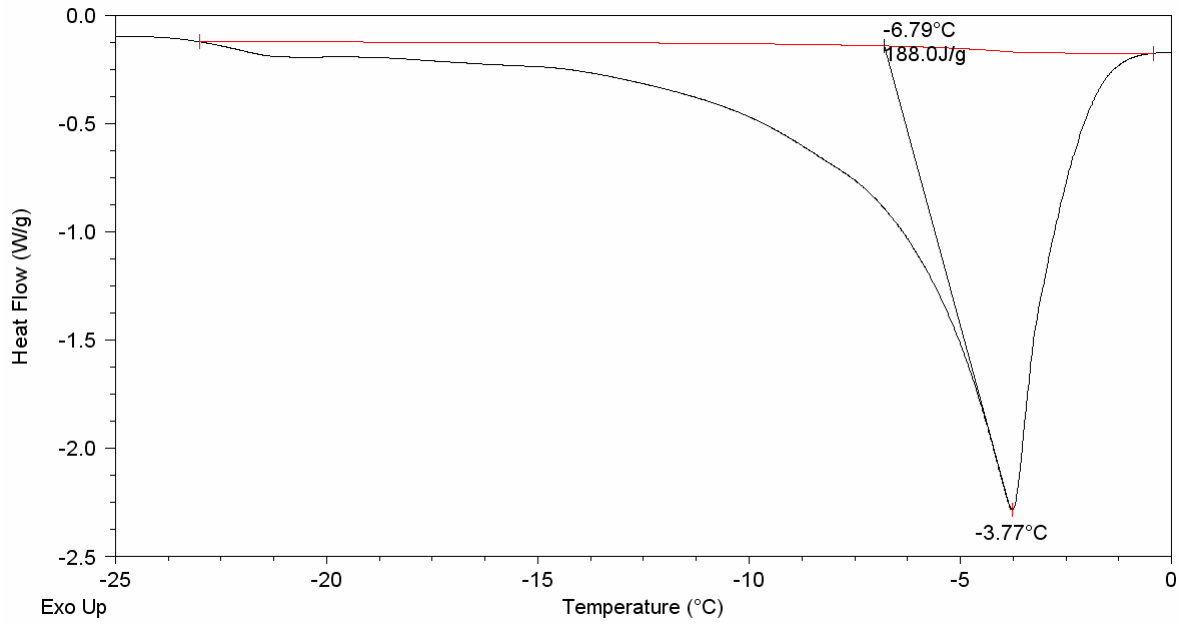

b) Expanded view of the melting endotherm portion of the curves shown above. The transition temperatures and enthalpy are as shown.

9.1.4 740 kDa hyaluronan

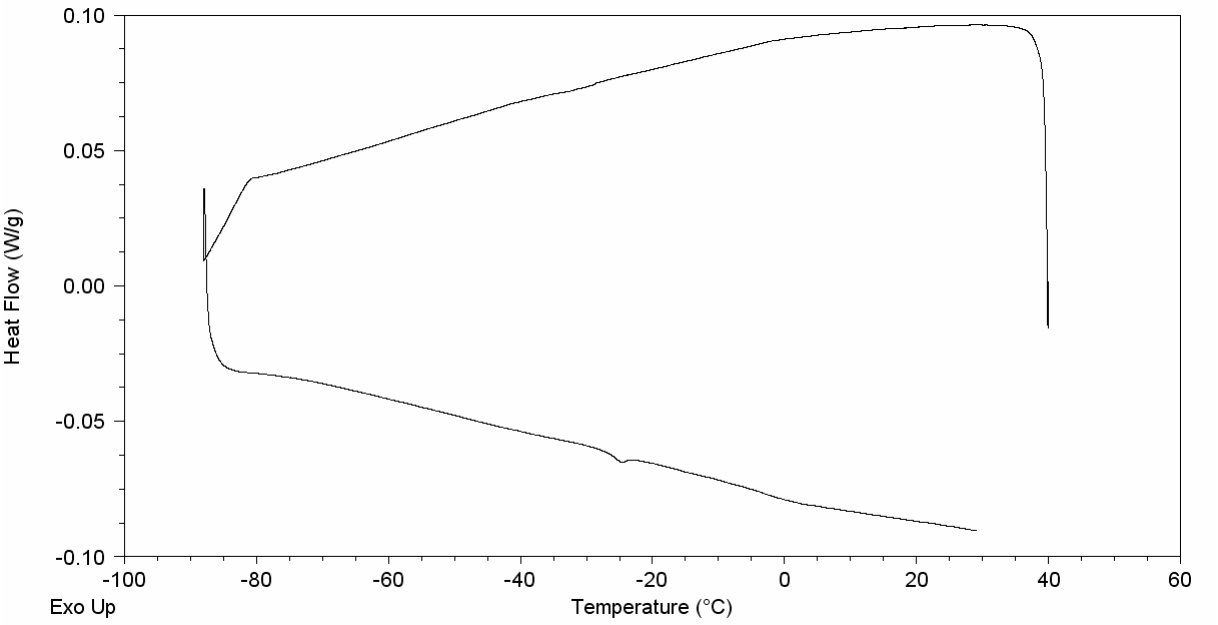

a) Cooling and heating curves for hyaluronan hydrogel of W_c 0.5.

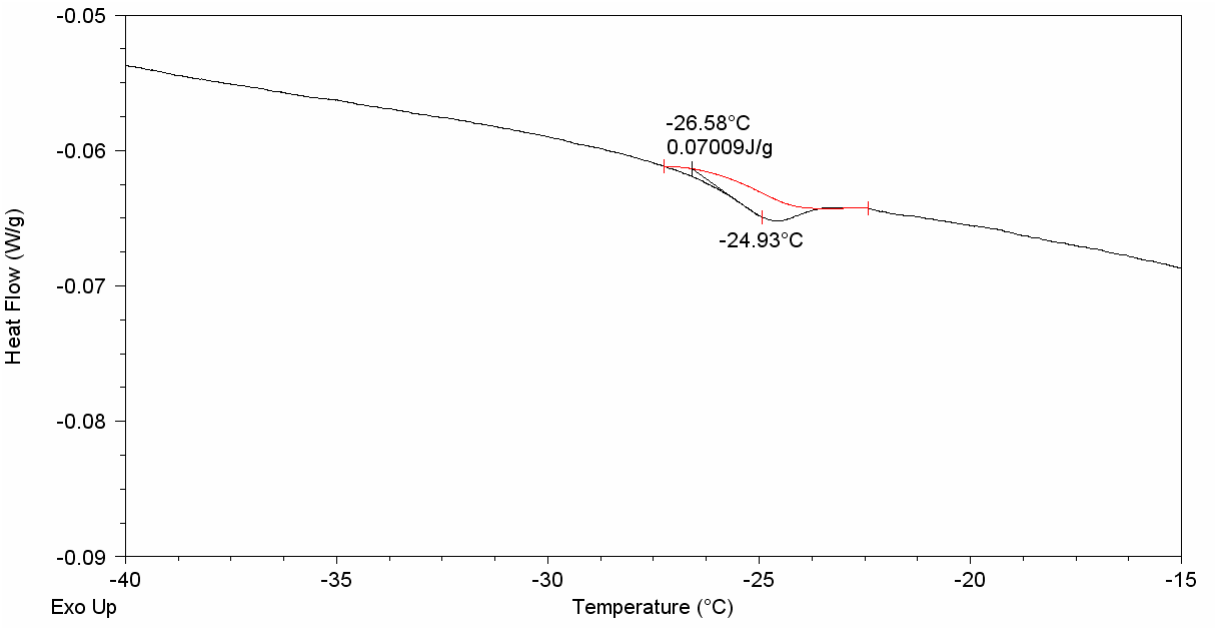

b) *Expanded view of the melting endotherm portion of the curves shown above. The transition temperatures and enthalpy are as shown.*

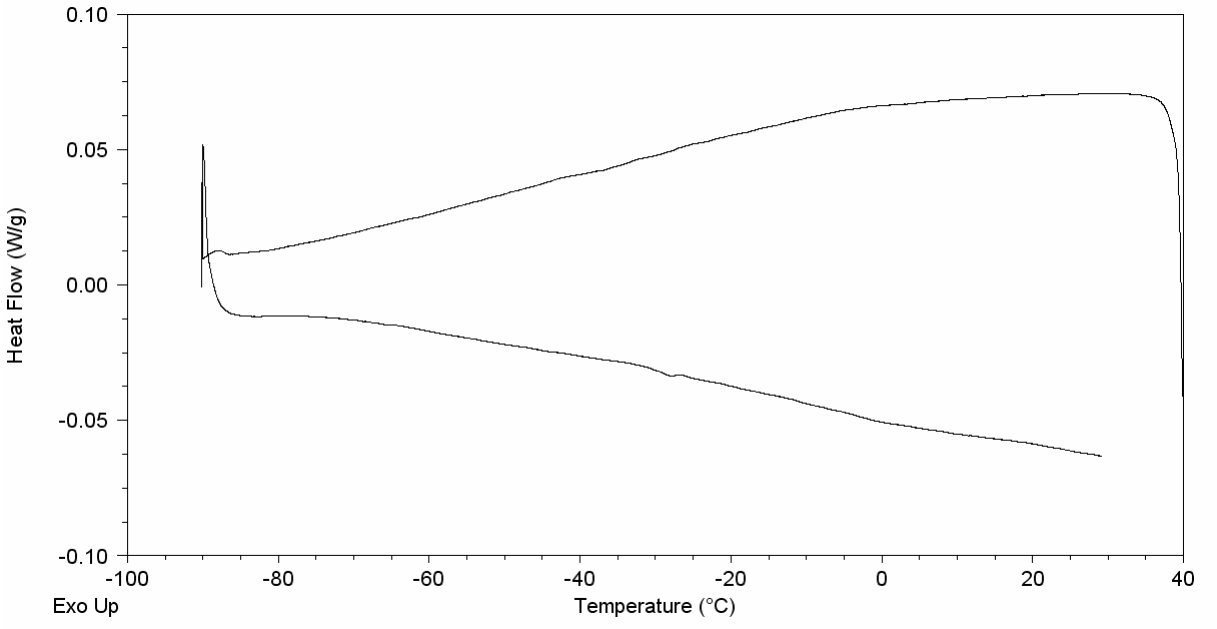

a) Cooling and heating curves for hyaluronan hydrogel of W_c 0.75.

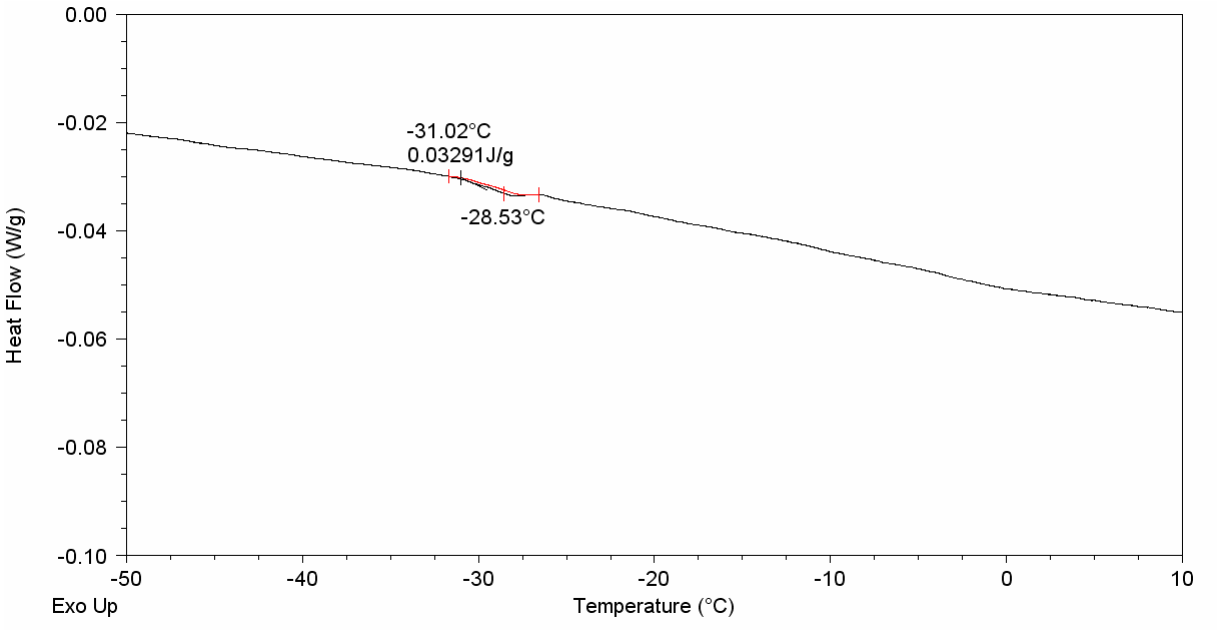

b) Expanded view of the melting endotherm portion of the curves shown above. The transition temperatures and enthalpy are as shown.

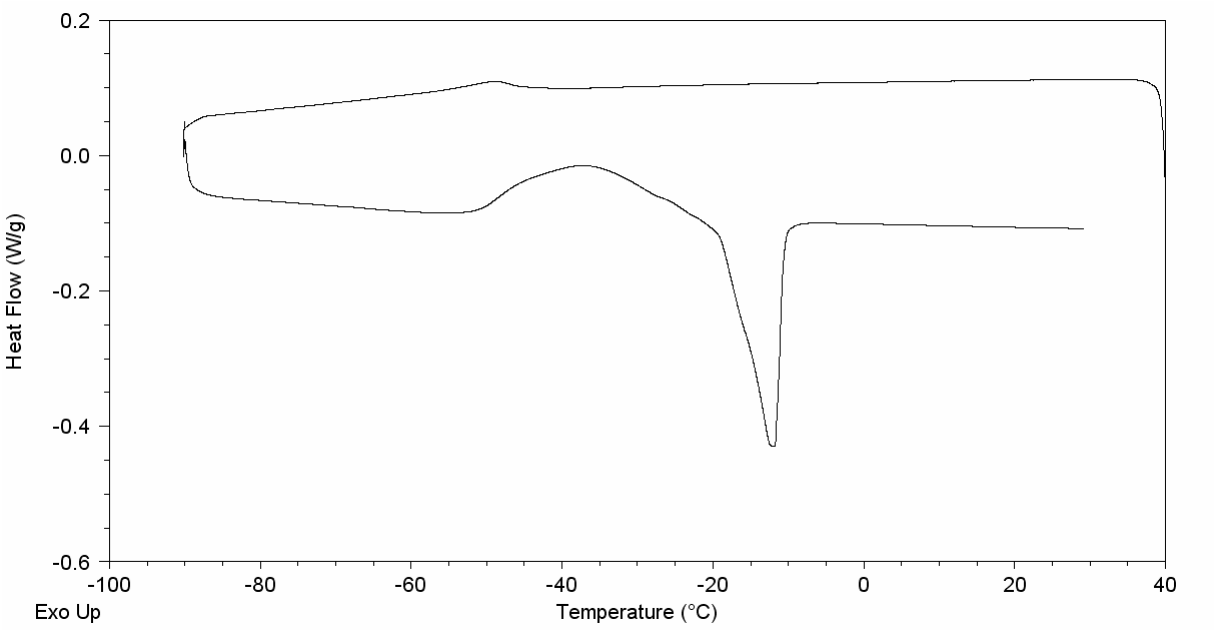

a) Cooling and heating curves for hyaluronan hydrogel of W_c 1.0.

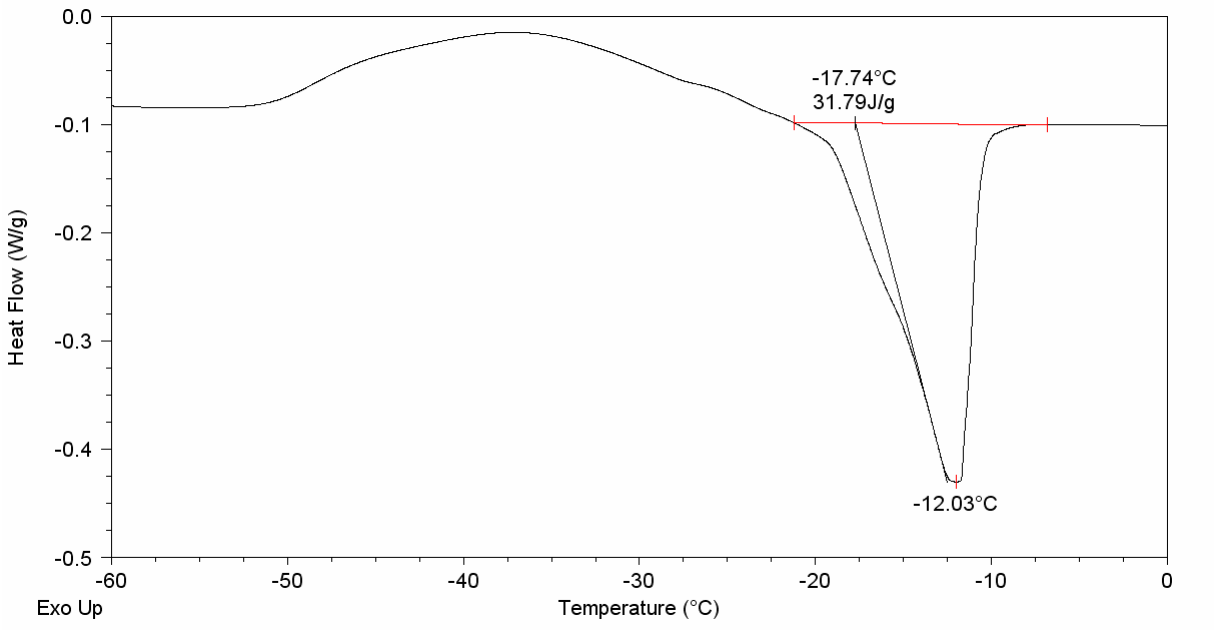

b) Expanded view of the melting endotherm portion of the curves shown above. The transition temperatures and enthalpy are as shown.

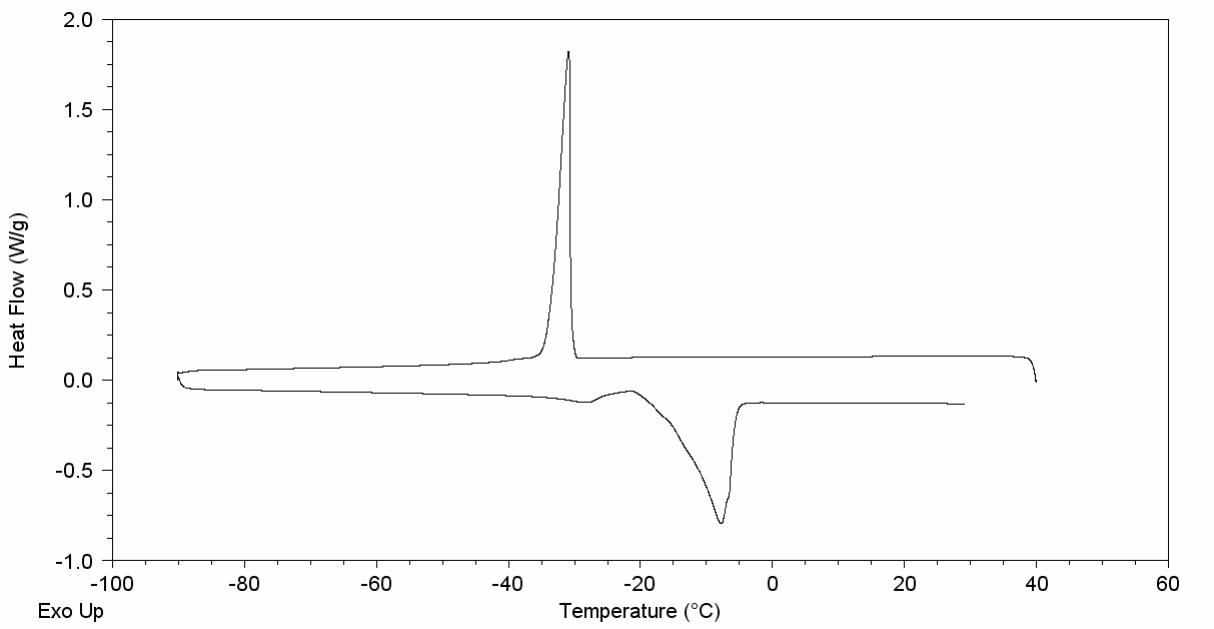

a) Cooling and heating curves for hyaluronan hydrogel of W_c 1.5.

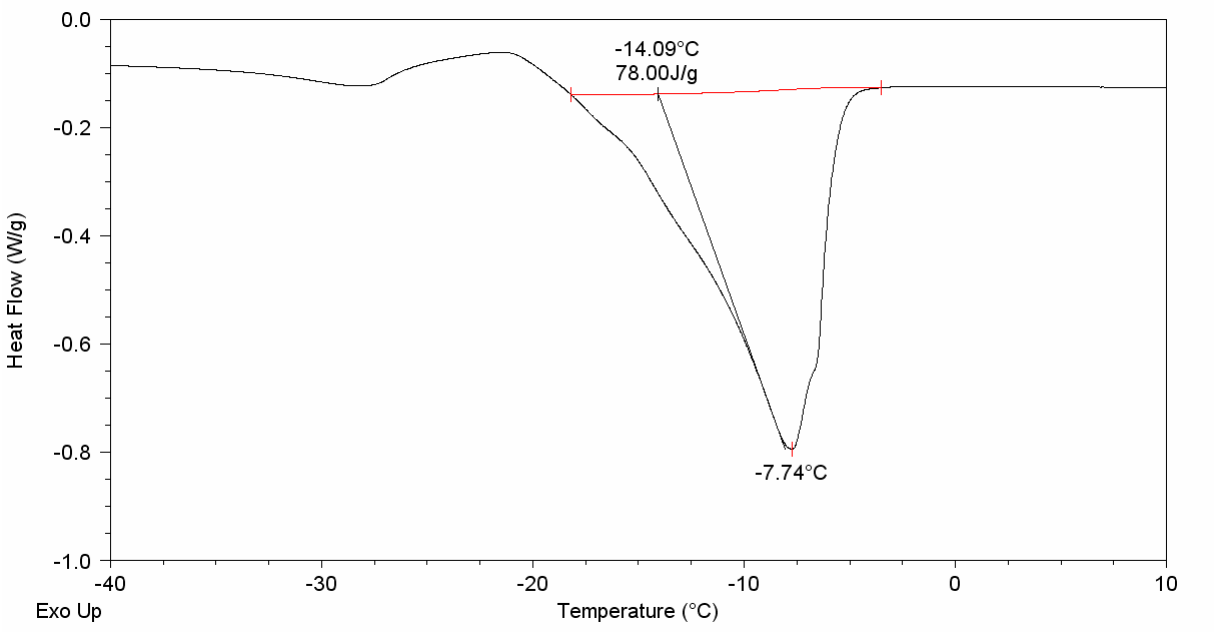

b) Expanded view of the melting endotherm portion of the curves shown above. The transition temperatures and enthalpy are as shown.

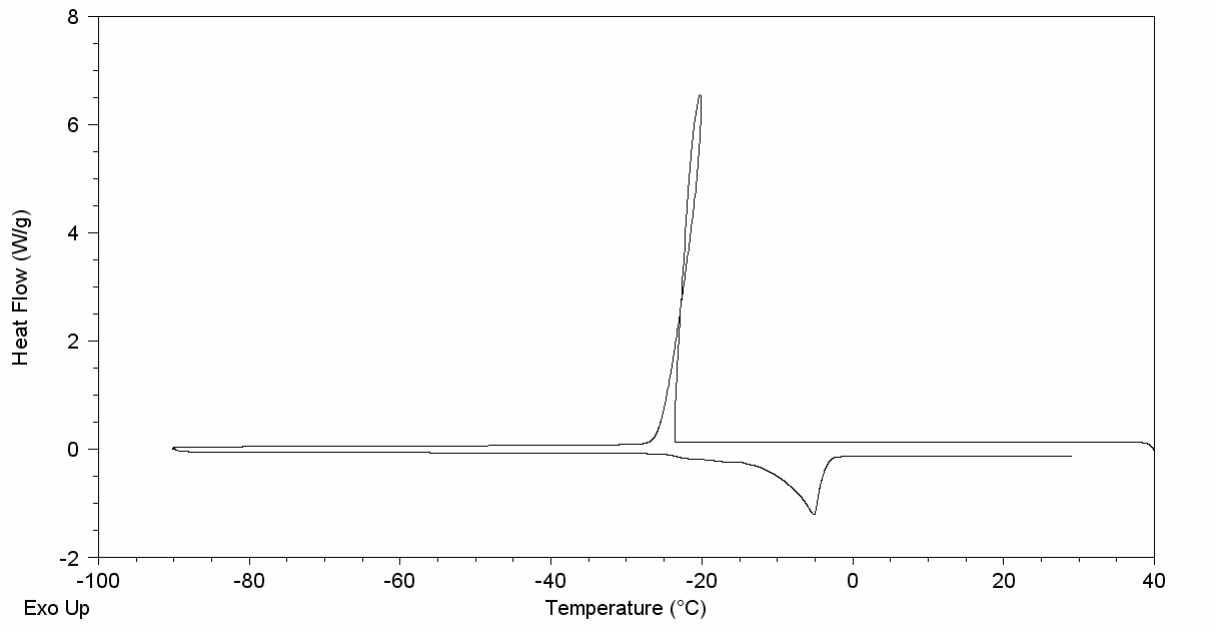

a) Cooling and heating curves for hyaluronan hydrogel of W_c 2.0.

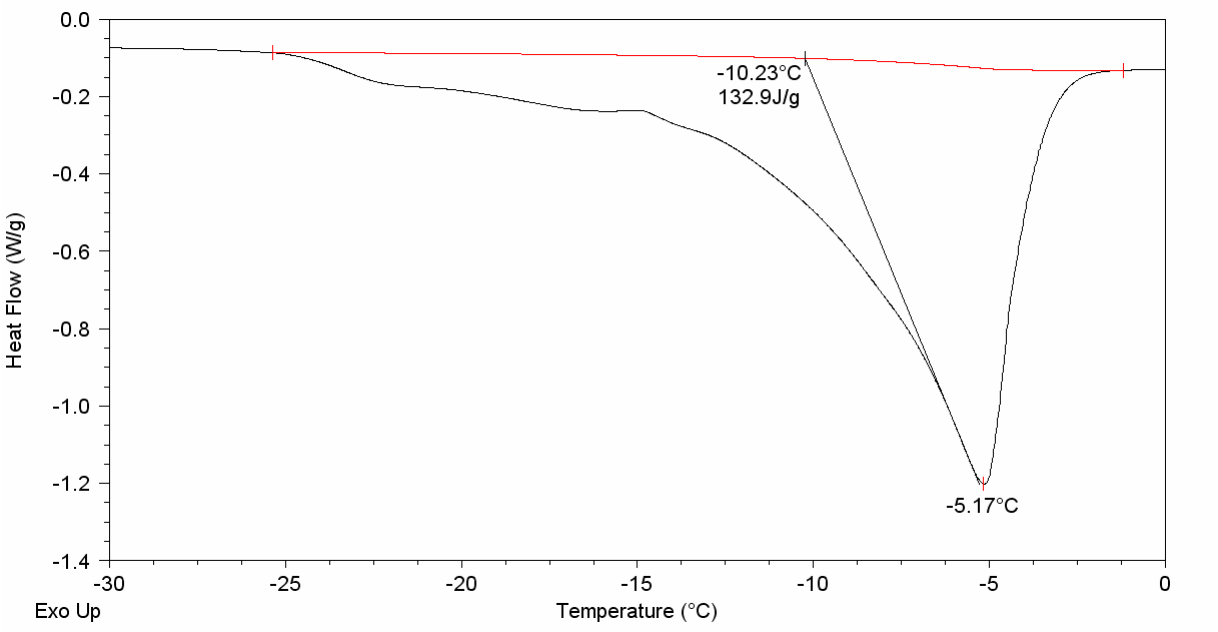

b) Expanded view of the melting endotherm portion of the curves shown above. The transition temperatures and enthalpy are as shown.

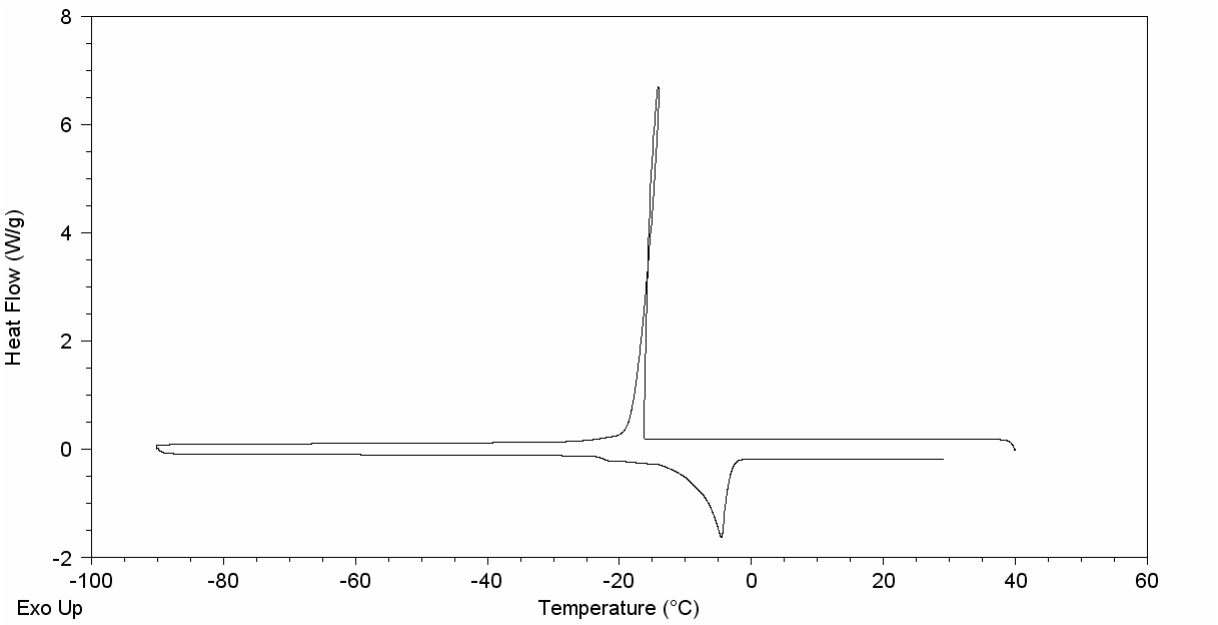

a) Cooling and heating curves for hyaluronan hydrogel of W_c 2.5

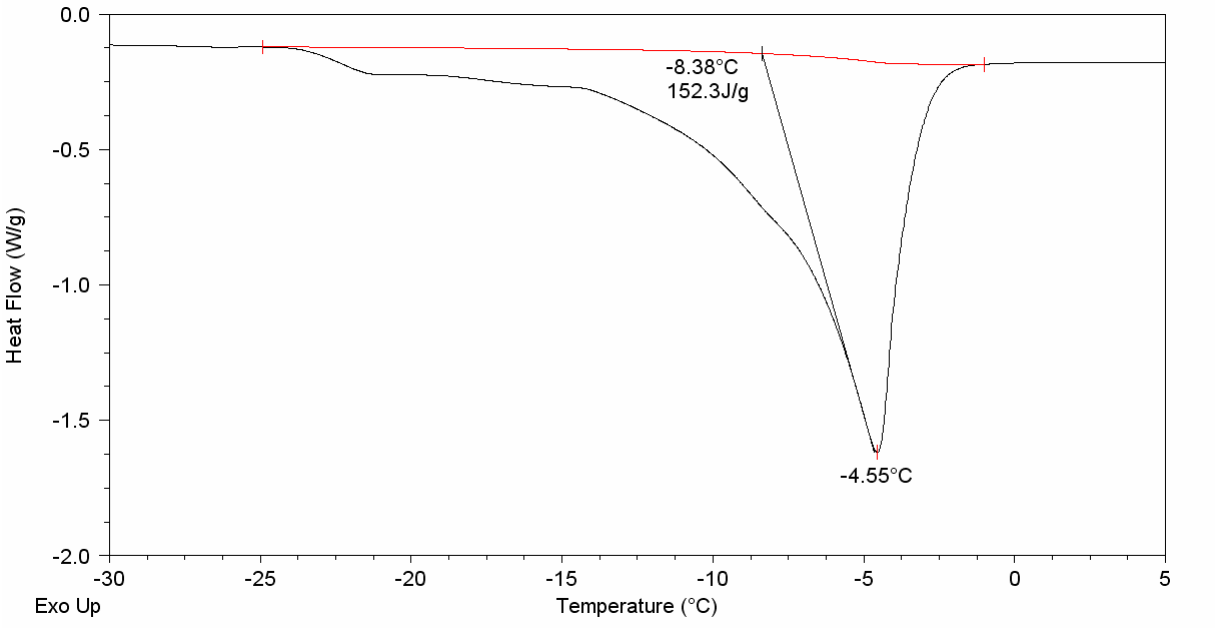

b) Expanded view of the melting endotherm portion of the curves shown above. The transition temperatures and enthalpy are as shown.

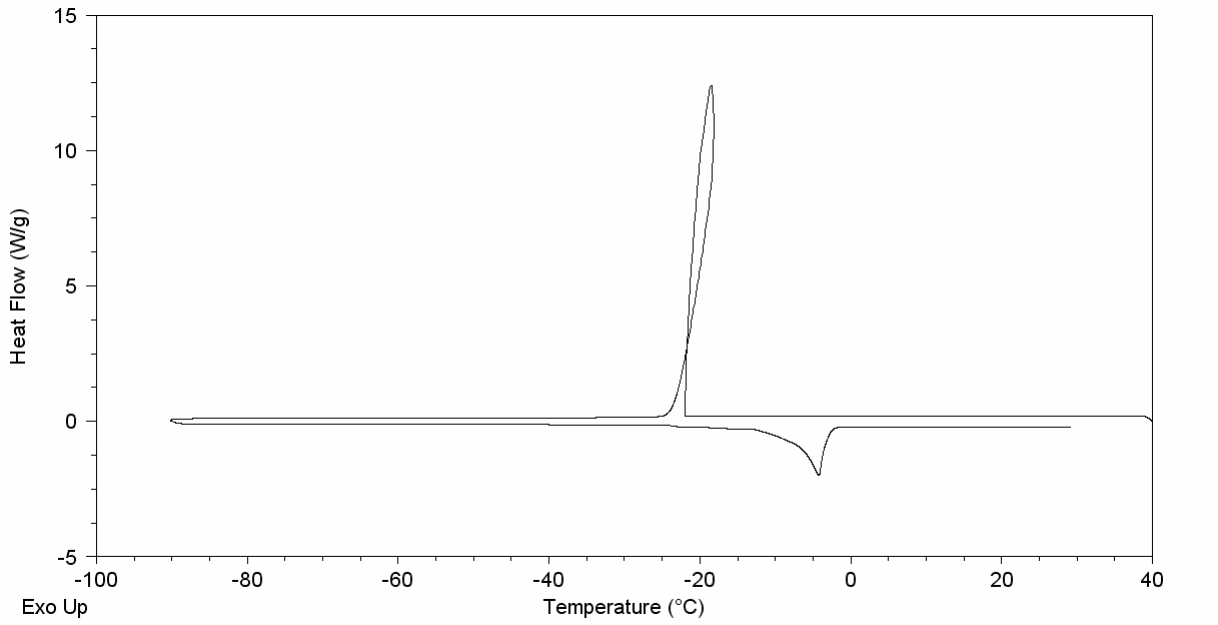

a) Cooling and heating curves for hyaluronan hydrogel of W_c 3.0.

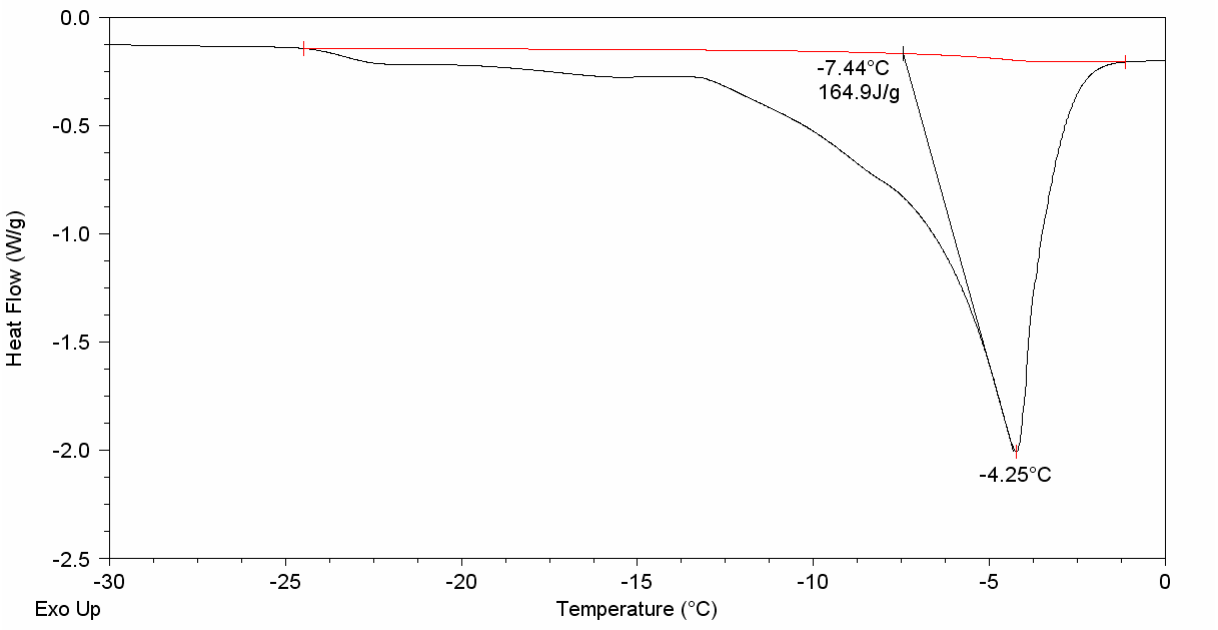

b) Expanded view of the melting endotherm portion of the curves shown above. The transition temperatures and enthalpy are as shown.

9.1.5 1390 kDa hyaluronan

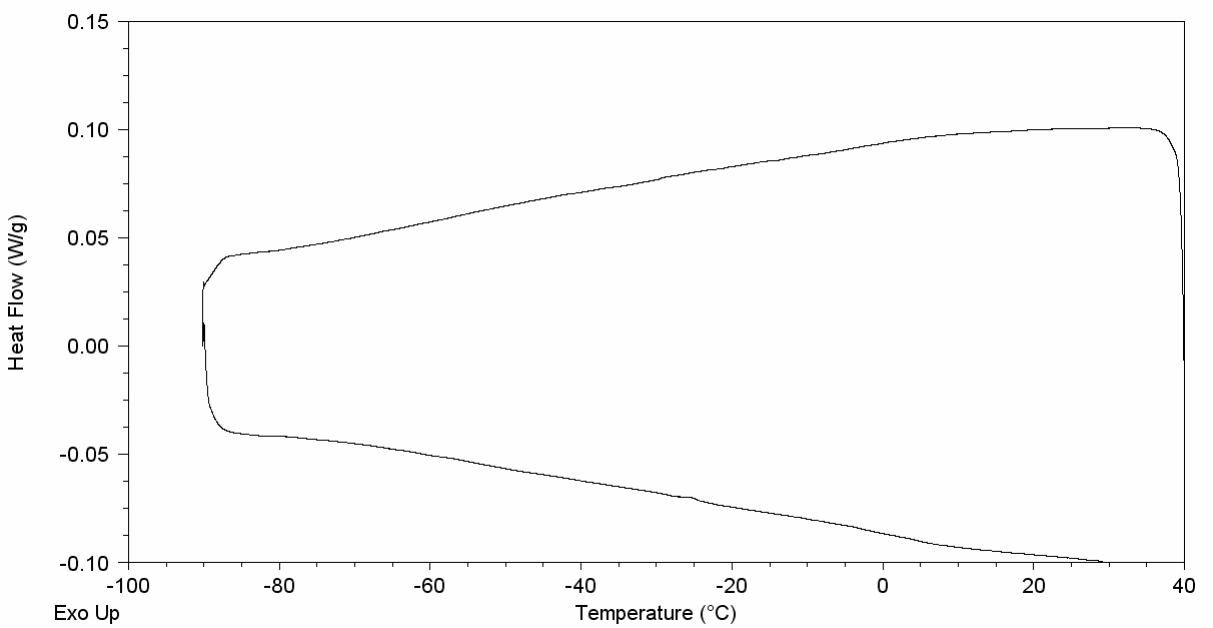

a) Cooling and heating curves for hyaluronan hydrogel of W_c 0.5. The expanded view of the melting curve is not reported because there is no endothermic transition.

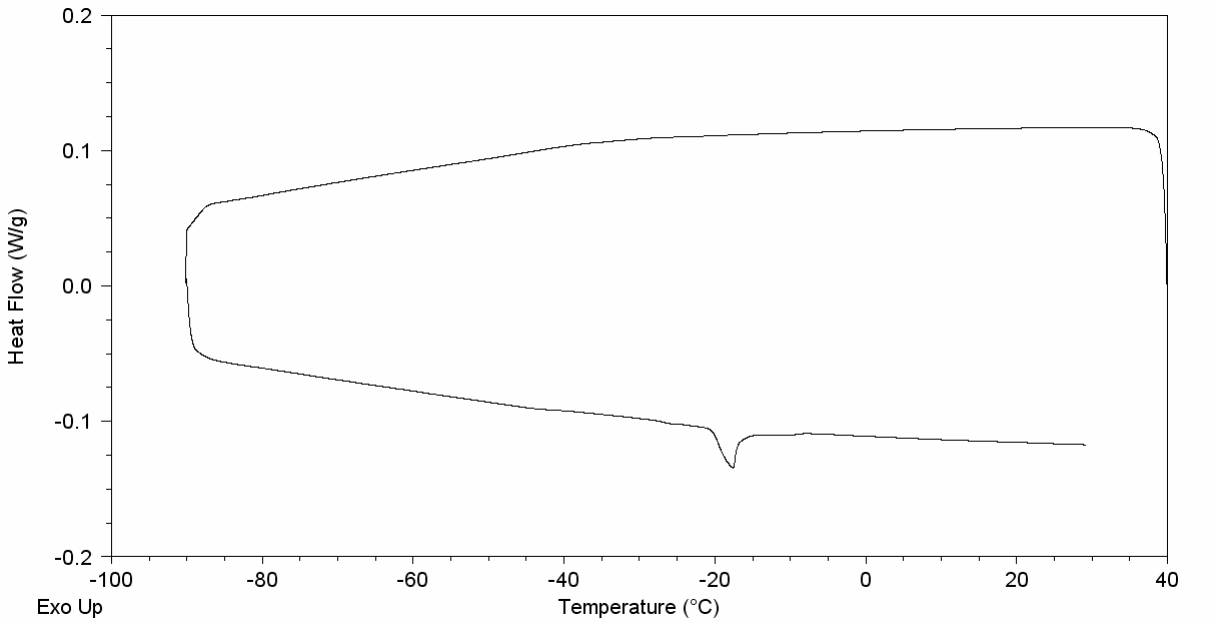

a) Cooling and heating curves for hyaluronan hydrogel of W_c 0.75.

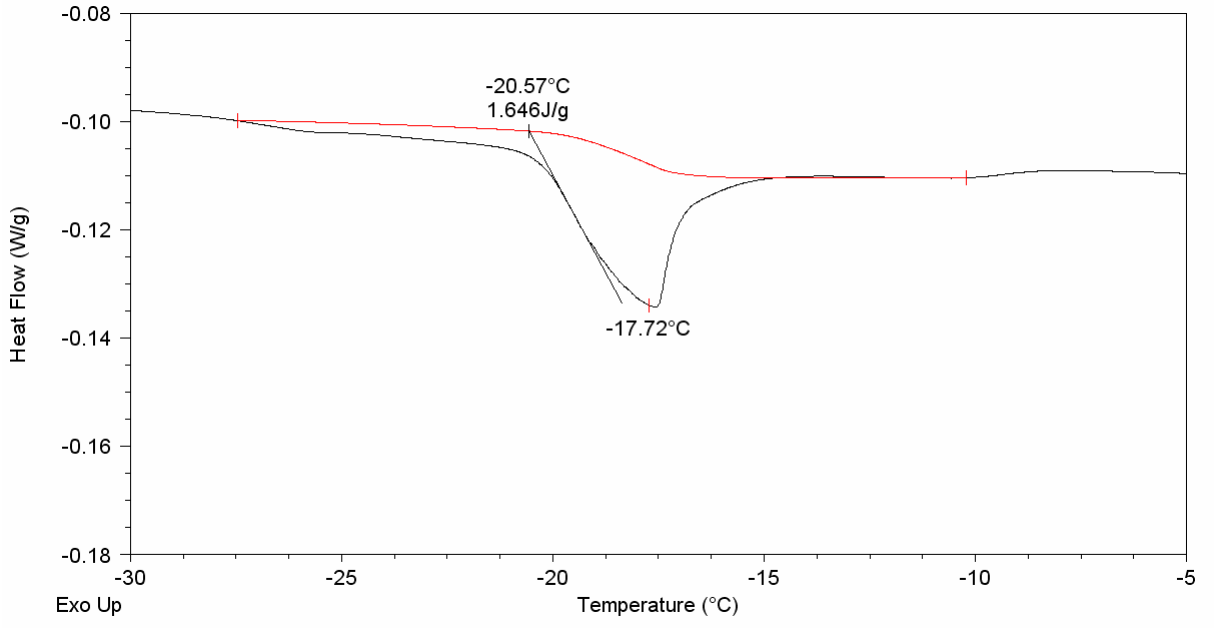

b) Expanded view of the melting endotherm portion of the curves shown above. The transition temperatures and enthalpy are as shown.

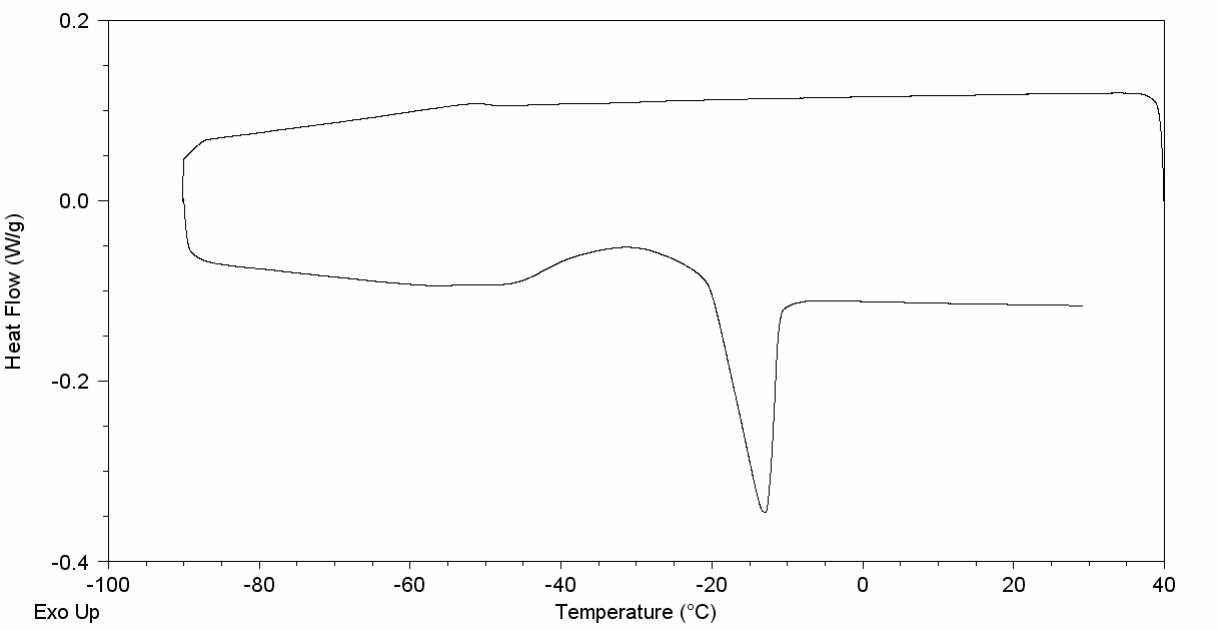

a) Cooling and heating curves for hyaluronan hydrogel of W_c 1.0.

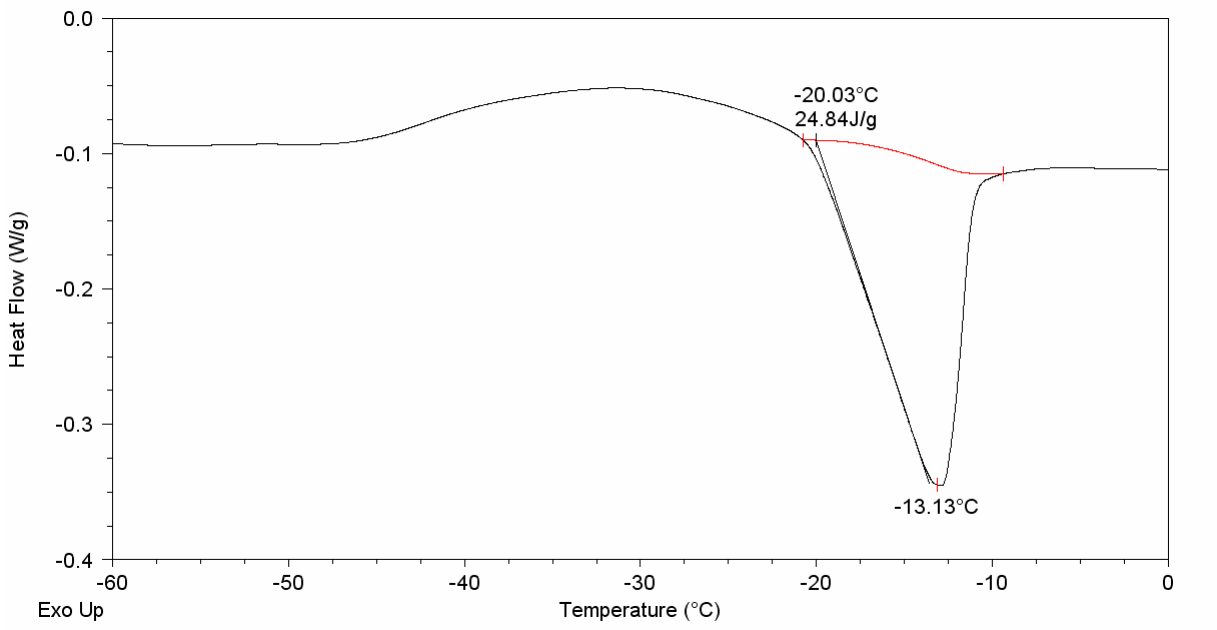

b) Expanded view of the melting endotherm portion of the curves shown above. The transition temperatures and enthalpy are as shown.

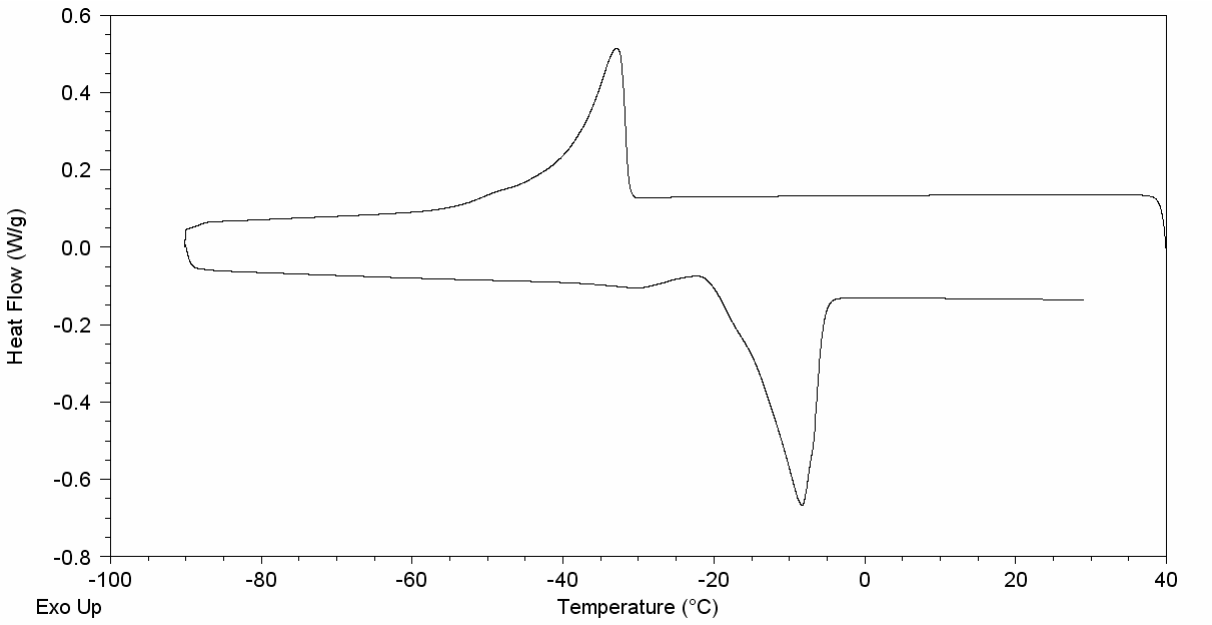

a) Cooling and heating curves for hyaluronan hydrogel of W_c 1.5.

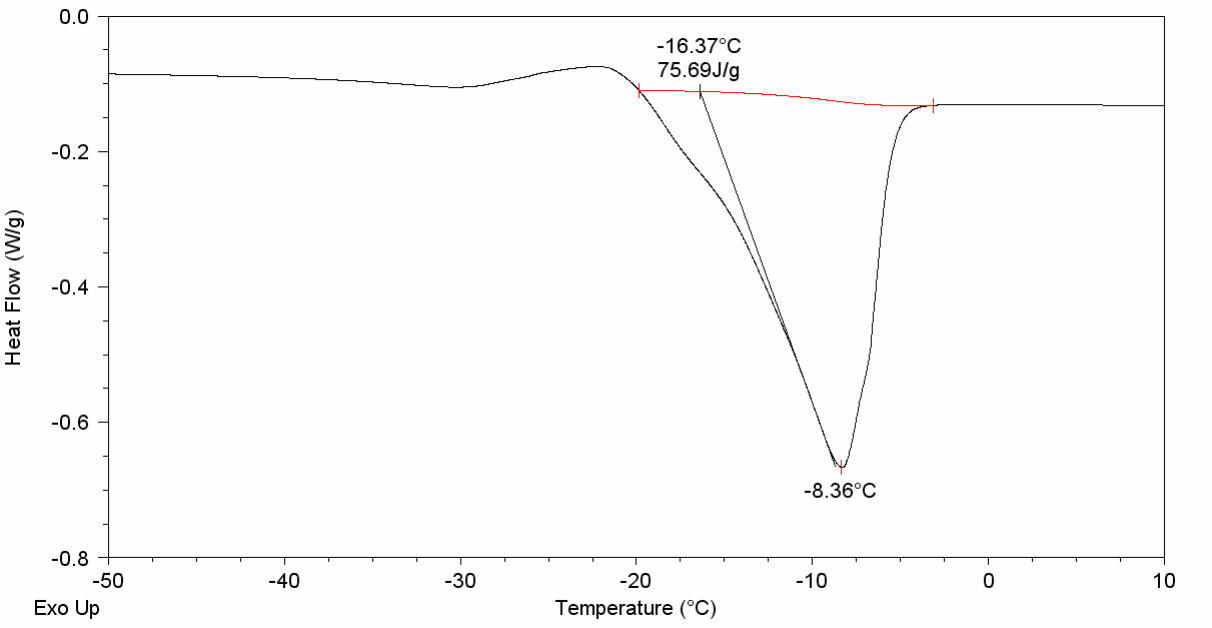

b) Expanded view of the melting endotherm portion of the curves shown above. The transition temperatures and enthalpy are as shown.

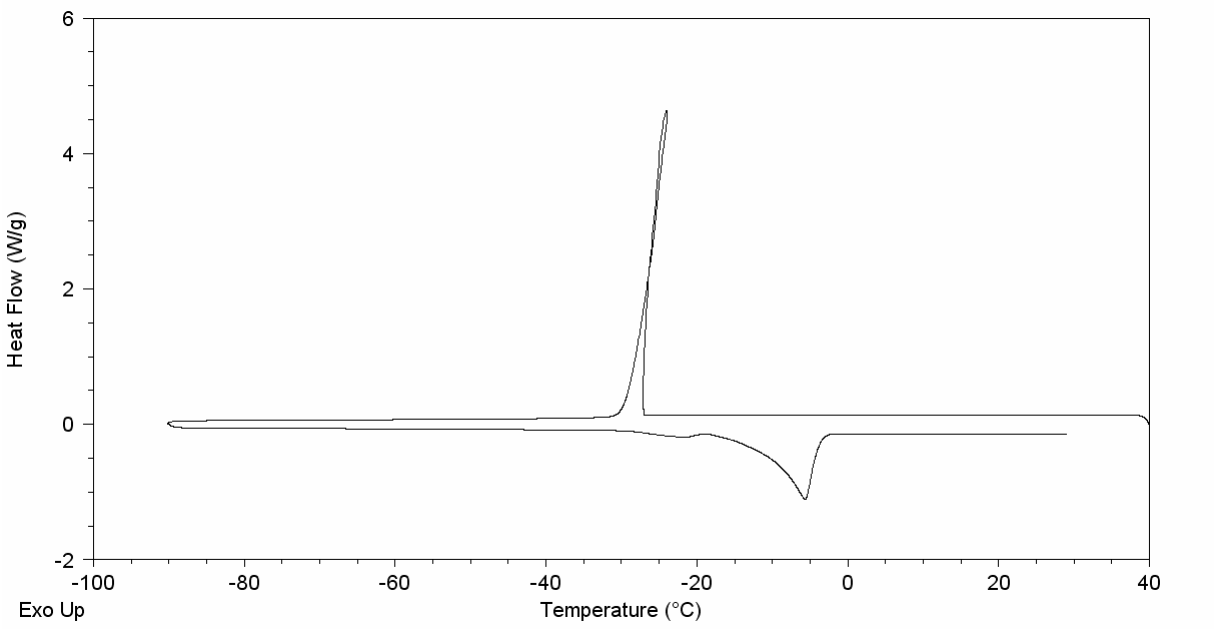

a) Cooling and heating curves for hyaluronan hydrogel of W_c 2.0.

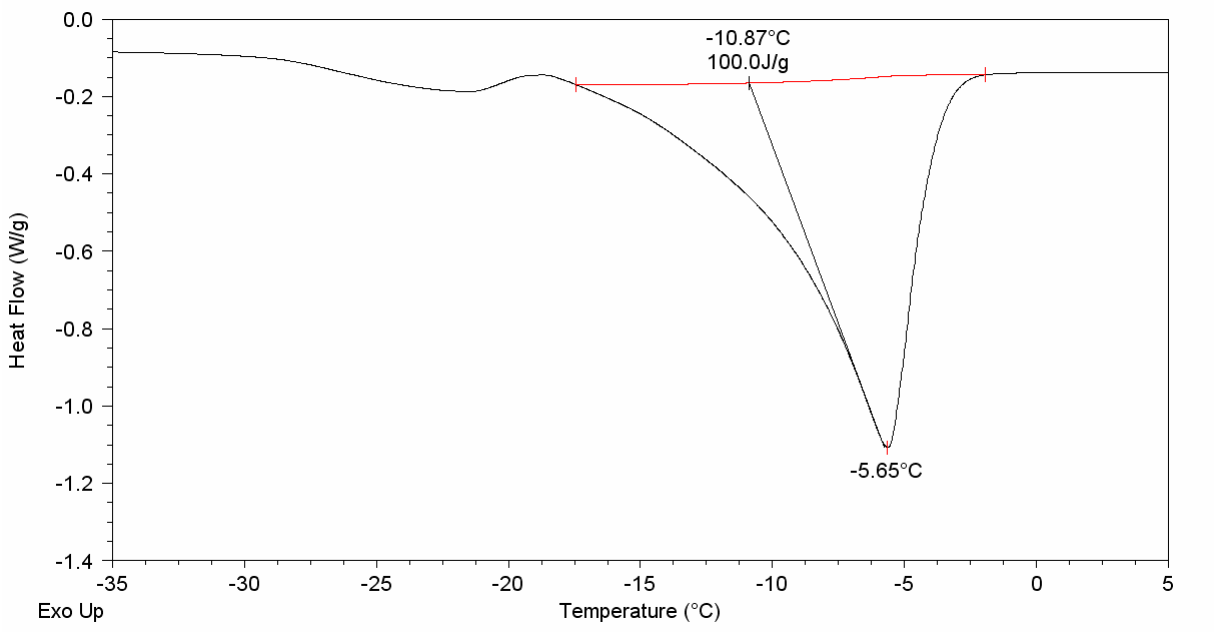

b) Expanded view of the melting endotherm portion of the curves shown above. The transition temperatures and enthalpy are as shown.

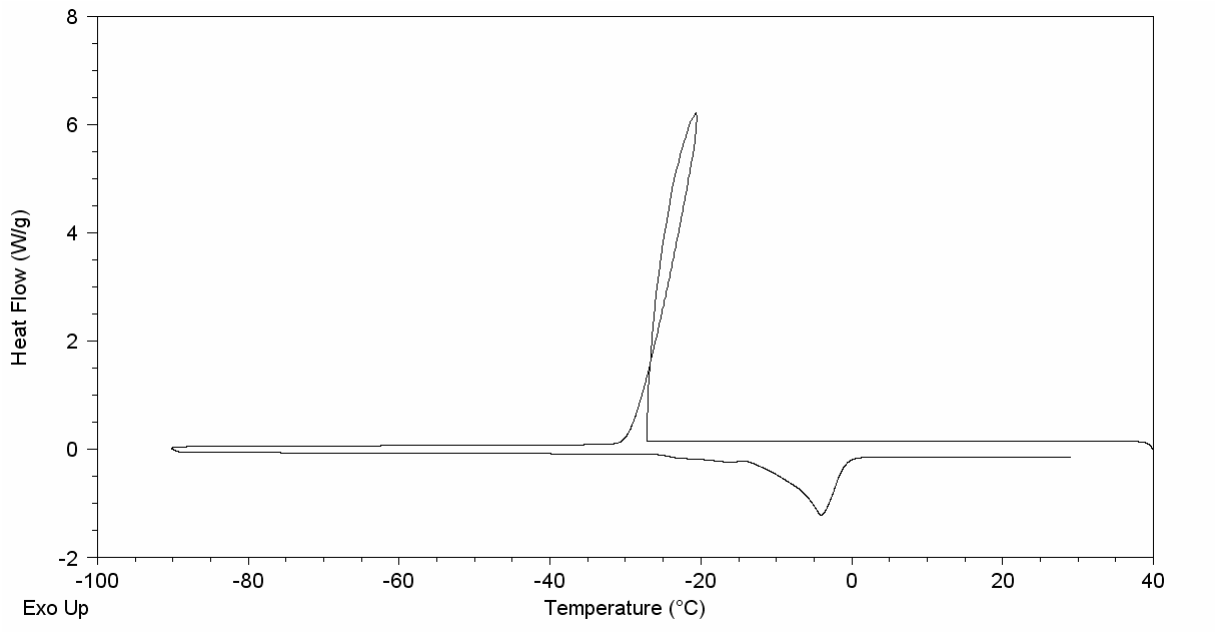

a) Cooling and heating curves for hyaluronan hydrogel of W_c 2.5.

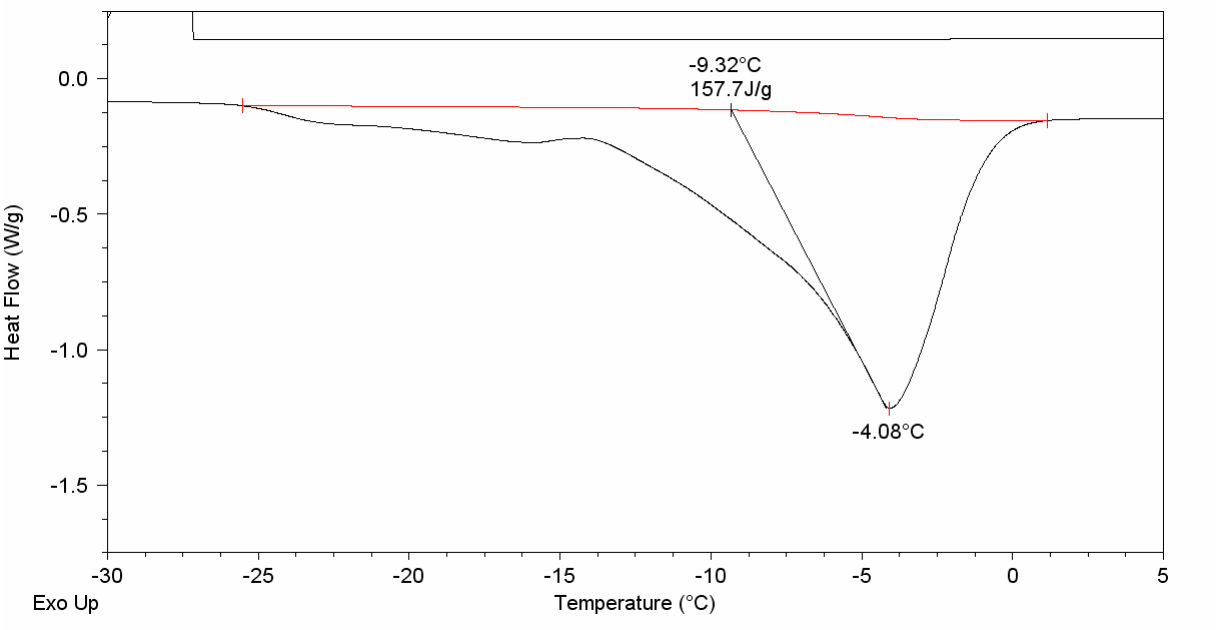

b) Expanded view of the melting endotherm portion of the curves shown above. The transition temperatures and enthalpy are as shown.

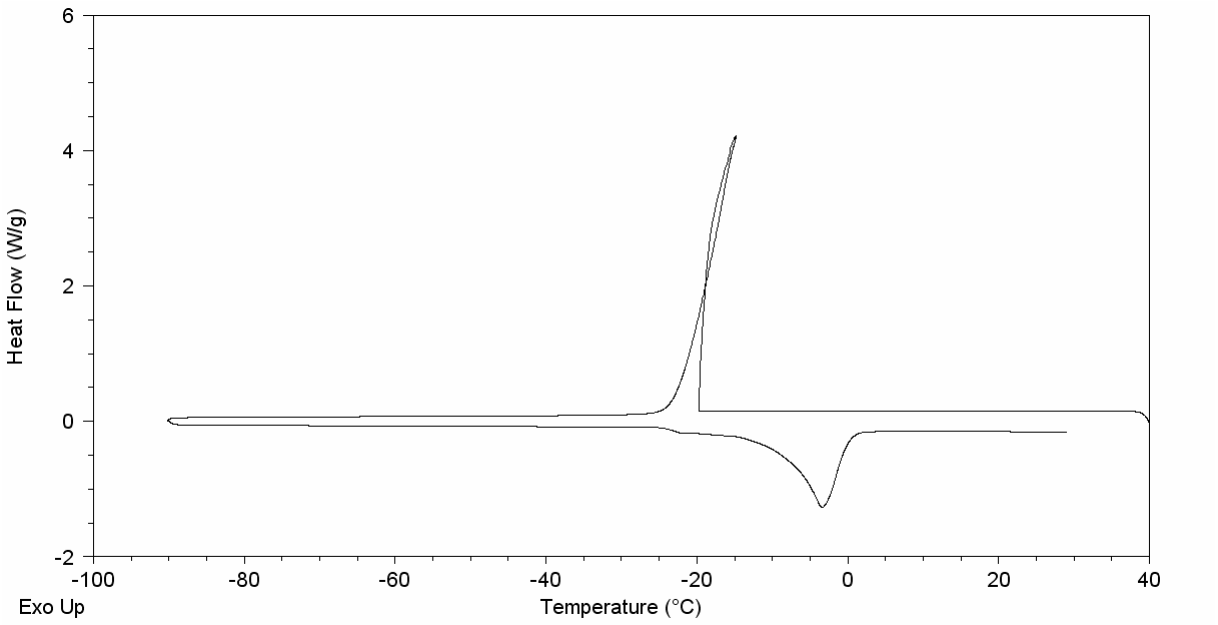

a) Cooling and heating curves for hyaluronan hydrogel of W_c 3.0.

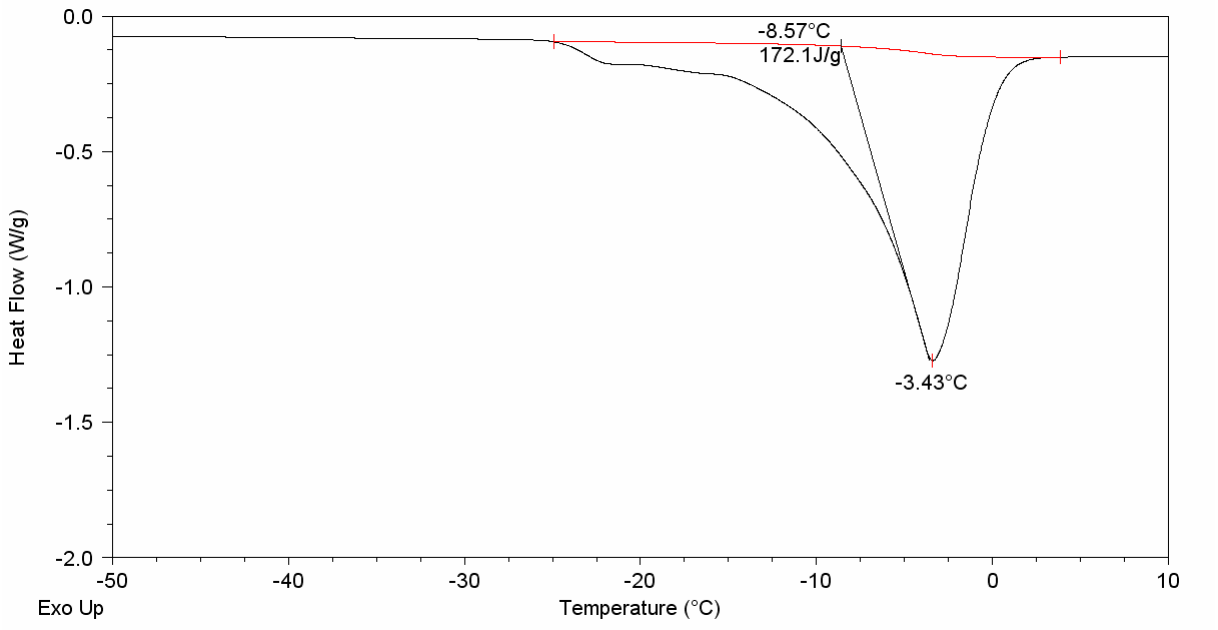

b) Expanded view of the melting endotherm portion of the curves shown above. The transition temperatures and enthalpy are as shown.